

N O T I C E

THIS DOCUMENT HAS BEEN REPRODUCED FROM
MICROFICHE. ALTHOUGH IT IS RECOGNIZED THAT
CERTAIN PORTIONS ARE ILLEGIBLE, IT IS BEING RELEASED
IN THE INTEREST OF MAKING AVAILABLE AS MUCH
INFORMATION AS POSSIBLE

NASA CR-159981



(NASA-CR-159981) INTERACTIONS BETWEEN
CONVECTIVE STORMS AND THEIR ENVIRONMENT
Final Report (National Oceanic and
Atmospheric Administration) 104 p
HC A06/MF A01

CSCL 04B G3/47

Unclas
21004

INTERACTIONS BETWEEN CONVECTIVE
STORMS AND THEIR ENVIRONMENT

Final Report

R. A. Maddox, L. R. Hoxit,
and C. F. Chappell

U. S. Department of Commerce
National Oceanic and Atmospheric Administration
Environmental Research Laboratories
Boulder, Colorado

Prepared for:

National Aeronautics and Space Administration
Goddard Space Flight Center
Greenbelt, Maryland

May 1979

Contract No. S-40336B



noaa

NATIONAL OCEANIC AND
ATMOSPHERIC ADMINISTRATION

Environmental
Research Laboratories

ABSTRACT

The ways in which intense convective storms interact with their environment are considered for a number of specific severe storm situations. A physical model of subcloud wind fields and vertical wind profiles is developed to explain the often observed intensification of convective storms that move along or across thermal boundaries. A number of special, unusually dense, data sets are used to substantiate features of the model. GOES imagery is used in conjunction with objectively analyzed surface wind data to develop a nowcast technique that might be used to identify specific storm cells likely to become tornadic. It is also shown that circulations associated with organized meso- α and meso- β scale (250 to 2500 km and 25 to 250 km respectively) storm complexes may, on occasion, strongly modify tropospheric thermodynamic patterns and flow fields.

FOREWORD

This paper constitutes the final project report for a study conducted by the Atmospheric Physics and Chemistry Laboratory, Environmental Research Laboratories, NOAA, for NASA under Contract S-40336B. The research effort was entitled "Thunderstorm/Environment Interactions that Affect Subsequent Convection" and was partially sponsored by the NASA Office of Applications under the direction of Goddard Space Flight Center, Meteorology Branch. Dr. C. F. Chappell acted as Principal Investigator with Dr. L. R. Hoxit and R. A. Maddox being Co-investigators. R. A. Maddox acted as Project Leader for the study and C. A. Peslen, NASA, GSFC, was Technical Officer.

ACKNOWLEDGMENTS

The studies of severe convective storms reported in this paper have been partially supported by NASA under Contract No. S-40336B and the authors gratefully acknowledge the NASA support without which this research would not have been possible. NSSL personnel supplied subsynoptic surface observations from Oklahoma sites and WKY tower data. Kelly Hill, NASA, Marshall Space Flight Center, provided several sets of AVE data that were used in the study. The authors also thank Mrs. Elaine Ardourel for carefully preparing the manuscript and NOAA Co-operative students Ken Crysler, Mike Dias, Brad Muller, and Nick Powell who assisted in data processing and reduction.

TABLE OF CONTENTS

	Page
FOREWORD	ii
ACKNOWLEDGMENTS	ii
TABLE OF CONTENTS	iii
LIST OF TABLES	iv
LIST OF FIGURES	iv
1. INTRODUCTION	1
2. THUNDERSTORM/THERMAL BOUNDARY INTERACTIONS	3
a. <u>The 27 May 1977 case</u>	20
b. <u>The 6 May 1975 (Omaha tornado) case</u>	24
c. <u>The 24 April 1975 (Neosho tornado) case</u>	30
3. ANALYSES OF SURFACE DATA AND CONCURRENT GOES IMAGERY	44
4. CONVECTIVE MODIFICATIONS OF THE ENVIRONMENT	51
a. <u>The 4 April 1977 (Birmingham tornado) case</u>	51
b. Upper-tropospheric flow fields on 24 and 25 April 1975	73
5. SUMMARY	86
REFERENCES	88
APPENDIX I	93

LIST OF TABLES

Table	Page
1 Mean value of θ_e (K) for the 950 - 900 mb layer	44

LIST OF FIGURES

Figure	Page
1a Surface mesoanalysis for 2100 GMT, 2 March 1977.	6
1b Surface mesoanalysis for 2200 GMT, 10 April 1979	7
1c Surface mesoanalysis for 1800 GMT, 4 May 1977.	8
1d Surface mesoanalysis for 0000 GMT, 6 June 1977	9
1e Surface mesoanalysis for 0000 GMT, 31 July 1977.	12
1f Surface mesoanalysis for 1500 GMT, 21 August 1977.	13
1g Surface mesoanalysis for 2100 GMT, 26 August 1977.	14
1h Surface mesoanalysis for 2100 GMT, 1 October 1977.	15
1i Surface mesoanalysis for 1200 GMT, 13 December 1977.	16
2 Schematic representation of boundary layer wind profiles within a typical severe thunderstorm producing surface pattern.	19
3 Surface mesoanalysis for 1200 GMT, 27 May 1977	21
4 Time series of observations from the NSSL tower on 27 May 1977	23
5 Time series of upper-air data taken at Oklahoma City on 27 May 1977	24
6 Surface mesoanalysis for 1800 GMT, 6 May 1975.	25
7 Surface mesoanalysis for 2100 GMT, 6 May 1975.	27
8 850 mb analysis for 0000 GMT, 7 May 1975	29
9 500 mb analysis for 0000 GMT, 7 May 1975	31

LIST OF FIGURES (Cont'd)

Figure	Page
10 Time series of surface observations for Lincoln, Nebraska, on 6 and 7 May 1975	32
11 Time series of surface observations for Omaha, Nebraska, on 6 and 7 May 1975	33
12 Surface mesoanalysis for 2200 GMT, 24 April 1975.	35
13 Surface mesoanalysis for 0000 GMT, 25 April 1975.	36
14 850 mb analysis for 2100 GMT, 24 April 1975	38
15 500 mb analysis for 2100 GMT, 24 April 1975	39
16 Surface observation time series for Ponca City, Oklahoma, on 24 and 25 April 1975	40
17 Surface observation time series for Tulsa, Oklahoma, on 24 and 25 April 1975	41
18 Surface observation time series for Joplin, Missouri, for 24 and 25 April 1975.	42
19 Upper-air time series for Monett, Missouri, on 24 April 1975	43
20 GOES full resolution, visible image for 1800 GMT, 6 May 1975.	47
21 GOES full resolution, visible image for 2000 GMT, 6 May 1975.	48
22 GOES full resolution, visible image for 2100 GMT, 24 April 1975	49
23 GOES full resolution, visible image for 2300 GMT, 24 April 1975	50
24a Surface mesoanalysis for 1200 GMT, 4 April 1977	54
24b Surface mesoanalysis for 1500 GMT, 4 April 1977	55
24c Surface mesoanalysis for 1800 GMT, 4 April 1977	55
24d Full resolution GOES visible image for 1800 GMT, 4 April 1977.	56

LIST OF FIGURES (Cont'd)

Figure		Page
24e	Surface mesoanalysis for 1900 GMT, 4 April 1977	58
24f	Surface mesoanalysis for 2000 GMT, 4 April 1977	58
24g	Surface mesoanalysis for 2100 GMT, 4 April 1977	59
24h	Full resolution GOES visible image for 2100 GMT, 4 April 1977.	60
24i	Surface mesoanalysis for 0000 GMT, 5 April 1977	61
25	Time series of surface observations for Birmingham, Alabama, on the afternoon of 4 April 1977	63
26	Time series of surface observations for Rome, Georgia, on the afternoon of 4 April 1977.	64
27a	Lower tropospheric conditions for 1200 GMT, 4 April 1977.	66
27b	Lower tropospheric conditions for 1800 GMT, 4 April 1977.	67
27c	Lower tropospheric conditions for 0000 GMT, 5 April 1977.	68
28a	Middle tropospheric conditions for 1200 GMT, 4 April 1977.	70
28b	Middle tropospheric conditions for 1800 GMT, 4 April 1977.	71
28c	Middle tropospheric conditions for 0000 GMT, 5 April 1977.	72
29a	Upper tropospheric/lower stratospheric conditions for 1200 GMT, 4 April 1977.	74
29b	Upper tropospheric/lower stratospheric conditions for 1800 GMT, 4 April 1977.	75
29c	Upper tropospheric/lower stratospheric conditions for 0000 GMT, 5 April 1977.	76

LIST OF FIGURES (Cont'd)

Figure	Page
30a Jetstream winds for 0000 GMT, 24 April 1975	77
30b Digitized IR satellite image for 0000 GMT, 24 April 1975	79
31a Jetstream winds for 0600 GMT and radar echoes for 0535 GMT, 24 April 1975	80
31b Digitized IR satellite image for 0600 GMT, 24 April 1975	81
32a Jetstream winds for 0000 GMT and radar echoes for 2335 GMT, 25 and 24 April 1975.	82
32b IR satellite image for 0000 GMT, 25 April 1975.	83
33a Jetstream winds for 0600 GMT and radar echoes for 0525 GMT, 25 April 1975	84
33b Digitized IR satellite image for 0600 GMT, 25 April 1975	85
A1 Response curve as a function of wavelength.	96

INTERACTIONS BETWEEN CONVECTIVE STORMS
AND THEIR ENVIRONMENT

R. A. Maddox, L. R. Hoxit, and C. F. Chappell

Mesometeorology Group, Atmospheric Physics
and Chemistry Laboratory
Environmental Research Laboratories, NOAA
Boulder, Colorado 80303

1. INTRODUCTION

The evolution and life cycle of severe thunderstorms and convective mesosystems is determined by complex interactions among dynamic, kinematic and thermodynamic processes on scales ranging from those of small cloud particles to those of mid-latitude cyclones. Once deep convection develops in the atmosphere numerous reactions and interactions occur. Some responses act to suppress or dissipate the convection while others may act to intensify or perpetuate storms by imposing organization on the convective system or by triggering new developments. Most research has (for lack of comprehensive data sets) focused upon perturbations and interactions that occur within clouds or in the boundary layer beneath and near the clouds.

The research effort reported here examined three specific types of thunderstorm/environment interactions. The first of these was the interaction of convective storms with shallow

baroclinic zones such as warm fronts or thunderstorm produced, cold air outflow boundaries. Storms that move across or along such baroclinic zones are often observed to intensify and become tornadic (Miller, 1967). The meso- β scale kinematic and thermodynamic features that might explain this preferred intensification have been examined for a number of cases.

Thunderstorms exist in and move through local mesoscale environments that may favor intensification because of specific spatial distributions of moisture, divergence, vorticity and conditional instability. It was hypothesized that these favorable meso- β scale regions might be detected and monitored utilizing conventional surface observations. Mappings of favorable fields or regions could then be superposed on concurrent satellite imagery to identify specific thunderstorm cells or complexes that were likely to intensify. These first two efforts considered down-scale interactions in which meso-scale environmental features interact with convective scale features in ways conducive to storm intensification.

The third type of interactions considered were up-scale feedbacks in which organized convective complexes affect and modify their background environment. One obvious way in which this occurs is through continued, organized convective overturning which modifies vertical temperature structure and consumes latent instability provided by the larger scale

environment (Fritsch, 1975a). The convective circulation is completed in regions of compensating mass subsidence. If this compensating subsidence occurs on organized, larger scales significant areas of warmer environmental temperatures result from the compressional heating. Mesoscale pressure and wind fields may be altered by these thermodynamic perturbations in ways which produce mesolow pressure systems (Hoxit et al., 1976), trigger new convection, act to organize and intensify existing convection, or even to modify large scale flow fields (Maddox, 1979a). A number of specific events have been studied in detail and the results are presented in subsequent sections.

2. THUNDERSTORM/THERMAL BOUNDARY INTERACTIONS

It has long been recognized that the area of intersection of a line of thunderstorms with a shallow baroclinic zone (e.g. warm front, another active squall-line, or a cool air outflow boundary produced by prior storms) was a favored location for the occurrence of severe, tornadic storms. Operational forecasting papers by Magor (1959) and Miller (1967) emphasized the importance of this frequently observed characteristic of mesoscale convective systems. Kuhn et al. (1958) showed in composite, pre-tornado thermal charts that the favored location for tornado occurrence was northeast of the axis of a surface thermal ridge within a region of strong temperature gradient. Purdom's (1975 and 1976) recent analyses of satellite imagery

have provided "photographic" verification of the characteristics noted by earlier investigators and have also shown that similar increases in intensity occur even when individual thunderstorms move across or along such boundaries.

Detailed studies of the thermodynamic and kinematic mechanisms responsible for these observed characteristics have not been undertaken. This has undoubtedly been because of a lack of mesoscale observations in the vicinity of such thermal boundaries. It has been assumed that ambient moisture convergence and relative vorticity must be maximized in these zones; and therefore, the most intense storms should be expected within these regions.

Storm Data reports of tornadoes were used in conjunction with 3-hourly surface charts to identify a number of thermal boundary tornado occurrences during 1977. (In addition, an important event that occurred in 1979 is also shown.) Examples of surface conditions preceding the tornadoes are shown for nine of these events in Figs. 1a through 1i. The GMT times of tornado occurrence from Storm Data are shown with the tornado tracks.

Figure 1a illustrates a case early in the spring when a number of short-track tornadoes occurred in Oklahoma along a warm frontal boundary. These particular storms occurred along a very strong thermal gradient and were moving rapidly north-eastward. As the storms moved into deeper cold air they decreased in intensity. The situation that spawned the

destructive Wichita Falls, Texas, tornado is illustrated in Fig. 1b. A number of intense tornadoes occurred along a thermal boundary that had been produced both by a large-scale warm front and by cool air outflow from storms to the north of the boundary.

A case in May is shown in Fig. 1c. Several strong tornadoes occurred in Missouri along the southern periphery of a thermal discontinuity that had been produced by thunderstorm activity. These storms occurred far to the east of a strong dryline and no tornado events were reported within the warm sector ahead of the dryline. Figure 1d illustrates a case in June when a single, long-track intense tornado occurred in southeastern Wisconsin. This storm tracked southeastward along the intense thermal gradient. The thermal boundary was likely produced by a combination of cool outflow from prior storms and by cooling from Lake Michigan. Once again no tornadoes were noted in the hot, moist air mass along and ahead of the surface cold front.

Figure 1e depicts a July situation in which four intense, but short-track, tornadoes occurred in northwestern Wisconsin along a warm frontal boundary. These storms were moving almost normal to the isotherms and thus moved into an increasingly hostile convective environment.

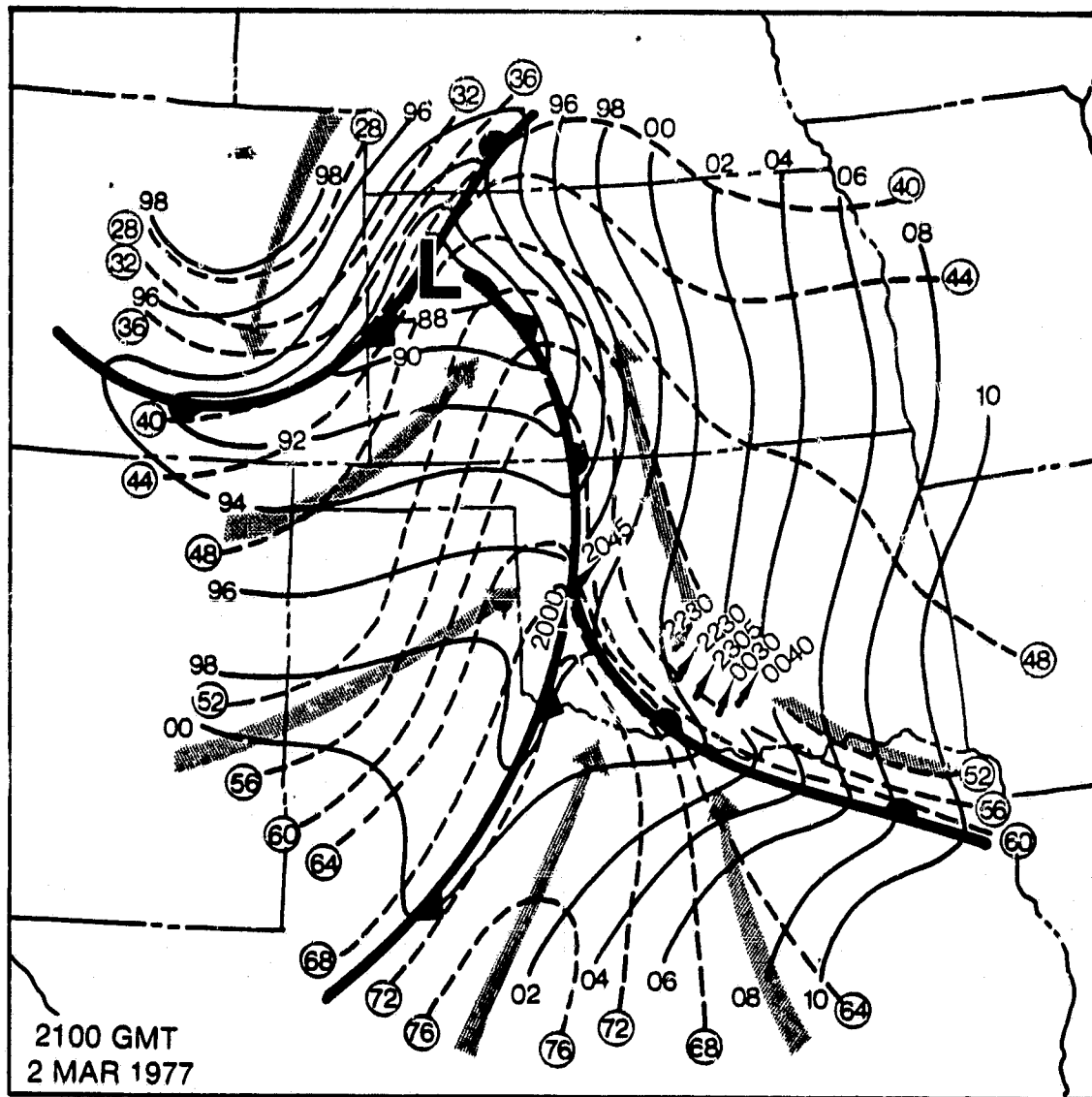


Fig. 1a. Surface mesoanalysis for 2100 GMT, 2 March 1977. Surface features are shown along with 2 mb isobars and 4°F isotherms. The arrows are streamlines for the observed surface winds. Tornado tracks are indicated along with reported times of occurrence (GMT).

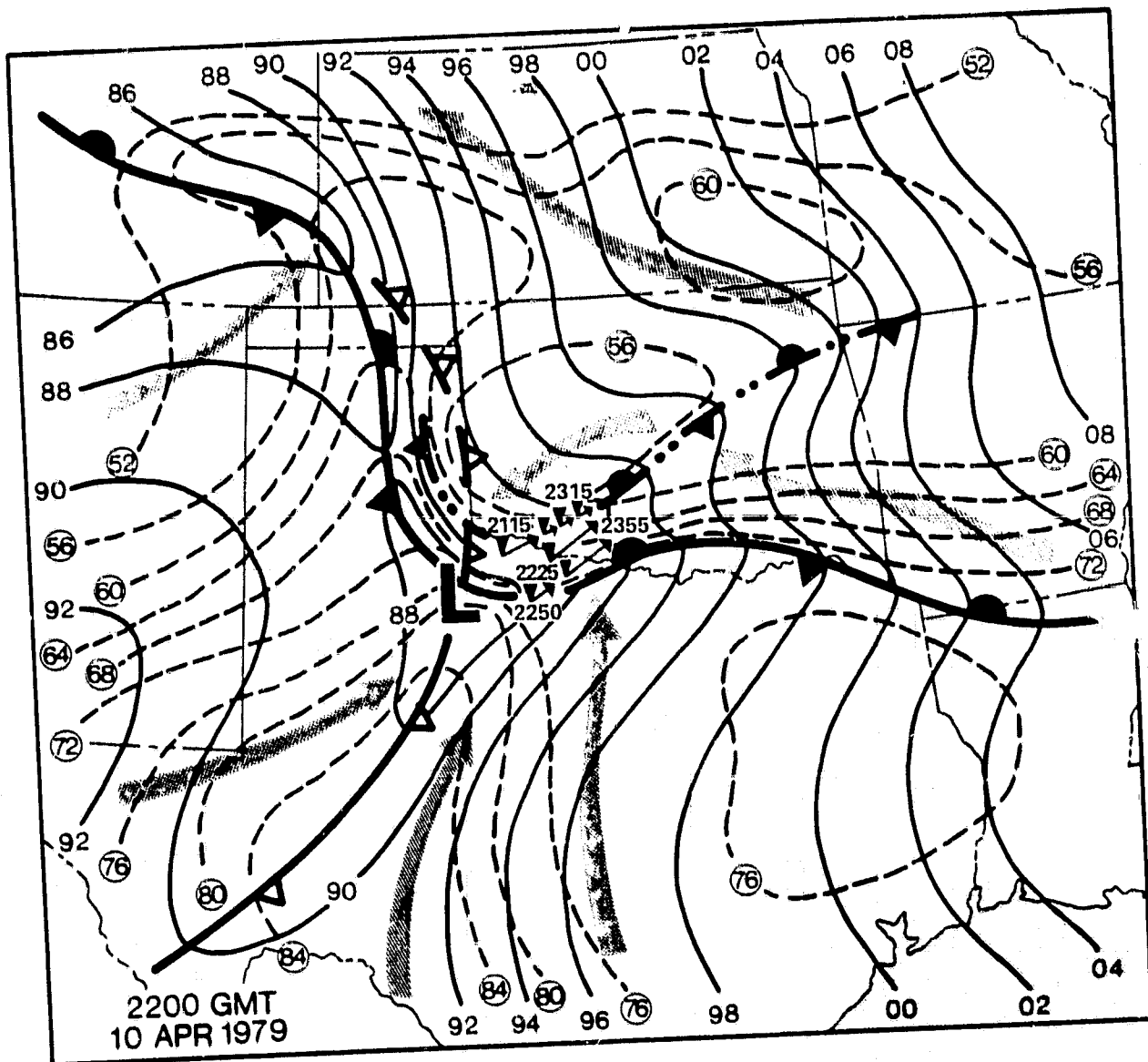


Fig. 1b. Surface mesoanalysis for 2200 GMT, 10 April 1979. A thunderstorm cold air outflow boundary is depicted by the squall symbol with barbs added to indicate its direction of movement. The open barbs denote the dryline. Other details as in Fig. 1a.

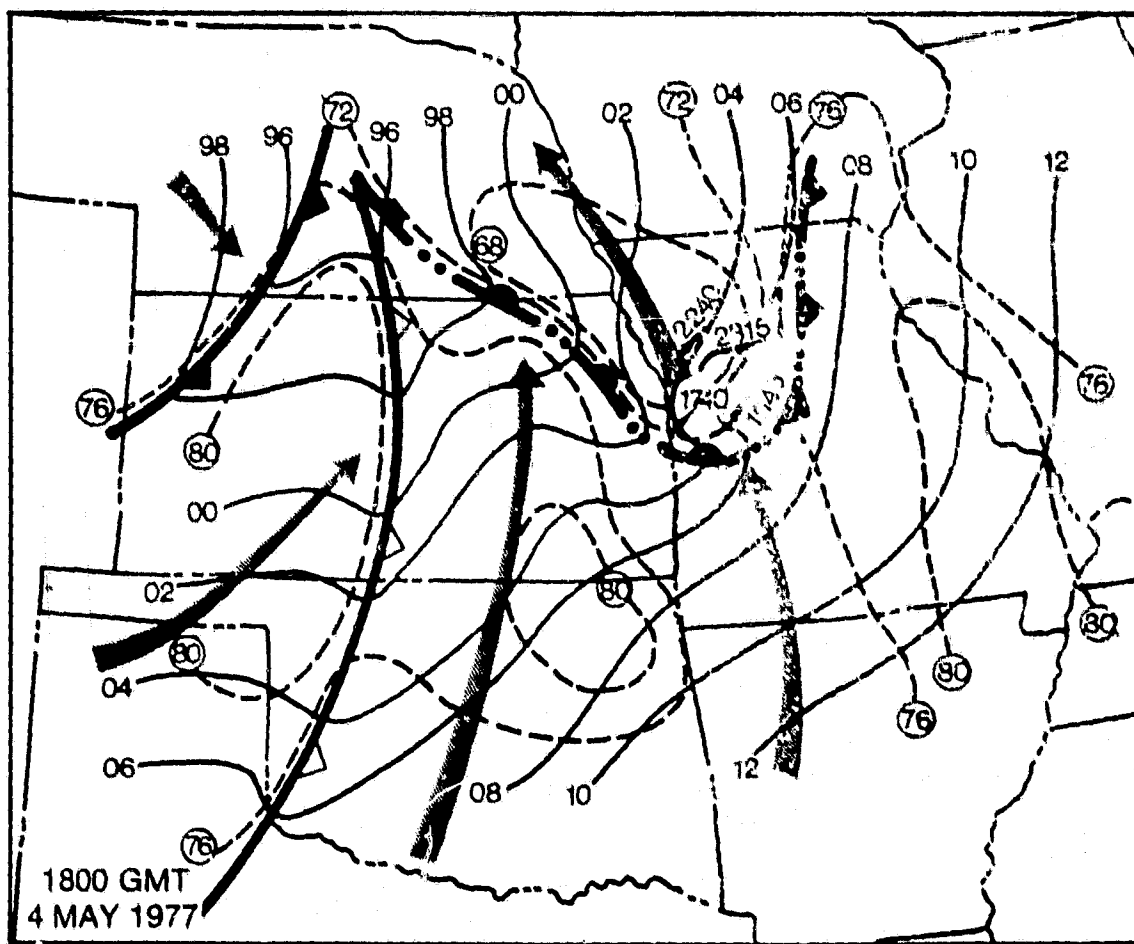


Fig. 1c. Surface mesoanalysis for 1800 GMT, 4 May 1977. Details as in Figs. 1a and 1b.

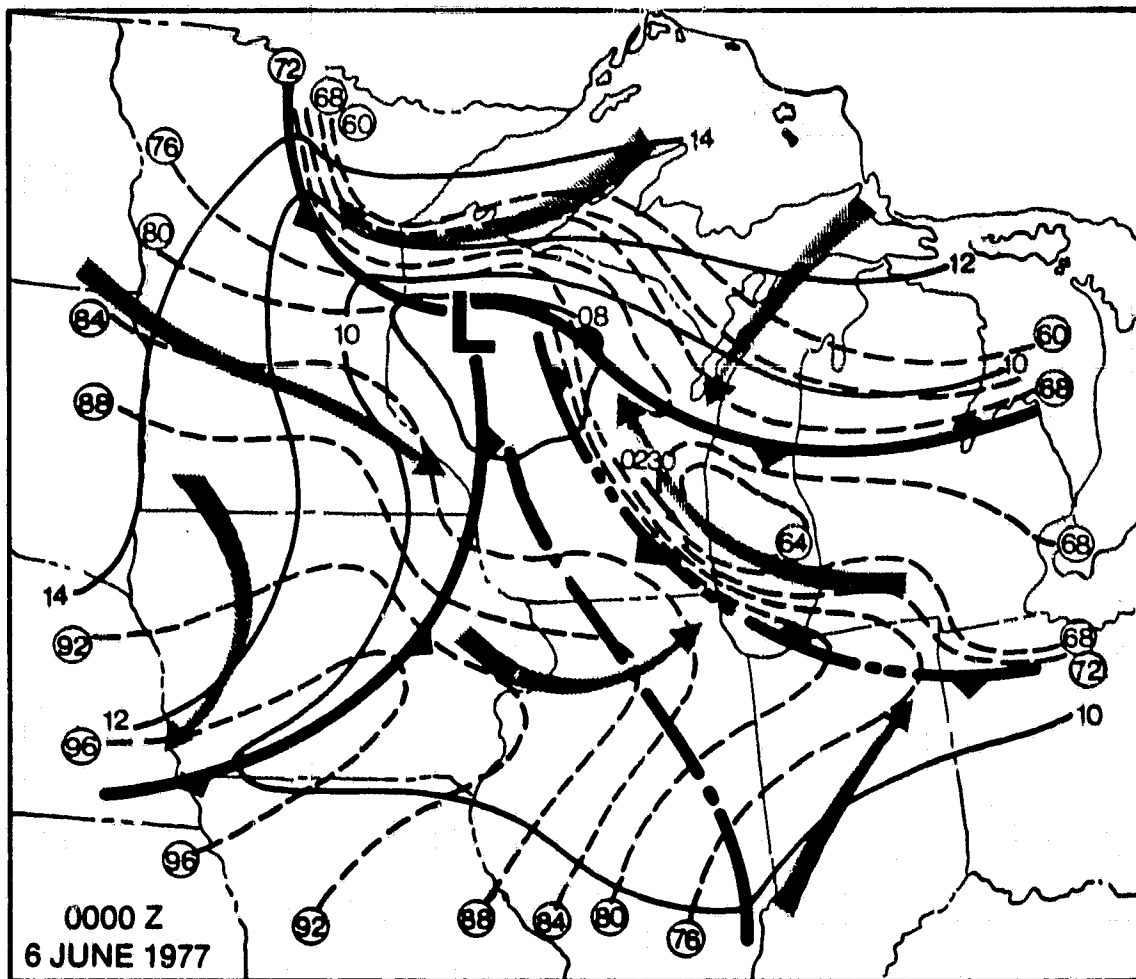


Fig. 1d. Surface mesoanalysis for 0000 GMT, 6 June 1977.
Details as in Figs. 1a and 1b.

A late summer (August) case in southeastern Illinois is shown in Fig. 1f. The single, intense, long-track tornado was apparently spawned by a storm cell moving along a thermal boundary produced by earlier storm activity. This case is quite similar to that shown in Fig. 1d. Figure 1g illustrates another August case that occurred in central Minnesota. Two tornadoes moved along, and slightly across, a strong thermal gradient associated with a stationary east-west surface front. It appears that lake effect cooling from Lake Superior helped maintain the strength of the front. Tornadoic storms were not reported in South Dakota and Nebraska ahead of the strong cold front. A fall situation (October) is shown in Fig. 1h. Four tornadoes were reported in eastern Tennessee along an outflow boundary produced by earlier storm activity. Once again these tornadoes were far removed from the very strong surface cold front. Figure 1i depicts a winter (December) tornado situation along the Gulf Coast. In this case a single, strong tornado moved through the north suburbs of Houston. The storm was moving across a weak thermal gradient along a warm frontal boundary.

These situations share many common features that are important whether they are considered relative to forecasting problems or to satellite data interpretation. The tornadoes tended to be intense (F2/F3 or greater, see Fujita, 1971) and destructive, but there were few individual occurrences. These

tornado events could thus be classified as small outbreaks - the type situation that may be harder to correctly forecast than a major (>10 tornadoes) outbreak (Galway, 1975). The storms that moved across the thermal boundary tended to produce intense, but short-track, tornadoes. Whereas, storms that moved along or parallel to such a thermal boundary produced intense, relatively long-track tornadoes. In all of the events shown, the thermal boundary tornadoes were the only tornado occurrences even though there were strong cold fronts and drylines pushing into the hot, moist air masses. This indicates that meso- α and meso- β scale conditions were probably not conducive to "family" type severe storm outbreaks. Tornadic storms were only able to develop in the meso- β scale thermal boundary zone. Therefore, the local environment along such boundaries must be considerably different than that of the hot, moist air mass.

Observational and theoretical studies suggest that in the vicinity of thermal boundaries a local environment conducive to severe storms is produced by horizontal variations in the boundary layer wind profile. Surface wind speeds over land are typically 50-60% of the geostrophic value and the flow is toward lower pressure with an isobaric crossing angle of about 35 degrees. The wind veers with height and the speed increases until geostrophic or gradient balance is reached - usually 1000 to 5000 feet above the surface. The surface crossing angle

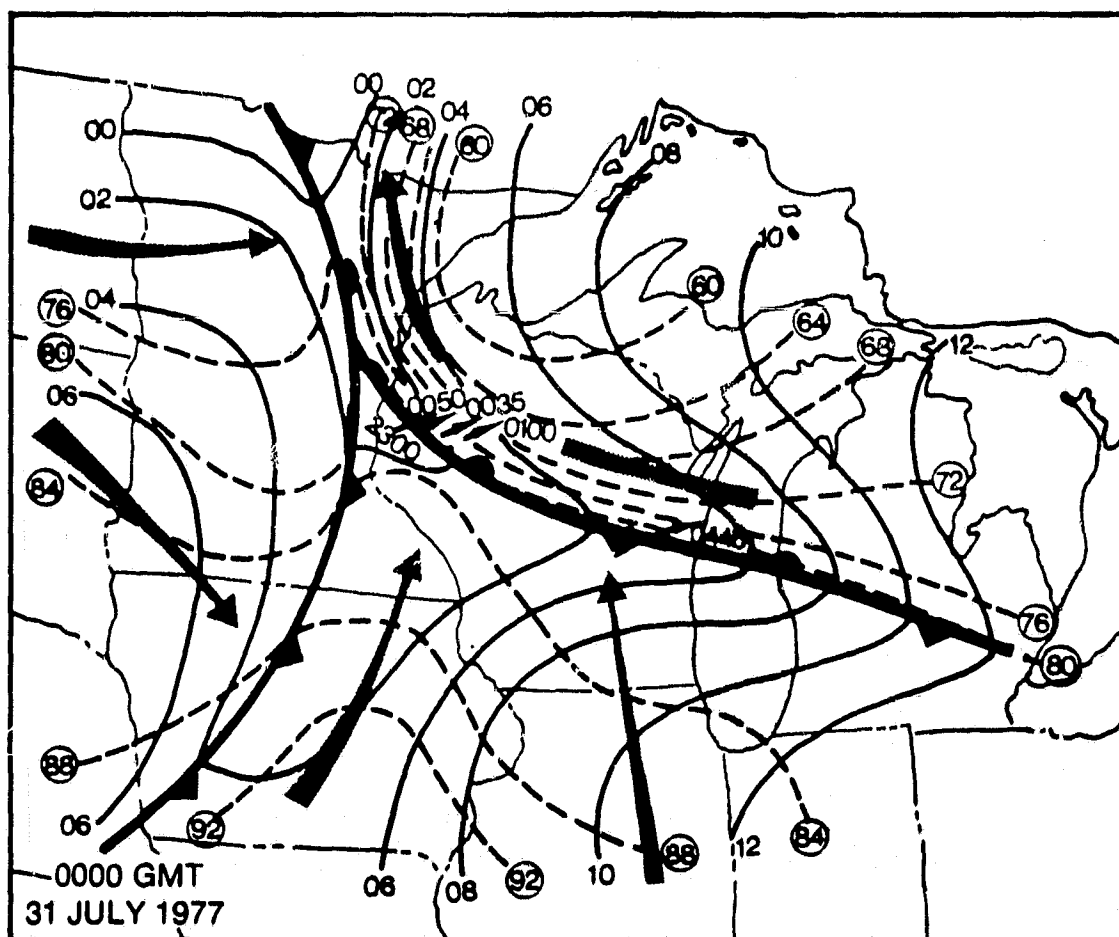


Fig. 1e. Surface mesoanalysis for 0000 GMT, 31 July 1977. Details as in Fig. 1a.

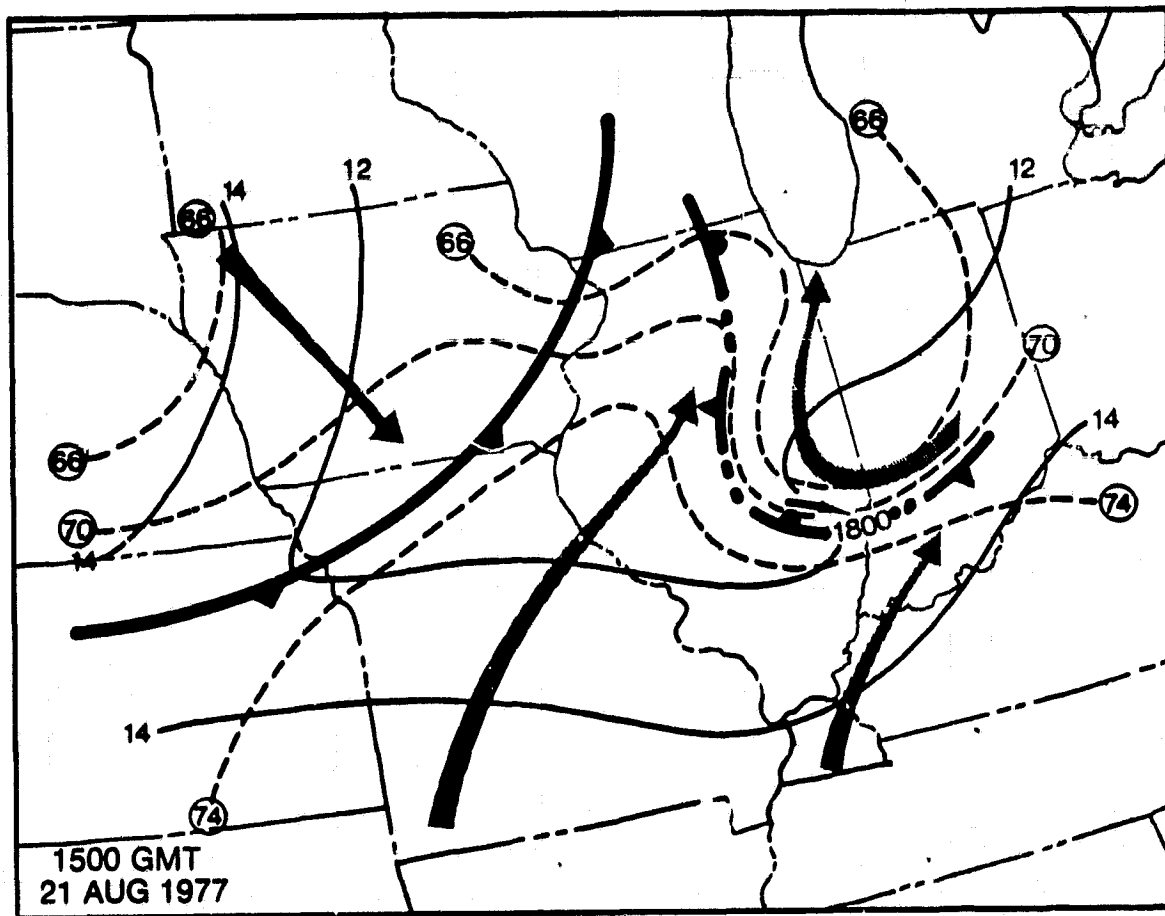


Fig. 1f. Surface mesoanalysis for 1500 GMT, 21 August 1977.
Details as in Figs. 1a and 1b.

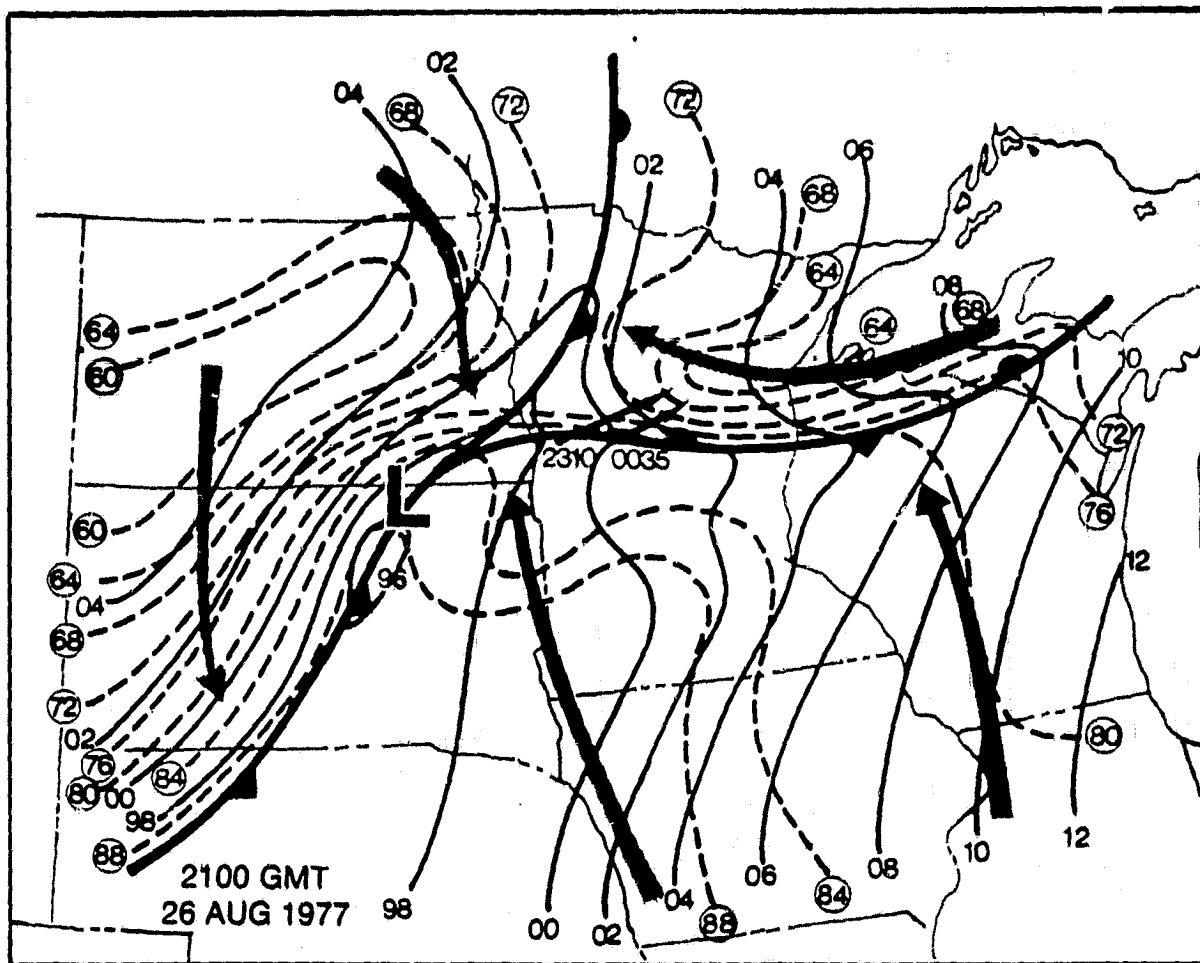


Fig. 1g. Surface mesoanalysis for 2100 GMT, 26 August 1977.
 Details as in Fig. 1a.

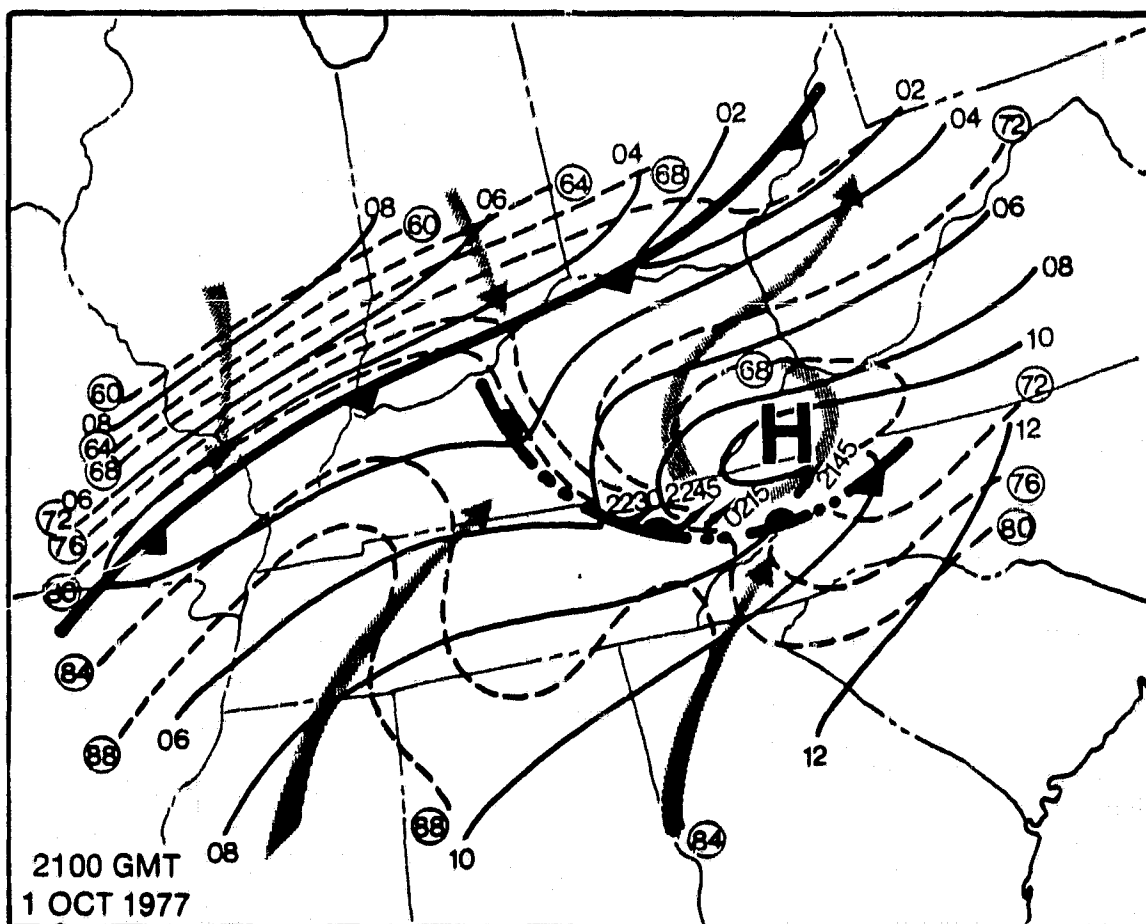


Fig. 1h. Surface mesoanalysis for 2100 GMT, 1 October 1977.
 Details as in Figs. 1a and 1b.

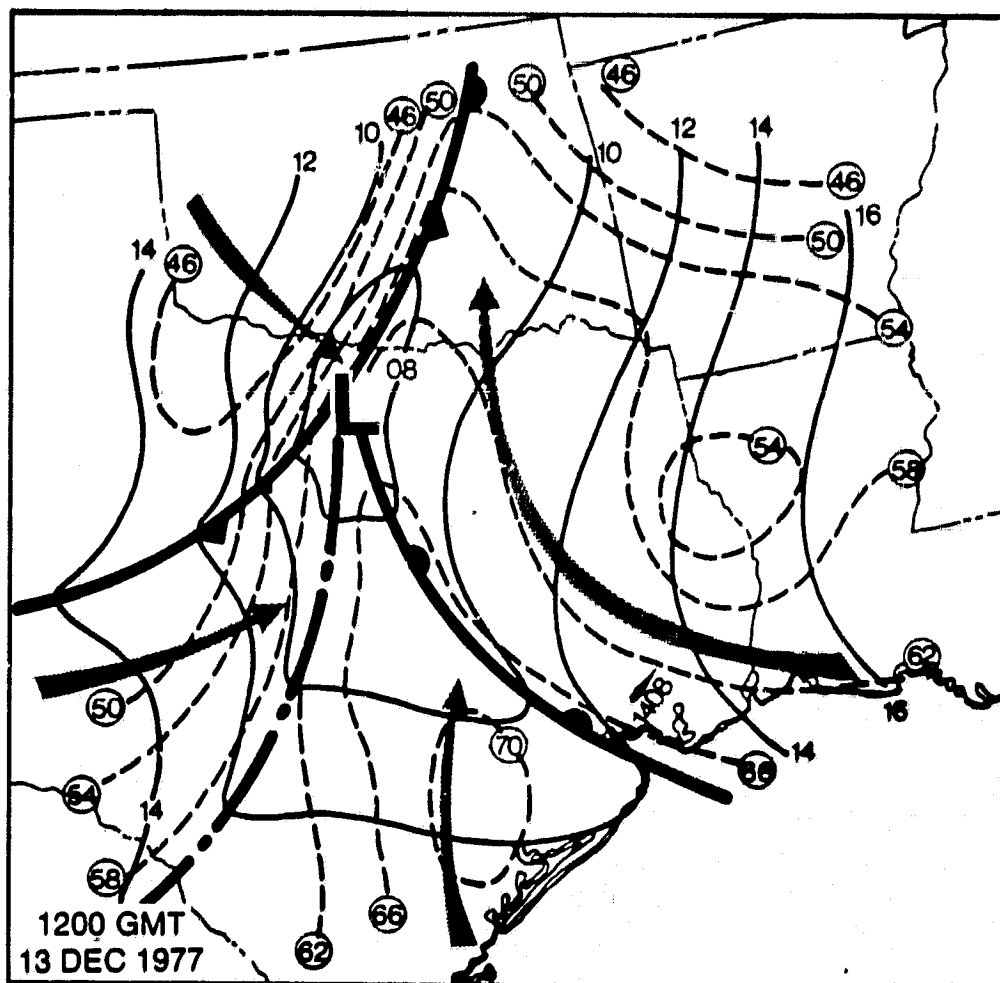


Fig. 1i. Surface mesoanalysis for 1200 GMT, 13 December 1977.
 Details as in Fig. 1a.

and the depth of the boundary layer are highly dependent upon atmospheric stability.

A direct effect of strong low level thermal gradients is a rapidly varying pressure gradient with height. In the case of warm thermal advection the veering of the wind is increased while the reverse is true for cold advection. These modifications of the basic Ekman wind profile have been documented in numerous studies (e.g. Blackadar, 1965; Lettau, 1967; and others). The change of the pressure gradient with height alters the vertical shear from that which would be present in barotropic conditions. Within a turbulent boundary layer the change in shear modifies vertical momentum transports further altering the boundary layer wind profile.

Sheppard et al. (1952) were the first to suggest such modifications. Theoretical studies by Blackadar (1965), Cattle (1971) and Arya and Wyngaard (1975) all suggested that the angle between the observed surface wind and the surface geostrophic wind is increased by low-level cold advection and decreased by warm advection. An extensive observational study by Hoxit (1974) produced similar results. Moreover, Hoxit's results indicated that the surface stress and ageostrophic wind component throughout the boundary layer were a function of the orientation and magnitude of the thermal wind vector relative to the surface geostrophic wind. The net result is that the average boundary layer ageostrophic wind component (directed

toward lower pressure) is greater in cases of cold thermal advection than in warm advection.

A conceptual model of sub-cloud wind profiles near thermal boundaries has been developed using three case studies, time-series of upper-air soundings, instrumented tower data, and the results of the observational and theoretical boundary layer studies cited above. Figure 2 shows a schematic representation of wind profiles for the lowest kilometer in three different air masses. This is a typical meso- α pattern often associated with severe thunderstorms. At point A (within a warm, dry and well-mixed air mass) the wind veers slightly with height and the speed increases slowly. In the hot, moist and conditionally unstable air mass (point B) warm thermal advection and surface friction produce a wind profile that veers and increases in speed with height. At Point C (in a cool, moist thunderstorm outflow region) the cold low-level thermal advection acts to decrease the veering of the winds. Winds at this point have maximum speeds near the surface and veer slowly with height until a transition occurs into the warmer air mass above. Within this cool, moist air mass cross-isobaric flow is often greater than it is within the hot, moist air mass. The Fig. 2 cross-section of wind profiles indicates that the vertical wind profiles are modified in a manner which acts to maximize meso- β scale convergence and cyclonic vorticity (mean for the sub-cloud layer) within a narrow "mixing zone" between points

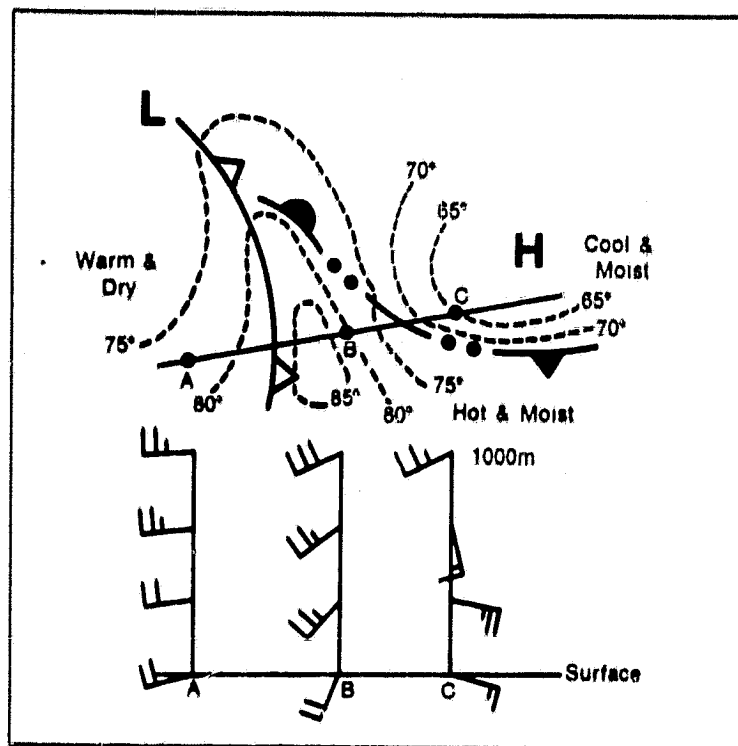


Fig. 2. Schematic representation of boundary layer wind profiles within a typical severe thunderstorm producing surface pattern. Surface features and isotherms ($^{\circ}\text{F}$) are indicated. Full wind barbs are 10 kt.

B and C. Note that between points A and B the mean sub-cloud layer convergence and vorticity are actually smaller in magnitude than they are for the surface winds alone.

The point C profile represents conditions that resulted from prior thunderstorm activity. The thunderstorm produced airmass will typically be meso- β in scale and therefore the

flow regime should not be balanced. However, the field should be evolving toward balanced flow and effects of cold air advection would be present in the vertical wind profiles.

Since precipitation also may play a major role in setting up and maintaining thermal boundaries (especially warm fronts and thunderstorm outflows), evaporation in the vicinity of such boundaries may increase absolute low-level moisture values, and thus produce local areas of enhanced convective instability. This could be especially true if the thermal boundary were retreating slowly northeastward. In this situation the southerly flow in the hot, moist air mass would move across wet terrain as it approached the thermal "mixing zone".

These hypothesized, systematic perturbations in planetary boundary layer wind profiles and moisture contents may, in part, explain why storms often reach maximum intensity and become tornadic as they approach thermal boundaries. Satellite imagery and satellite derived low-level wind fields might, on some occasions, be utilized to locate wind shear zones associated with thermal boundaries (see Maddox and Vonder Haar, 1979).

a. The 27 May 1977 case

NASA conducted an Atmospheric Variability Experiment (AVE) on 27 May 1977 that included a number of additional upper-air soundings over the central United States (see Hill and Turner, 1977 for details of the AVE's). This day was chosen for study because serial soundings were taken at Oklahoma City

and instrumented tower data from NSSL were available. Figure 3 shows a mesoanalysis of surface conditions at 1200 GMT, on 27 May 1977, over Oklahoma and north Texas. Two weak outflow boundaries stretched across Oklahoma from northeast to southwest. These boundaries did not become active again during the afternoon and were not notable except for the special data taken within the cool air outflow region.

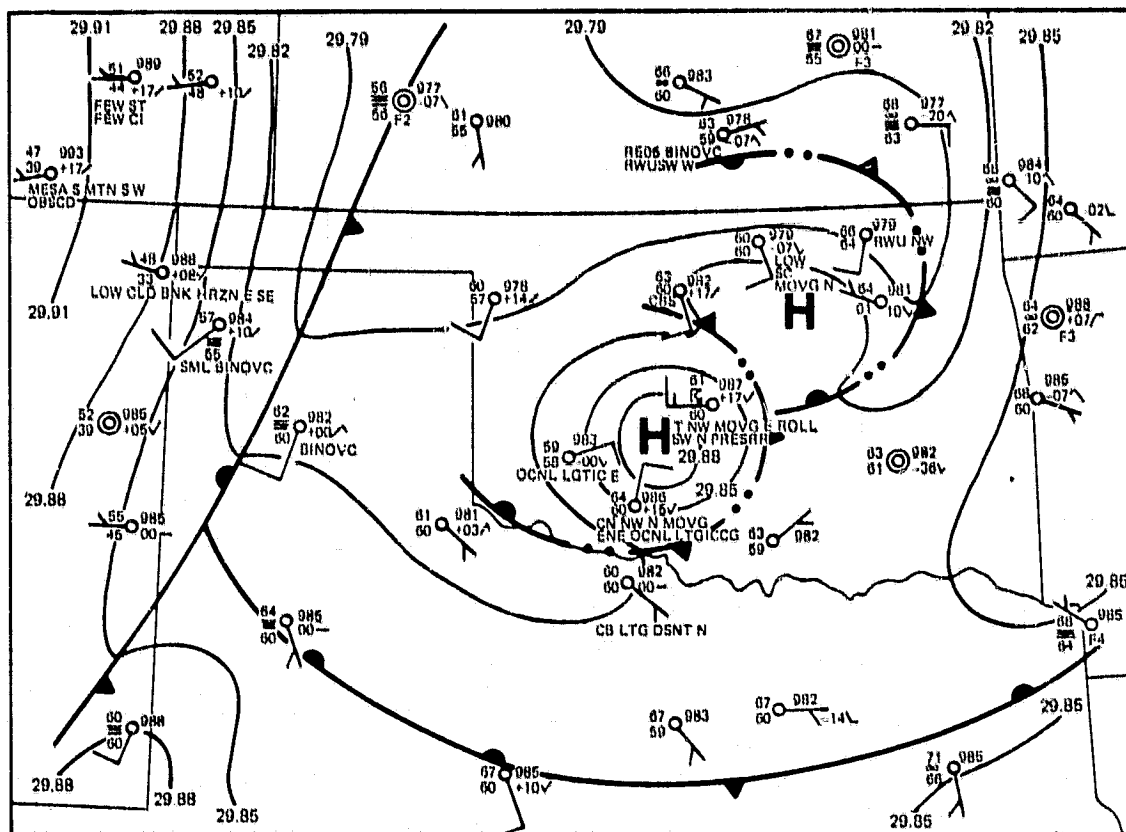


Fig. 3. Surface mesoanalysis for 1200 GMT, 27 May 1977. Pressure analysis is of altimeter setting.

Time series of wind, temperature and wetbulb temperature data from the instrumented NSSL tower (WKY Television Systems 481 m TV transmitting tower located 39 km north of NSSL and 10 km northeast of downtown Oklahoma City) are presented in Fig. 4. The meteorological instrumentation and operation of the tower was explained by Carter (1970). Cool outflow air spread over the tower site between 1200 and 1300 GMT with an inversion persisting until about 1700 GMT. The vertical wind profiles from 1400 GMT on exhibit little veering with height and backing is evident within lower layers from 1330 to 1630 GMT. Tremendous modifications of the thermodynamic structure occur from 1600 to 1700 GMT as surface heating modifies and destroys the cool air dome. Wetbulb temperatures rise rapidly and are quickly mixed through the tower layer (the region with wetbulb temperatures $\geq 16^{\circ}\text{C}$ is shaded).

A time series of the Oklahoma City AVE soundings is shown in Fig. 5. The shallow dome of cool outflow air extended up to about 900 mb (slightly deeper than the layer shown in the Fig. 4 time series). The wind profiles at 1400 and 1730 GMT are very similar to the hypothesized profile for point C on Fig. 2. A rapid change in the thermodynamic structure of the boundary layer between 1600 and 1700 GMT is also indicated by the Oklahoma City data. Of most interest is the rapid increase in moisture and θ_e values that rapidly mix upward to the 825 mb level. At Stephenville, Texas, (approximately 350 km south-

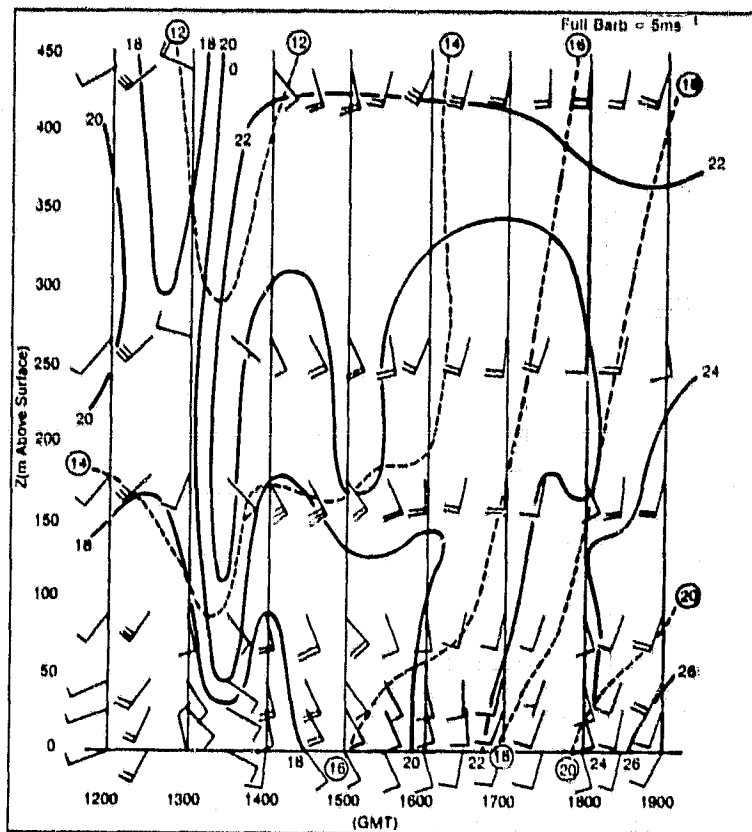


Fig. 4. Time series of observations (60 second averages at the hour and half hour) from the NSSL tower on 27 May 1977. Solid lines are temperature ($^{\circ}\text{C}$); dashed lines are wetbulb temperature ($^{\circ}\text{C}$); and a full wind barb represents 5 m s^{-1} .

southwest of Oklahoma City) AVE soundings that were not affected by thunderstorm outflows were taken deep within the warm, moist

airmass. These soundings indicated a more gradual diurnal modification of a deeper moist layer. At 2100 GMT the mixing ratio values at Oklahoma City exceeded the Stephenville values from the surface to 850 mb. Evaporation of surface moisture left by the morning thunderstorms may be partly responsible for the elevated mixing ratios in the Oklahoma City vicinity.

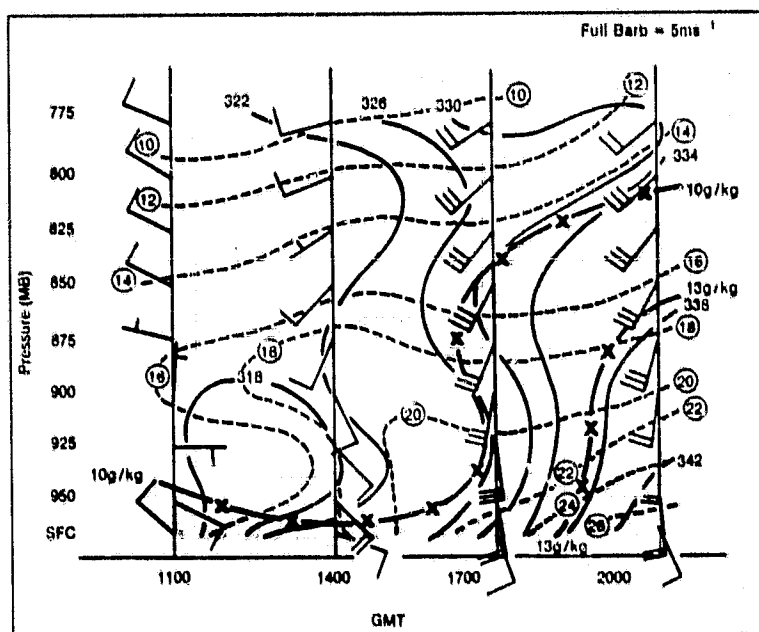


Fig. 5. Time series of upper-air data taken at Oklahoma City on 27 May 1977. Dashed lines are temperature ($^{\circ}\text{C}$); solid lines are θ (K); dash/X lines are mixing ratio; and a full wind barb represents 5 m s^{-1} .

b. The 6 May 1975 (Omaha tornado) case

On 6 May 1975, a number of intense tornadoes occurred in eastern Nebraska along a very strong thermal gradient

associated with a warm front. This day was also a NASA AVE day; however, the experimental area was located south of Nebraska and no sequential soundings were available in the storm area. Hourly surface data, conventional soundings, radar data, and GOES imagery were utilized to study this event. Figures 6 and 7 depict mesoanalyses of surface conditions at

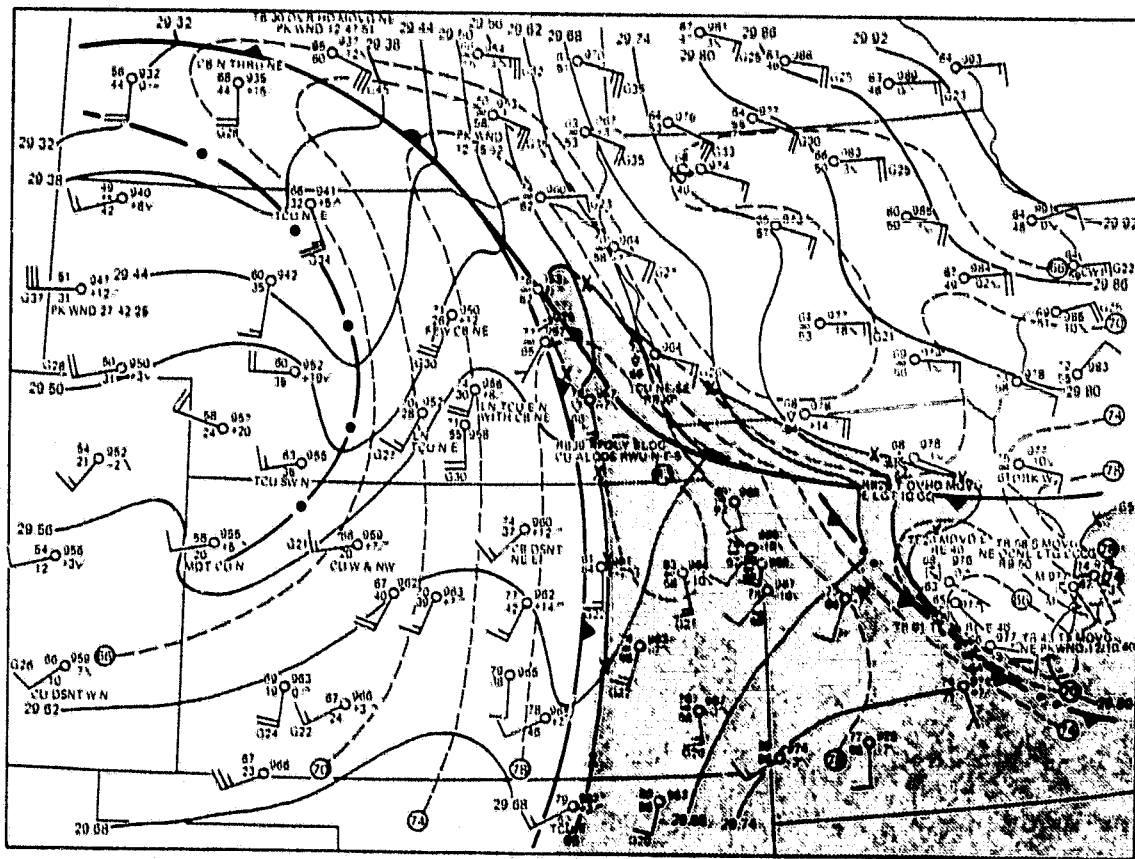


Fig. 6. Surface mesoanalysis for 1800 GMT, 6 May 1975. Solid lines are altimeter setting; dashed lines are 4°F isotherms; and regions with dewpoint temperature $> 65^{\circ}\text{F}$ are shaded.

1800 and 2100 GMT, on 6 May 1975. A Pacific front and occlusion was moving slowly eastward across eastern Kansas and Nebraska. A very slow moving warm front stretched from northeastern Nebraska east-southeastward across northeastern Missouri. There was a strong temperature gradient north of the front that persistent cloudiness and thunderstorm activity in southern Iowa and northern Missouri helped maintain. Another area of active storms remained over central Missouri during the analysis period.

The tornado events are shown on Fig. 7 with their reported times of occurrence. The storms were generally moving across the isotherms and all but one tornado had short tracks. A storm in northeastern Nebraska apparently moved northward almost parallel to the isotherms and produced a long-track tornado. Three of these tornadoes were F3 or greater in intensity. The storms fed upon a very narrow tongue of moist air that had been pulled up into eastern Nebraska. As the cells moved northward over cooler, drier air they weakened and were no longer tornadic. The general surface pattern is similar to that of the model in Fig. 2. The most favorable meso- β scale environment for severe storms should according to the model, lie along the warm front from northeastern Missouri to extreme southeastern South Dakota, which is exactly where the most intense storms occurred. Indeed, radar film from Grand Island, Nebraska, and Des Moines, Iowa, indicated that the cell which spawned the Omaha tornado developed in the warm air sector south-southwest of Omaha. The storm became

tornadoic as it moved across the "mixing zone" over the southwest suburbs of Omaha.

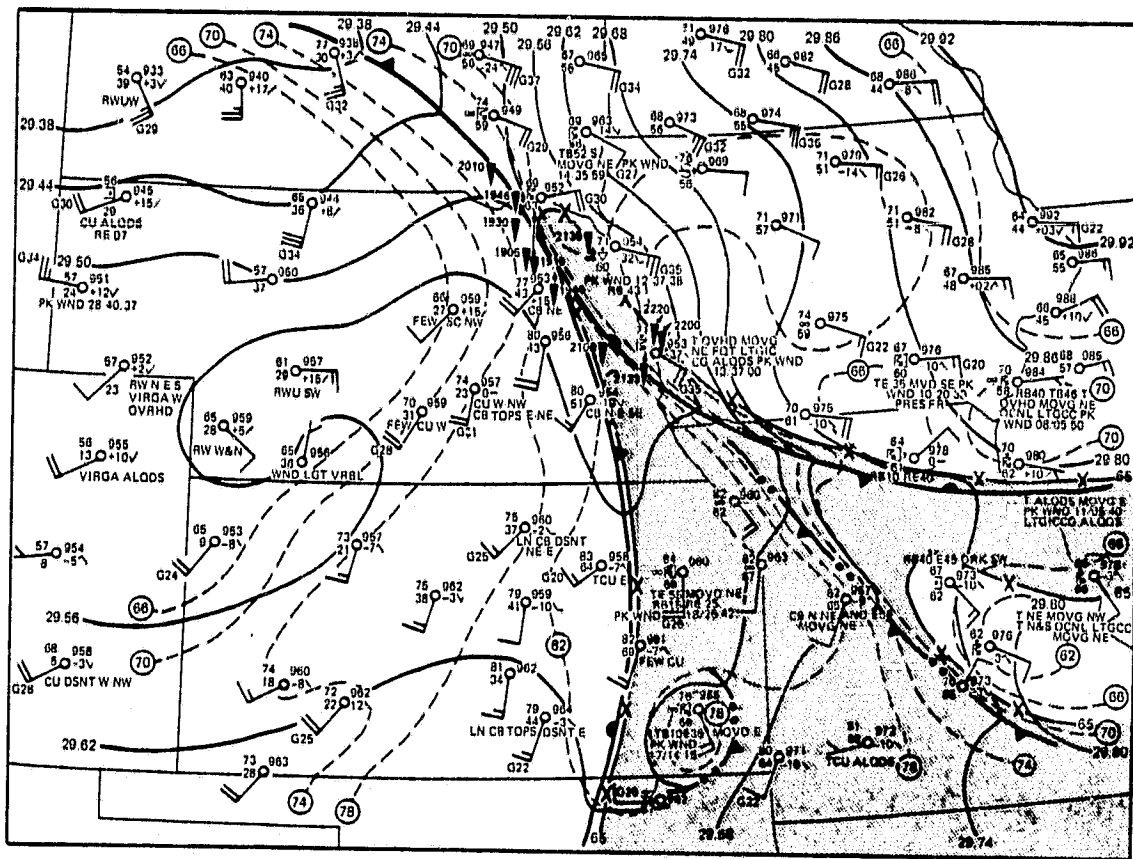


Fig. 7. Surface mesoanalysis for 2100 GMT, 6 May 1975. Tornado events logged at the National Severe Storms Forecast Center are indicated (dark triangles) along with the GMT time of occurrence. Other details are as in Fig. 6.

Figures 8 and 9 present 850 mb and 500 mb analyses for 0000 GMT, 7 May 1975 (approximately two hours after the Omaha tornado). At 850 mb the Pacific front was very weak and is indicated to be dissipating. The surface warm front was shallow with the 850 mb position well to the north. Thus the storms might have remained severe as they moved north-northeastward were it not for the very narrow tongue of warm, moist air that was feeding them. Persistent storms in Missouri and Illinois had generated a mesohigh circulation that was detectable at 850 mb. At 500 mb an intense cutoff low was moving slowly northward over Wyoming. The Pacific front and severe storm outbreak were associated with a weakening short-wave trough that was rotating around the cutoff.

Time series of surface observations for Lincoln and Omaha, Nebraska, are shown in Figs. 10 and 11. (Lincoln is located approximately 90 km southwest of Omaha.) At Lincoln the warm front moved north of the station between 1700 and 1730 GMT. Thunderstorms developed in the warm air sector just west of Lincoln around 1800 GMT. These storms moved northward ahead of the Pacific front which passed Lincoln shortly after 2000 GMT. At the time of the Omaha tornado (2140 GMT) Lincoln reported a temperature of 78°F with a dewpoint of only 45°F and west-southwest winds at 15 knots. Later in the evening the entire system took on the characteristics of a warm occluded system with the cool, moist surface air over Iowa pushing back

westward. The cool air moved westward across Lincoln at about 0200 GMT.

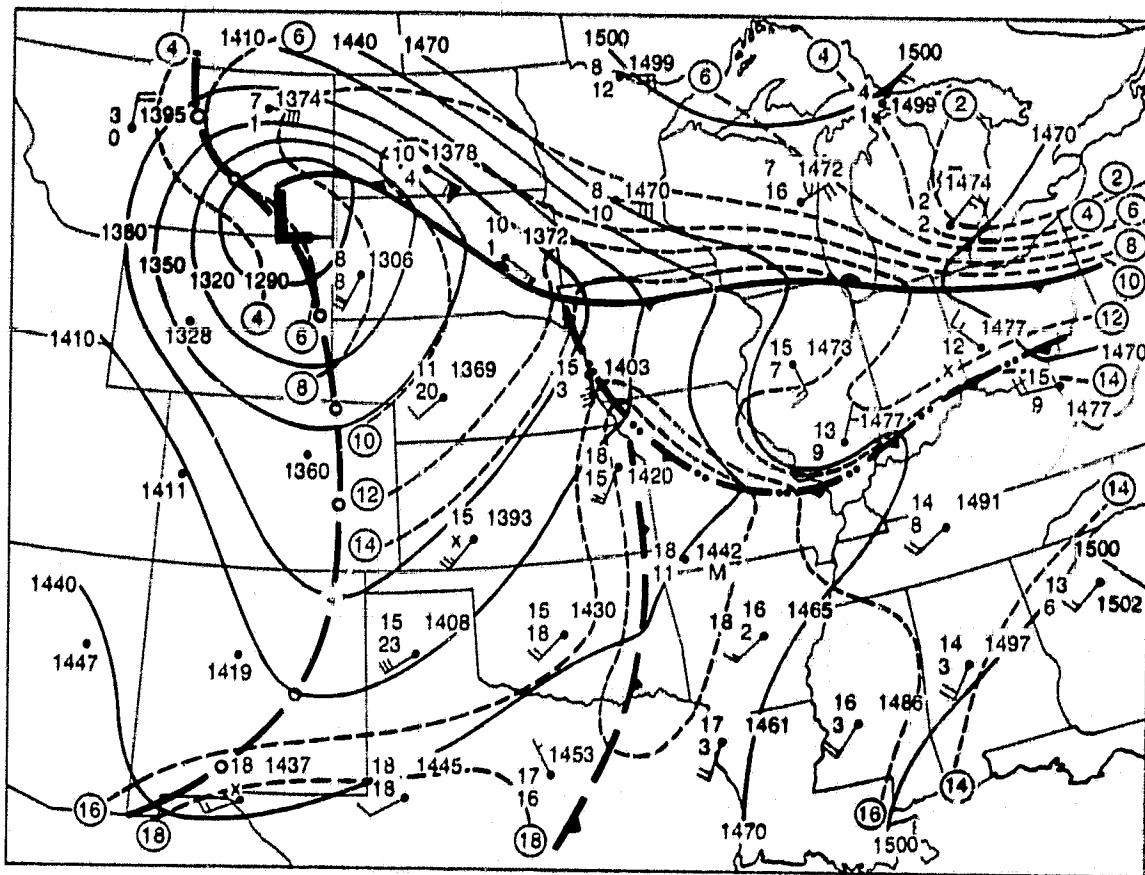


Fig. 8. 850 mb analysis for 0000 GMT, 7 May 1975. Fronts, troughs, and outflow boundaries are indicated, as are 30 m height contours (solid lines) and 2°C isotherms.

The Omaha time series shows that the warm front remained south of Omaha throughout the period and that the Pacific front did not penetrate eastward to Omaha. The region just north of the warm front was characterized by strong and gusty east-southeasterly winds. These winds became very strong as the thunderstorm activity began. Between 2200 and 2300 GMT the surface winds reflect the passage of a small scale cyclonic circulation in which the tornado was apparently embedded. Although the surface pressure fluctuates violently between 2100 and 2300 GMT, the surface temperature and dewpoint remain relatively constant. At the time of the tornadic storm Lincoln is located in about the relative position of point A and Omaha is at about point C as indicated on Fig. 2. Tornadic thunderstorms and severe hailstorms occurred along the strong thermal gradient northeast of the axis of hottest surface temperatures.

c. The 24 April 1975 (Neosho tornado) case

During the NASA AVE IV (see Fucik and Turner, 1975) experiment three to six hourly soundings were taken over much of the eastern 2/3rds of the United States during the period 0000 GMT, 24 April through 1200 GMT, 25 April 1975. An intense tornado (F4) struck Neosho, Missouri, at about 0040 GMT on 25 April 1975. (Neosho is located about 25 km south-southeast of Joplin, Missouri, and about 145 km east-northeast of Tulsa, Oklahoma.) Serial upper-air soundings were taken at Monett,

Missouri (Monett is 40 km east of Neosho), during AVE IV.
 The AVE data were used in conjunction with surface data, radar
 data, and GOES imagery to study this situation.

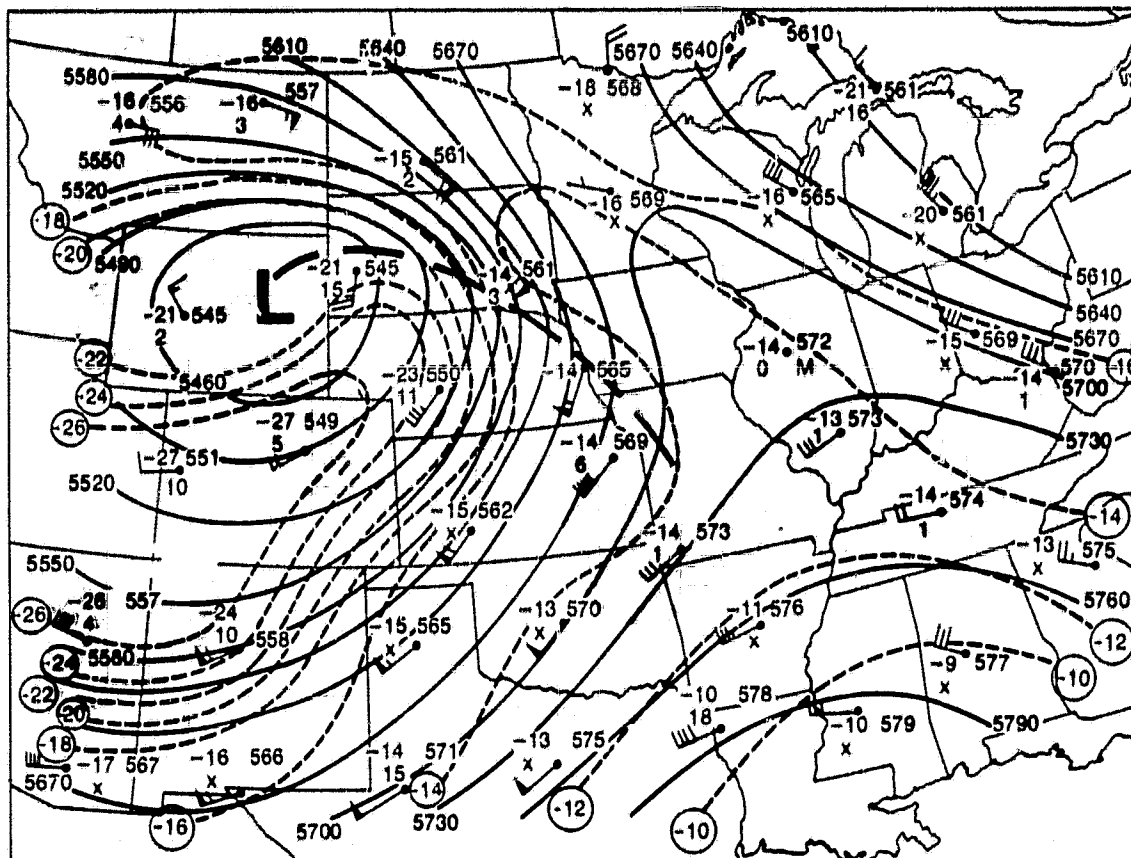


Fig. 9. 500 mb analysis for 0000 GMT, 7 May 1975.
 Short-wave trough position is shown by the
 heavy dashed line with other details as in
 Fig. 8.

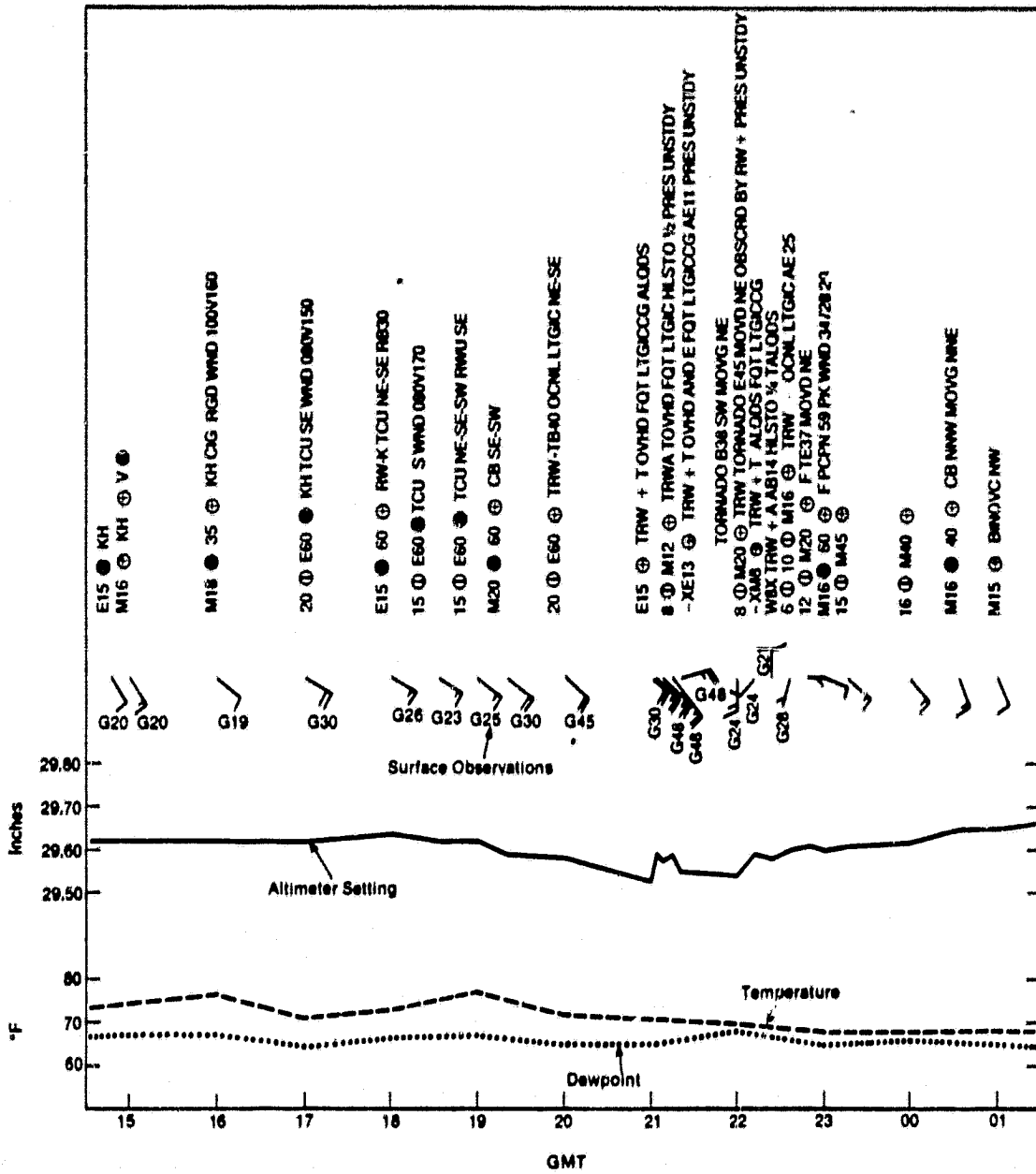


Fig. 11. Time series of surface observations for Omaha, Nebraska, on 6 and 7 May 1975. Details as in Fig. 10.

Mesoscale surface analyses for 2200 GMT, 24 April and 0000 GMT, 25 April 1975, are shown in Figs. 12 and 13. The surface situation was very complex with a number of mesoscale features present at 2200 GMT. The thunderstorm cool air outflow boundary that stretched across northern Arkansas into southeast Kansas and the mesohigh over southern Missouri had both been generated by early morning storm activity that moved from central Missouri into northern Arkansas before it dissipated. A strong temperature gradient was present along the southern and western peripheries of this outflow boundary. A mesolow pressure system was moving southeastward along the Oklahoma/Kansas border. Very warm surface temperatures were noted near the center of this mesolow and a tongue of very dry air had been pulled across central Oklahoma into its circulation. Very moist conditions were indicated by the band of 65°F plus dewpoints east and south of the mesolow. Dewpoints were high along the western edge of the outflow boundary.

A mesohigh/low pressure couplet and another outflow boundary were located southeast of Kansas City. These features were associated with a severe thunderstorm that was producing large hail. A slow moving, large scale frontal system curved from the Texas panhandle northeastward across central Illinois. Thunderstorm cells were rapidly developing in Oklahoma in the warm, moist air mass southeast of Oklahoma City, and southeast and northeast of Tulsa (indicated on GOES photo but not shown).

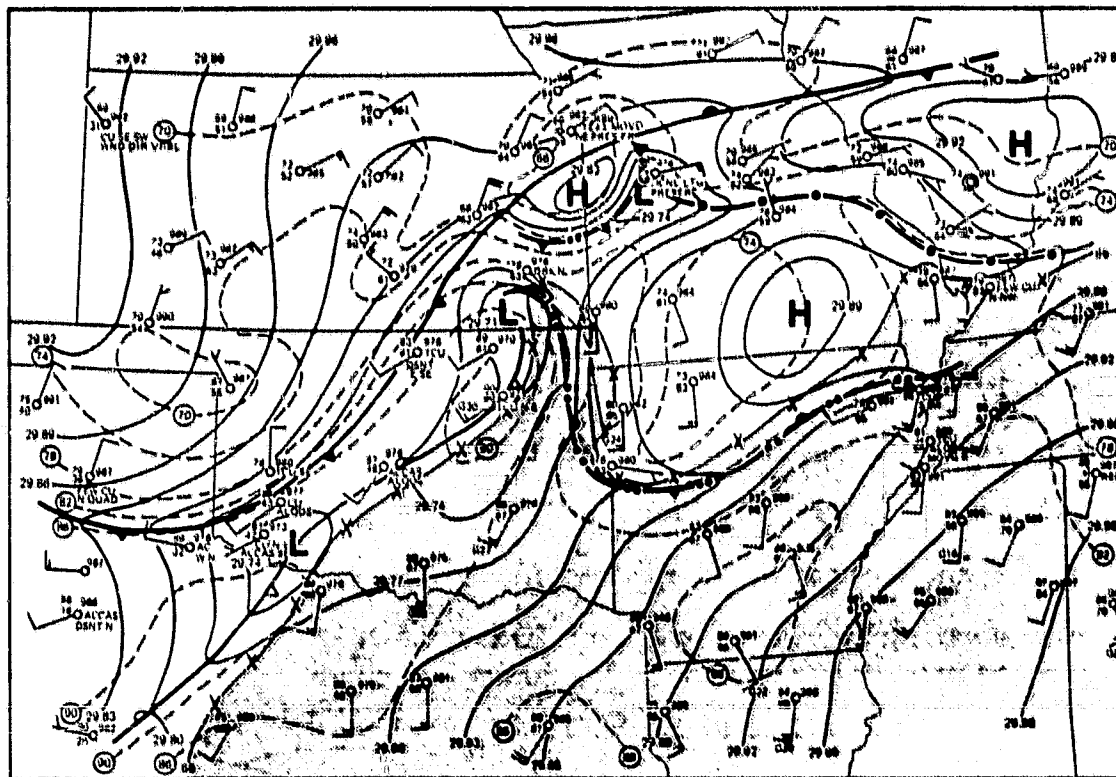


Fig. 12. Surface mesoanalysis for 2200 GMT, 24 April 1975. Pressure analysis (solid lines) is of altimeter setting; isotherms (dashed lines) are shown for 4°F intervals; and the region where dewpoints were $\geq 65^{\circ}\text{F}$ is shaded.

By 0000 GMT the large scale front had pushed south over central and western Oklahoma pinching off the narrow dry tongue, and a large, severe hailstorm was in progress south and east of Oklahoma City. Two important mesolows were present, one in central Missouri and one between Joplin and Tulsa. A tornadic storm was in progress near Miami, Oklahoma, east-

northeast of one of the mesolow centers. This storm produced the Neosho tornado a few minutes later as it moved eastward across the thermal boundary zone. Neither tornado had a long track. The outflow boundary moving down from the north may also have been interacting with the tornadic cell by the time of the Neosho event. The two thermal boundary tornadoes were the only two reported during the afternoon and evening although there were many severe thunderstorms reported over eastern Oklahoma, southern Missouri and western Arkansas. Several funnels and tornadoes were reported during the late night and early morning hours in eastern Arkansas and Tennessee.

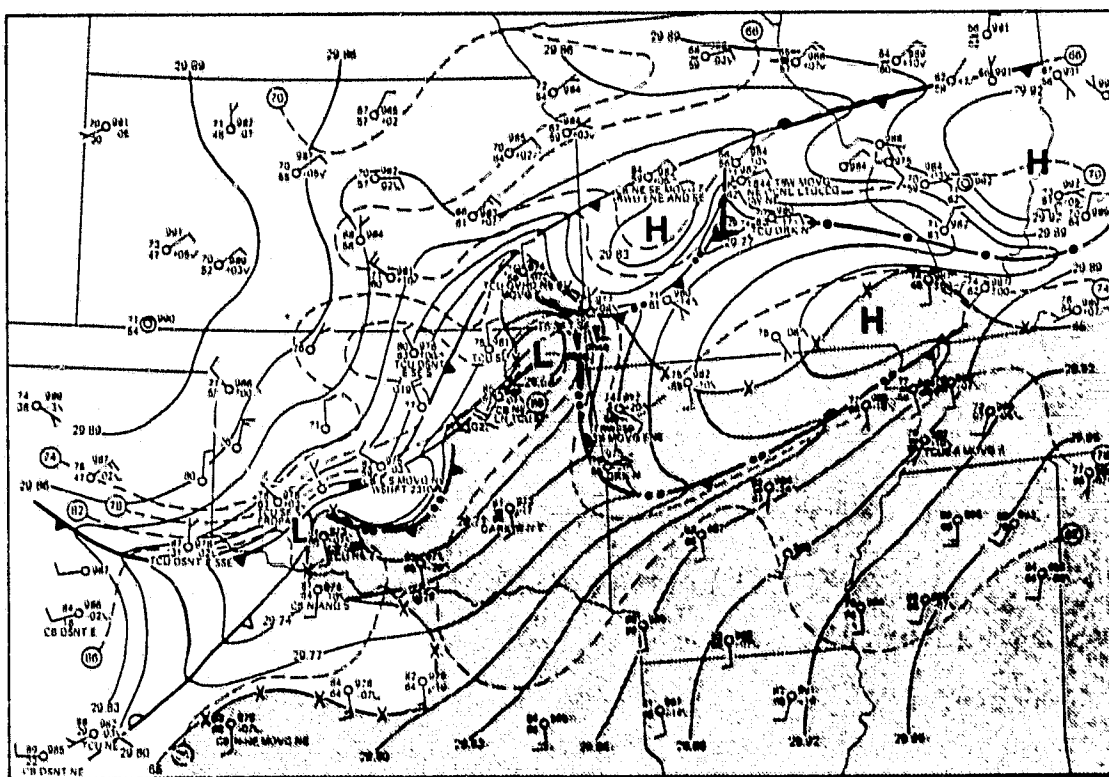


Fig. 13. Surface mesoanalysis for 0000 GMT, 25 April 1975, with details as in Fig. 12.

Analyses for 850 and 500 mb are presented in Figs. 14 and 15 for 2100 GMT, 24 April 1975, approximately three hours prior to the tornadoes. Radar echoes from the 2035 GMT radar summary chart have been superposed upon the analyses. At 850 mb a cyclonic circulation was located over south central Kansas and the dry-line and large scale front were detectable. The outflow air over southern Missouri and northern Arkansas was shallow with a south-southwesterly flow of warm, moist 850 mb air overriding the cool surface air. A stationary, thunderstorm generated thermal boundary stretched eastward from central Missouri. At 500 mb one weak short-wave trough was moving eastward over the Ohio Valley while an intensifying short-wave was moving across the Central Plains. A broad area of shower and thunderstorm activity was associated with the eastern trough and a number of storms were developing along and ahead of the western trough.

Time series of the surface conditions at Ponca City, Oklahoma (located approximately 125 km west-northwest of Tulsa), Tulsa, Oklahoma, and Joplin, Missouri, are presented in Figs. 16, 17, and 18. (At 2100 GMT Ponca City, Tulsa, and Joplin were located at about points A, B, and C on Fig. 2.) At Ponca City winds became westerly and the relative humidity decreased from 1500 to 2100 GMT while the station was within the tongue of dry air. The synoptic scale front pushed south of Ponca City about 2300 GMT and cooler, very moist air moved over the

station. At Tulsa very strong and gusty southwesterly winds were reported during the early morning hours. The thunderstorm outflow boundary appears to have moved just south of Tulsa between 1500 and 1800 GMT. After 1900 GMT winds became southerly

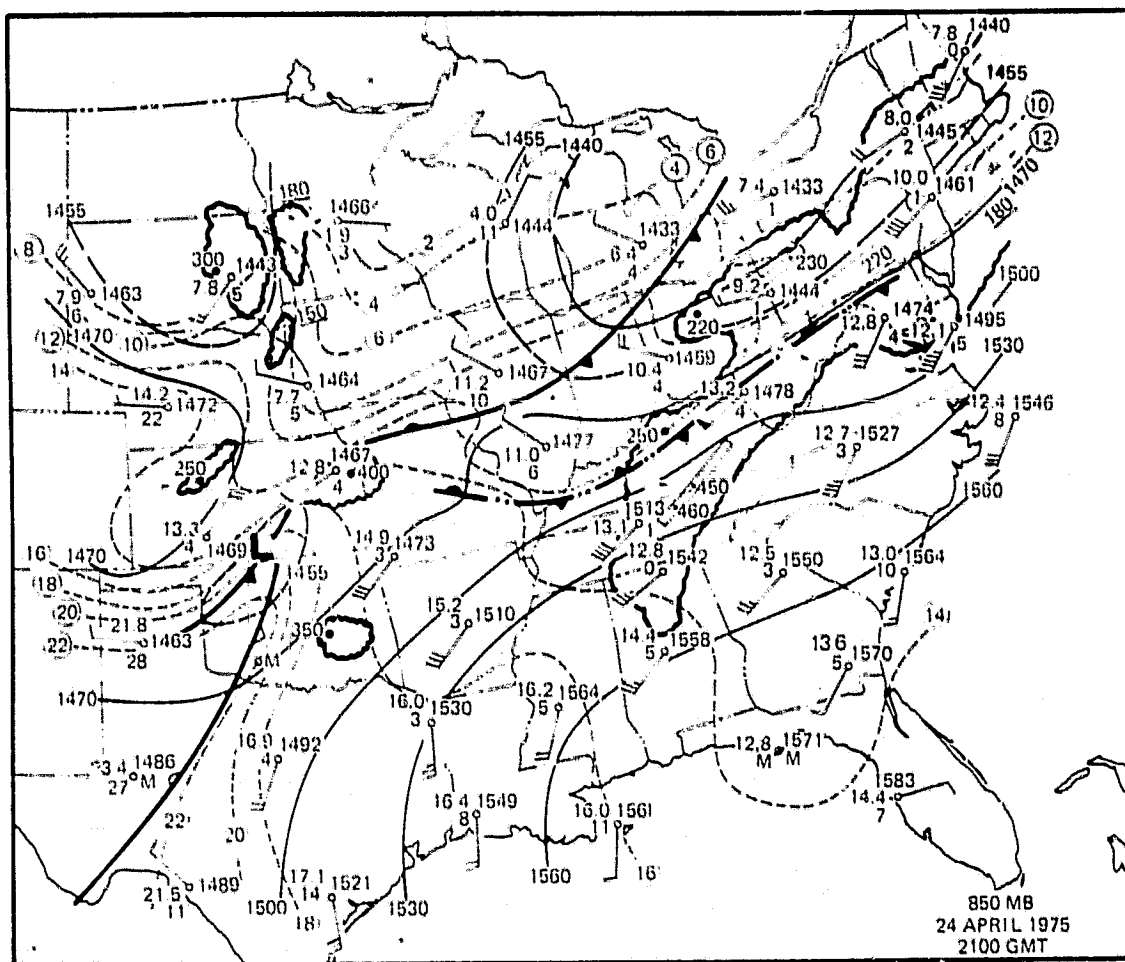


Fig. 14. 850 mb analysis for 2100 GMT, 24 April 1975. Frontal boundaries and thunderstorm outflow boundaries are shown, as are 2°C isotherms (dashed), 30 m height contours (solid), and 2035 GMT radar echoes (shaded).

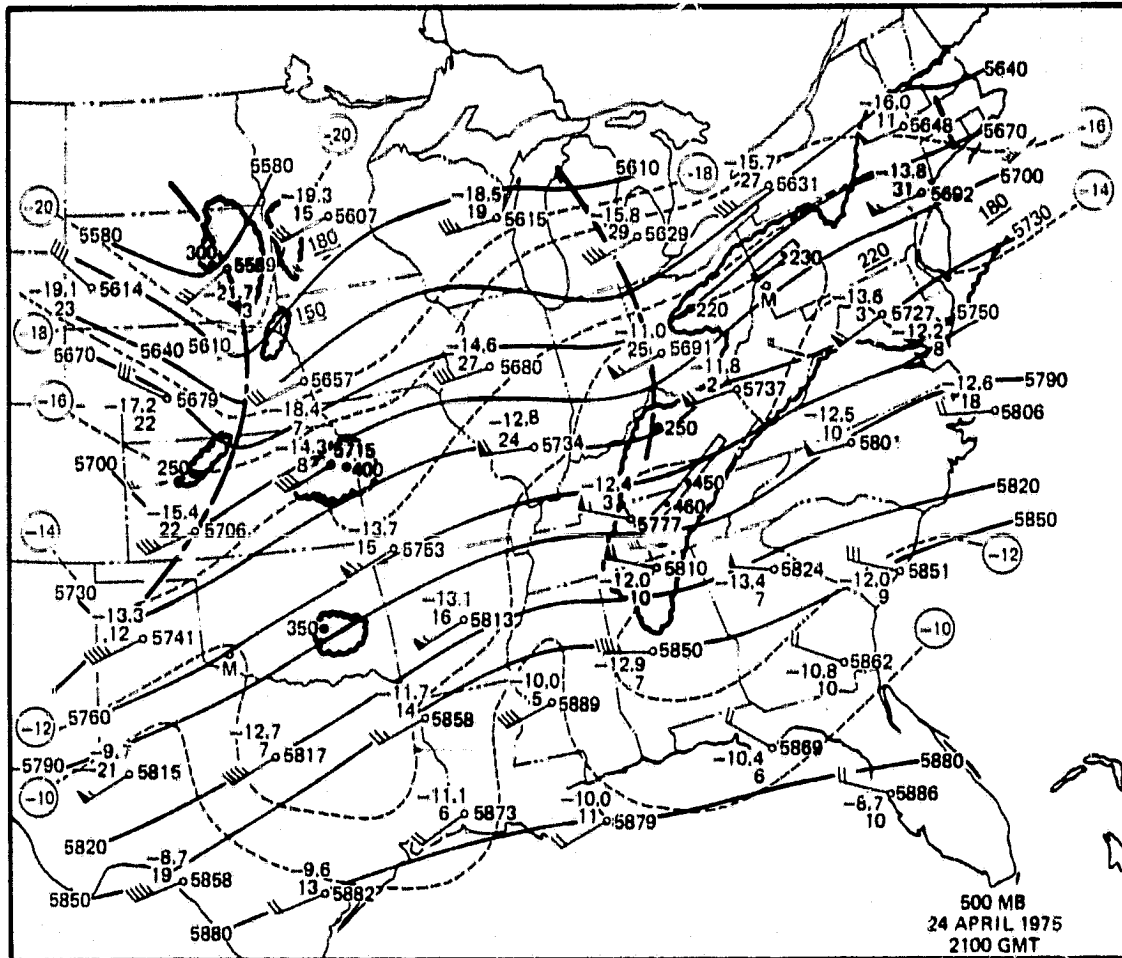


Fig. 15. 500 mb analysis for 2100 GMT, 24 April 1975. Short-wave troughs are shown as heavy dashed lines with other details as in Fig. 14.

and then southwesterly and increased in speed. The relative humidity decreased markedly between 2100 and 2300 GMT as the

station was under the influence of the dry tongue. The synoptic scale cold front did not pass Tulsa until after 0500 GMT on the 25th. The Joplin time series shows the influence of several mesoscale features. During the early morning hours the jump in surface pressure and the abrupt drop in surface temperature occurred shortly after 1000 GMT as the thunderstorm outflow boundary moved past the station. The temperature remained quite cool until about 1600 GMT when the low cloud deck dissipated. After this time the surface temperature and

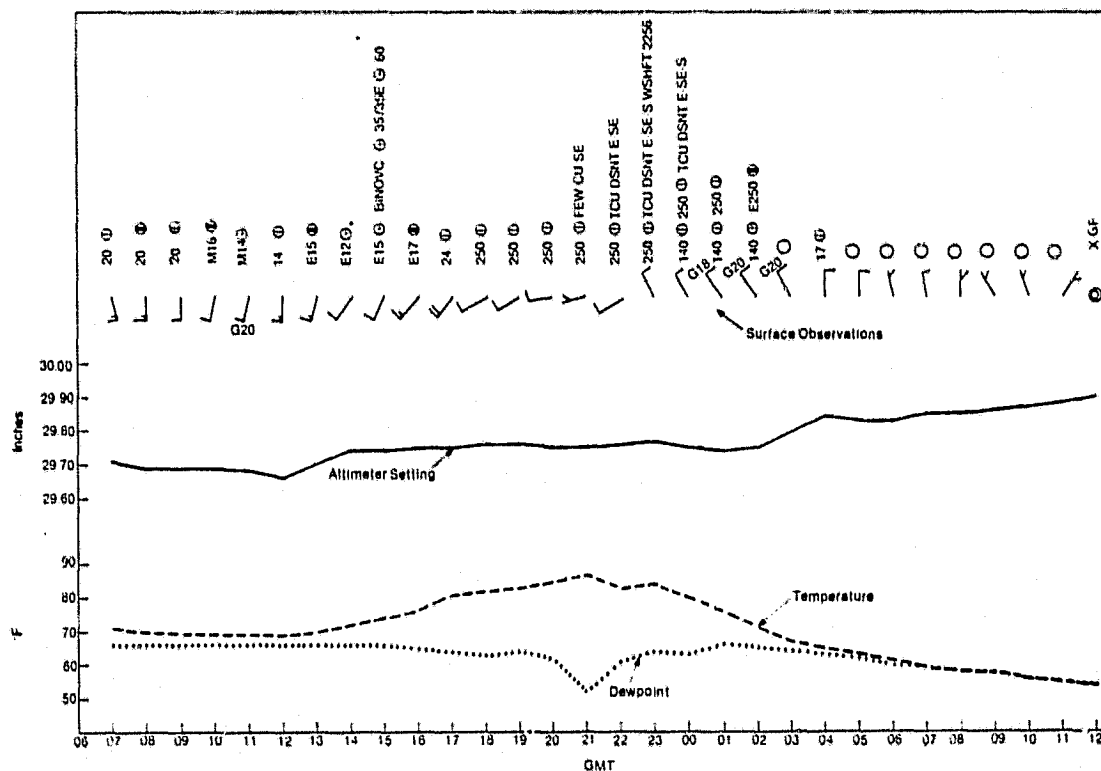


Fig. 16. Surface observation time series for Ponca City, Oklahoma, on 24 and 25 April 1975.

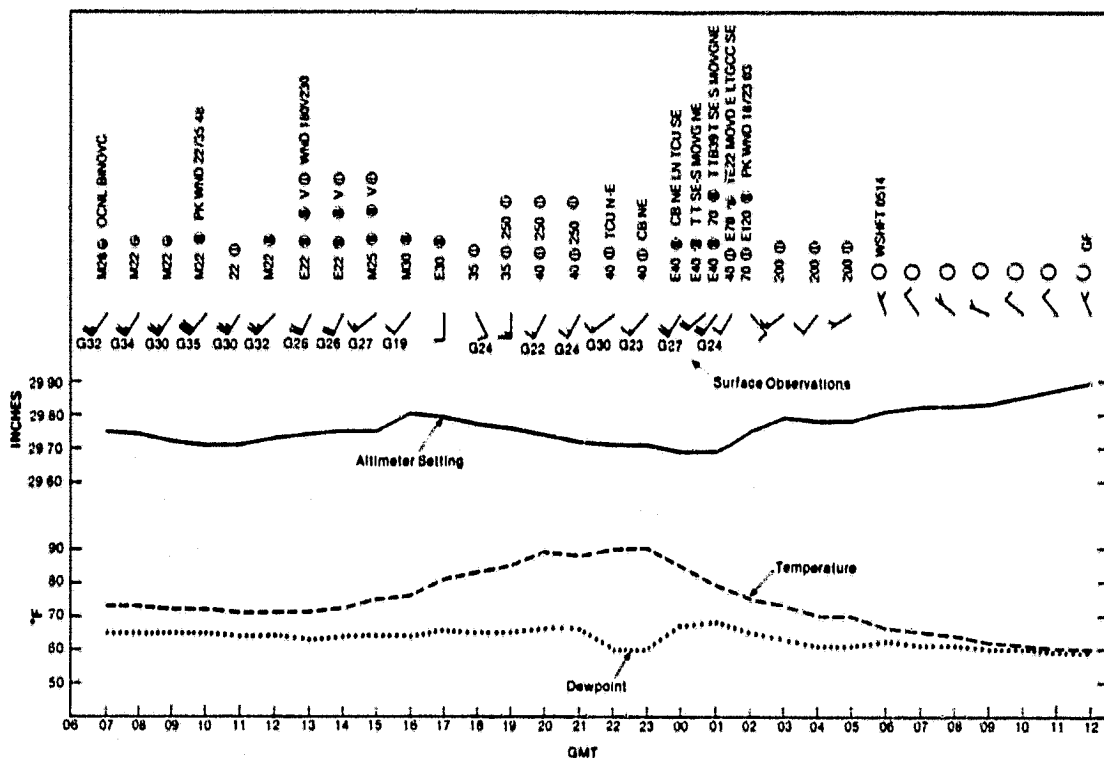


Fig. 17. Surface observation time series for Tulsa, Oklahoma, on 24 and 25 April 1975.

the dewpoint increased slowly as surface heating modified the cool air dome. Until 2300 GMT the surface wind slowly veered and decreased in speed as the mesohigh and attendant pressure gradient weakened. At 2300 GMT the temperature at Tulsa was more than 10°F warmer than the temperature at Joplin. After this time the winds shifted to the east as the outflow boundary from the north eased over the station and thunderstorms began to develop in the area. Between 0000 and 0200 GMT the pressure dropped rapidly and then increased slowly as the tornado cyclone passed to the south of the station. The temperature fell slowly during the period of pressure fluctuations and the wind speed never exceeded 10 kt.

similar to the point C profile shown in Fig. 2. After 1900 GMT the boundary layer air mass modifies very rapidly as θ_e increases and mixes quickly upward. The surface temperature increases slowly (1800 to 2315 change of $\sim + 5^\circ\text{C}$) while θ_e

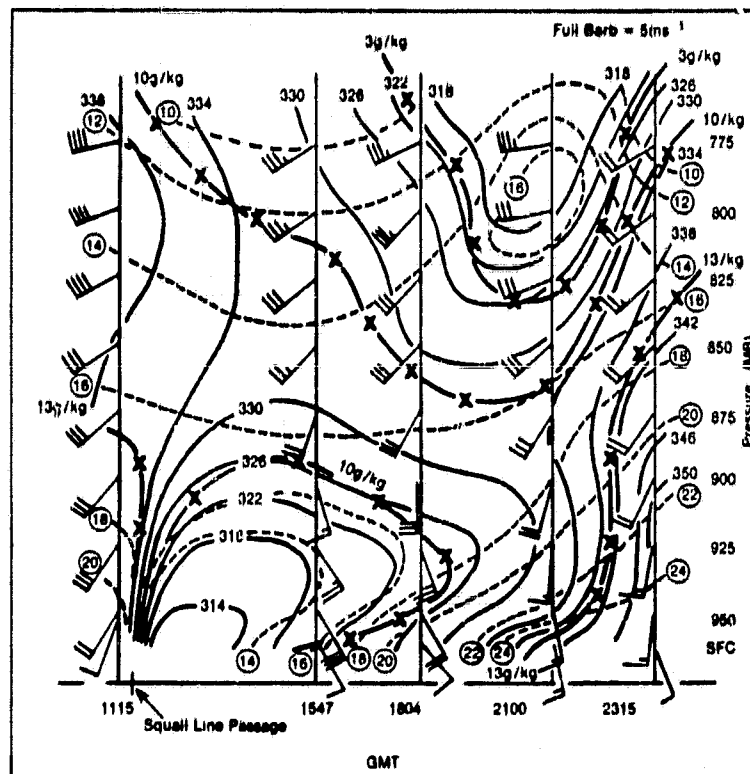


Fig. 19. Upper-air time series for Monett, Missouri, on 24 April 1975. Isotherms (dashed) are shown for 2°C intervals; θ_e (K) is analyzed in solid lines for 4K intervals; mixing ratio lines (dash/X) are shown for selected values, with the region of mixing ratio $> 10\text{g/kg}$ shaded and the region of $< 3\text{g/kg}$ lightly hatched; and winds are in m s^{-1} with a full barb equal to 5 m s^{-1} .

at the surface jumps dramatically (1800 to 2315 change of $\nu + 22K$). These changes are very similar to those shown for the 27 May Oklahoma case. The dramatic change in θ_e is, in large part, due to rapid increases in the local mixing ratio. Table 1 shows mean values of θ_e for the 950-900 mb layer for a number of stations.

Table 1. Mean value of θ_e (K) for the 950 - 900 mb layer

	Topeka Kansas	Ft. Sill Oklahoma	Stephenville Texas	Monett Missouri	Little Rock Arkansas	Shreveport Louisiana
2100 GMT	325	334*	336	332	333	336
0000 GMT	322	345	339	349	337	338

*1900 GMT value

The tremendous increase in θ_e at Monett may, in part, be due to the effects of very warm air moving across the damp terrain south-southwest of the station.

3. ANALYSES OF SURFACE DATA AND CONCURRENT GOES IMAGERY

A number of researchers have related surface thermodynamic and kinematic fields to the development of severe thunderstorms (e.g. Hudson, 1971; Newman, 1972; Sasaski, 1973; Doswell, 1977; and Barnes, 1978a). Other investigators have utilized satellite data sets to diagnose the severe thunderstorm environment.

Peslen (1977) and Houghton and Lee (1977) computed kinematic

fields using winds derived from tracking clouds in satellite imagery. Negri et al. (1977) used satellite derived winds and satellite sounder precipitable water values to estimate moisture divergence. Adler and Fenn (1977) utilized IR cloud temperature to relate the rate of expansion of cold cloud tops to severe storm events. Purdom (1976) combined satellite data and surface observations to refine subjective mesoanalyses and Maddox et al. (1977) combined objective analyses of satellite derived winds and surface mixing ratio to estimate moisture divergence. It was surmised that important insights into storm severity might be gained by simply co-mapping gridded analyses of surface parameters and GOES imagery.

Barnes (1978b) suggested that a tornado cyclone's ability to produce vortices in the friction layer depended upon ambient vorticity exceeding a threshold of 10^{-3} s^{-1} on scales of about 25 km. Although features on such small scales are not detectable in routine surface data, it was hypothesized that analyses of meso- β scale ambient vorticity fields might indicate the likelihood of the vorticity threshold being reached at smaller scales. To investigate this hypothesis the vorticity equation was rewritten retaining only the terms (divergence and advection) that may be computed using surface winds:

$$\frac{\partial \xi}{\partial t} = -(\xi + f) \nabla \cdot \mathbf{V} - \mathbf{V} \cdot \nabla (\xi + f). \quad (1)$$

The observed vorticity is $(\xi + f)$ and the time it would take the mesoscale environment to spin up to 10^{-3} s^{-1} , due to divergence and advection (with $\frac{\partial \xi}{\partial t}$ assumed invariant), was called the Vorticity Time Parameter (VTP), given by:

$$\text{VTP} = \frac{10^{-3} - (\xi + f)}{-(\xi + f) \nabla \cdot \mathbf{V} - \mathbf{V} \cdot \nabla (\xi + f)} \text{ s.} \quad (2)$$

Although the mesoscale environment (on scales resolved by surface observations) certainly won't spin up to 10^{-3} s^{-1} , relatively smaller values of VTP (negative values are not allowed) may indicate that mesoscale ambient conditions are more favorable for the occurrence of intense tornadic storms.

This hypothesis was investigated for the Omaha and Neosha tornado situations. The surface observations were extracted from WBAN-10 forms and analyzed using an objective analysis scheme developed by Barnes (1964 and 1973). The analysis response for the examples shown retained > 80% of the amplitude of waves longer than 200 km. (A detailed explanation of the analysis procedure is presented in Appendix I.)

GOES images for 1800 and 2000 GMT, 6 May 1975, are shown in Figs. 20 and 21. Corresponding surface mesoanalyses and contoured values of the VTP have been mapped onto the satellite images. At 1800 GMT the favorable VTP region stretches along the frontal zone from southern Nebraska into central South Dakota. Several thunderstorms are developing in this zone from east central Nebraska into extreme southern South Dakota.

The VTP analysis indicates that these cells should be monitored for the next 1 to 2 hours. This is valuable "nowcast" information since strong storms are also indicated over Iowa, Missouri, Kansas, and Oklahoma.

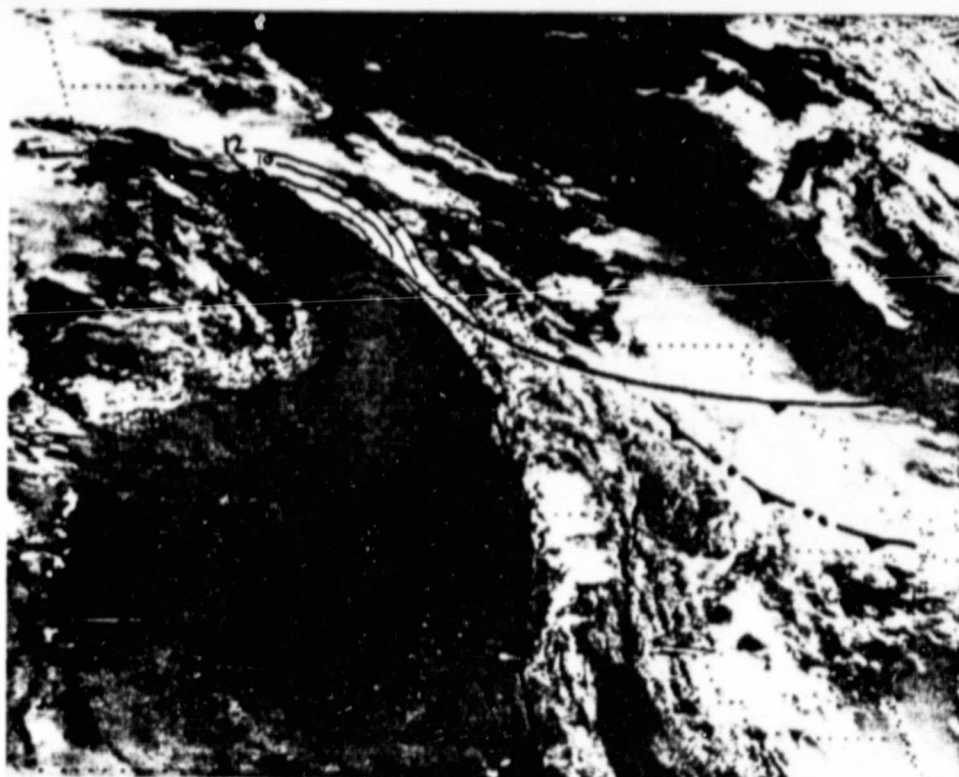


Fig. 20. GOES full resolution, visible image for 1800 GMT, 6 May 1975. Surface features and VTP contours (values of 12×10^4 s and less) have been superposed upon the image.



Fig. 21. GOES full resolution, visible image for 2000 GMT, 6 May 1975. Details as in Fig. 20.

At 2000 GMT the VTP pattern had split and showed two very favorable regions. One favorable area existed behind the surface front in a region where very dry air was being pulled into the low pressure circulation. No thunderstorms existed in this dry zone and the thunderstorms in southeast South Dakota were moving away from this favorable VTP region and into increasingly deeper low-level cold air. A second favorable VTP area was indicated along the Missouri River in eastern Nebraska. Several strong thunderstorms are indicated in the region and these would be the storms of concern for the next 1 to 2 hours. Indeed a check of the tornado locations

and times shown on Fig. 7 shows that the VTP analyses, when used with the GOES imagery, accurately specified the regions of tornadic activity.

GOES images for 2100 and 2300 GMT, 24 April 1975, are presented in Figs. 22 and 23. At 2100 GMT there was a small region of favorable VTP associated with the mesolow circulation in southeast Kansas. There were no thunderstorms indicated in, or near to, this area. The location of the tongue of hot, dry air over central Oklahoma is quite apparent in the image. By 2300 GMT the VTP values had decreased dramatically in the vicinity of the mesolow circulation. One large storm was almost centered within the favorable VTP region while two smaller cells were located on the peripheries of the region.

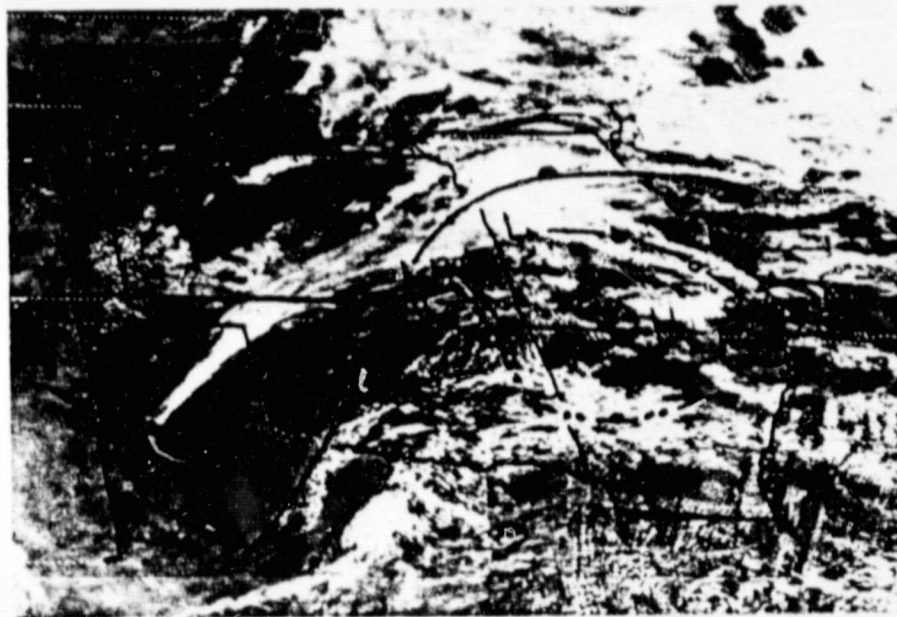


Fig. 22. GOES full resolution, visible image for 2100 GMT, 24 April 1975. Details as in Fig. 20.

The large cell spawned the Miami and Neosho tornadoes an hour and an hour and forty minutes later. Once again the combination of VTP and GOES imagery provides a valuable nowcast tool since the visual appearances of storms over southern Oklahoma and northern Missouri were more impressive than that of the tornadic storm.

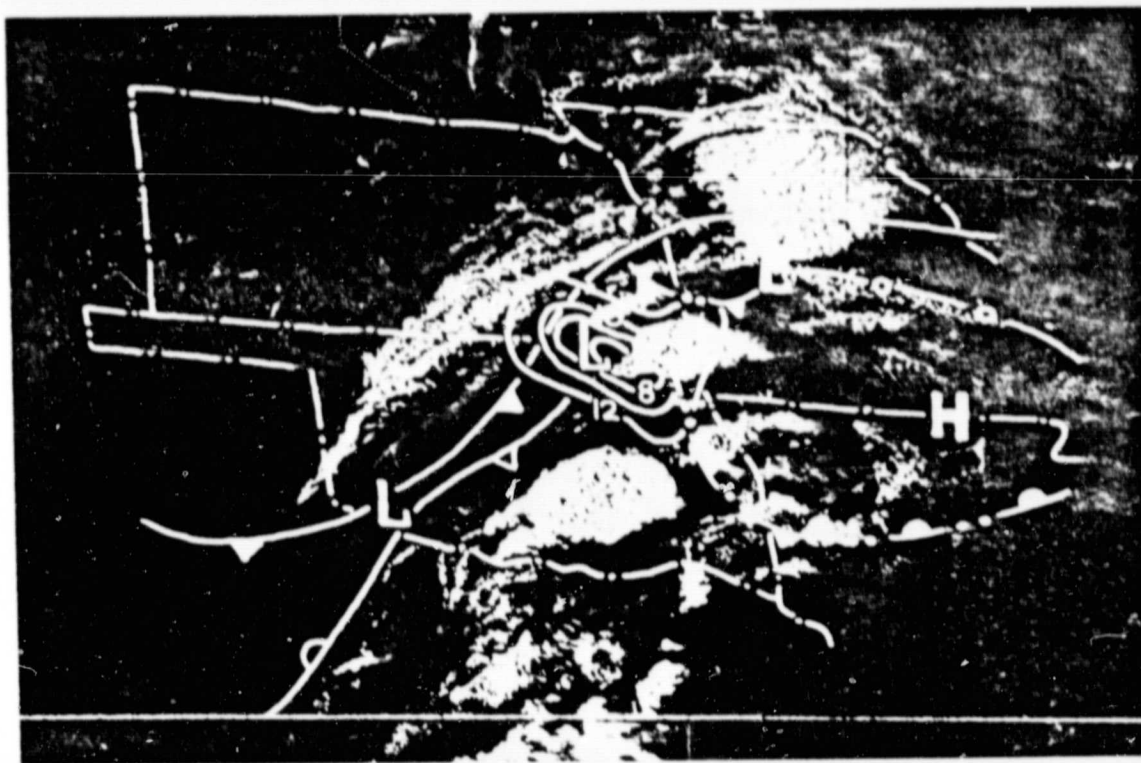


Fig. 23. GOES full resolution, visible image for 2300 GMT, 24 April 1975. Details as in Fig. 20.

Although only two cases have been examined, the results are encouraging and indicate that fields derived from conventional observations might be used in conjunction with satellite data to specify regions where the threat of intense tornadic storms is maximum. The nowcast forecasting and warning applications could be quite valuable once such a technique is tested and refined for a variety of tornado situations. An interactive data processing and analysis system, such as AOIPS, would be necessary to compute, analyze, contour, and display these types of data blends in a real time mode.

4. CONVECTIVE MODIFICATIONS OF THE ENVIRONMENT

The preceding two sections have considered ways in which the near environment acts to control the intensity and evolution of convective storms. This section presents results documenting the life cycle of mesoscale pressure systems and relates these features to thermodynamic feedbacks that were produced by convective storm complexes. Many of the findings are from a detailed case study of a major severe thunderstorm outbreak that utilized satellite, radar, surface, and conventional upper-air data along with a set of special 1800 GMT sounding data.

a. The 4 April 1977 (Birmingham tornado) case

On 4 April 1977, a major outbreak of severe weather occurred over the southeastern United States. Twenty-two tornadoes were reported including one of F5 intensity at

Birmingham, Alabama, that killed 22 people while inflicting tremendous damage. An intense storm, with associated large hail and tornadic activity, was partly responsible for the crash of Southern Airways Flight 242 in northern Georgia and the deaths of 71 persons. Special 1800 GMT rawinsonde data were taken over the southeast U.S. as part of a SESAME '77 experiment (see Kreitzberg, 1977). These soundings were used in conjunction with surface observations, radar data, and GOES imagery to prepare detailed analyses of the meteorological conditions associated with the event. Miller (1978) has also analyzed this particular severe storm situation.

Mesoanalyses of surface conditions over the Southeast are presented for the period 1200 GMT, 4 April to 0000 GMT, 5 April 1977, along with selected satellite images, in Figs. 24a through 24i. Analyses of mesoscale pressure perturbations (large scale pressure subjectively estimated from time series data and then subtracted from the observed pressure) are on the 1200, 1500, 1800, 2100 and 0000 GMT charts. At 1200 GMT (Fig. 24a) considerable thunderstorm activity was already in progress, especially over Tennessee and Mississippi. A mesolow pressure center was located over northwestern Mississippi and a squall-line trailed southwestward into eastern Louisiana. The thunderstorm activity was occurring well to the east of the synoptic scale cold front that was just pushing into western Arkansas. Moist (dewpoints $\geq 65^{\circ}\text{F}$) southerly flow was indicated

from the Gulf Coast northward to Tennessee. As the day progressed the thunderstorm outflow boundary over western Mississippi moved slowly eastward. A series of mesoscale pressure systems developed along this boundary and moved rapidly northeastward. Most of the reported tornadoes were associated with these mesolows. The tornado events are indicated on the surface charts with their reported times of occurrence. During the afternoon mesoscale pressure perturbations of $-.10$ to $-.20$ inches (4-8 mb) existed along the leading edge of the severe convection. By middle to late afternoon the mesohigh pressure area to the rear of the major squall-line became stronger with surface pressure perturbations in excess of $+0.04$ inches (~ 2 mb).

By 1800 GMT (Fig. 24b) several tornadoes had occurred with the mesolow center that was moving northeastward over northwestern Alabama. Strong and gusty southerly flow was indicated in Mississippi, Alabama, and Georgia to the south and east of the squall-line. All of the significant convective storms continued to occur well in advance of the synoptic scale cold front. At 1800 GMT (Fig. 24c) a major mesolow pressure area was present in eastern Mississippi with pressure perturbations as great as -0.20 inches indicated. The first mesoscale low pressure center had moved to northeastern Alabama with two tornadoes reported in this region between 1800 and 1900 GMT. Pressures were reported to be falling

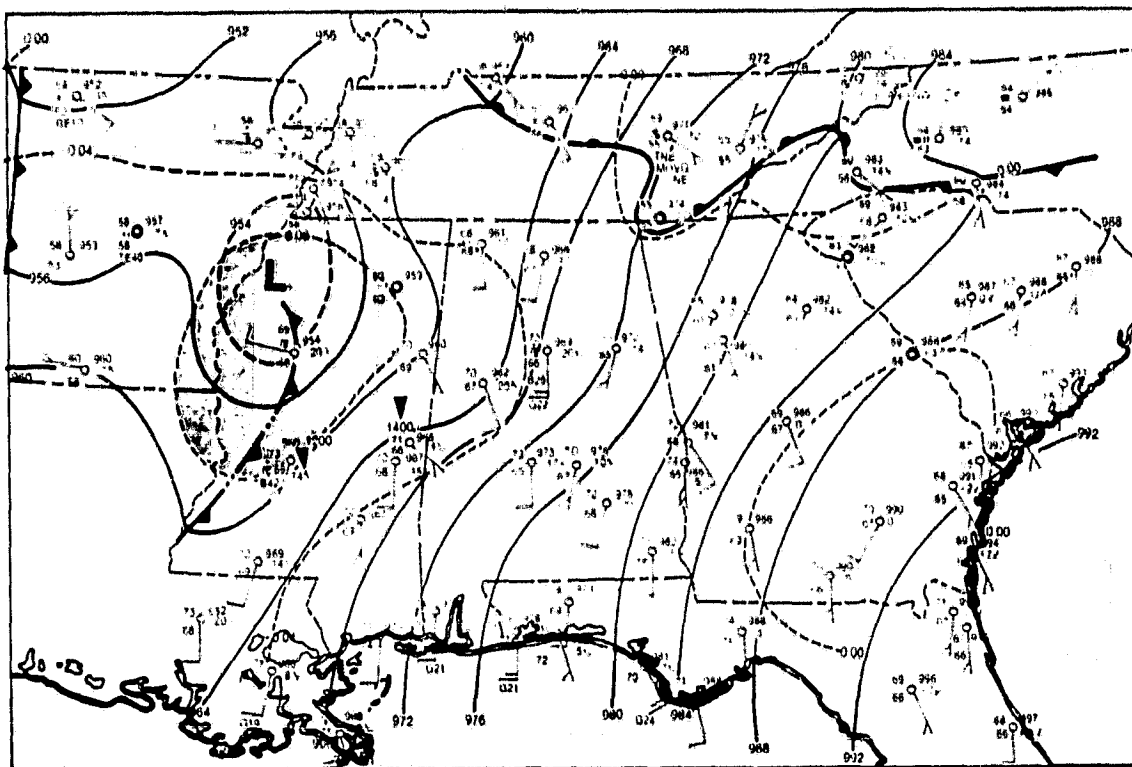


Fig. 24a. Surface mesoanalysis for 1200 GMT, 4 April 1977. Pressure analysis (of altimeter settings), fronts, trough lines, and thunderstorm outflow boundaries are solid black lines. Analyses of mesoscale pressure perturbations (dashed lines) are shown with areas of < -0.08 inches shaded and areas of $> +0.04$ cross-hatched. Tornado events logged at The National Severe Storms Forecast Center are indicated (shaded triangles) along with the GMT time of occurrence.

rapidly at many stations in Alabama, northern Florida and western Georgia. There was a marked temperature contrast across the squall-line with mid-eighties reported over southeastern Alabama compared with upper-sixties temperatures over northeastern Alabama. A concurrent GOES visible image

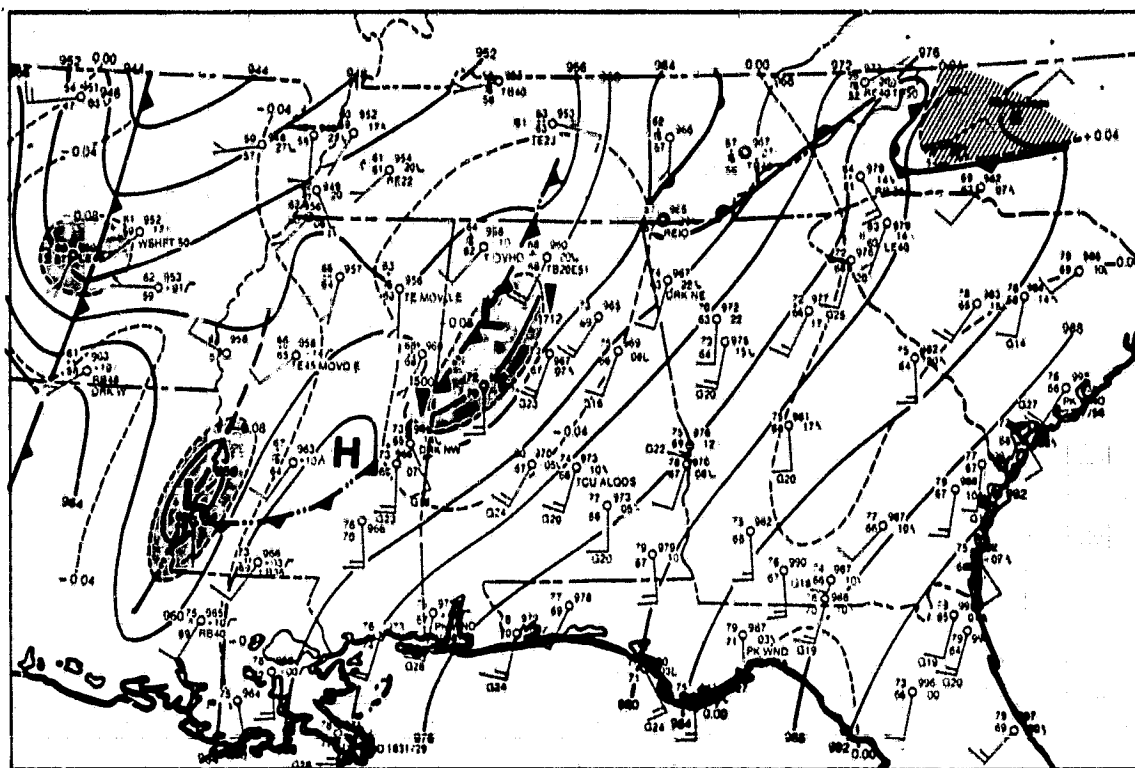


Fig. 24b. Surface mesoanalysis for 1500 GMT, 4 April 1977.
 Details as in Fig. 24a.

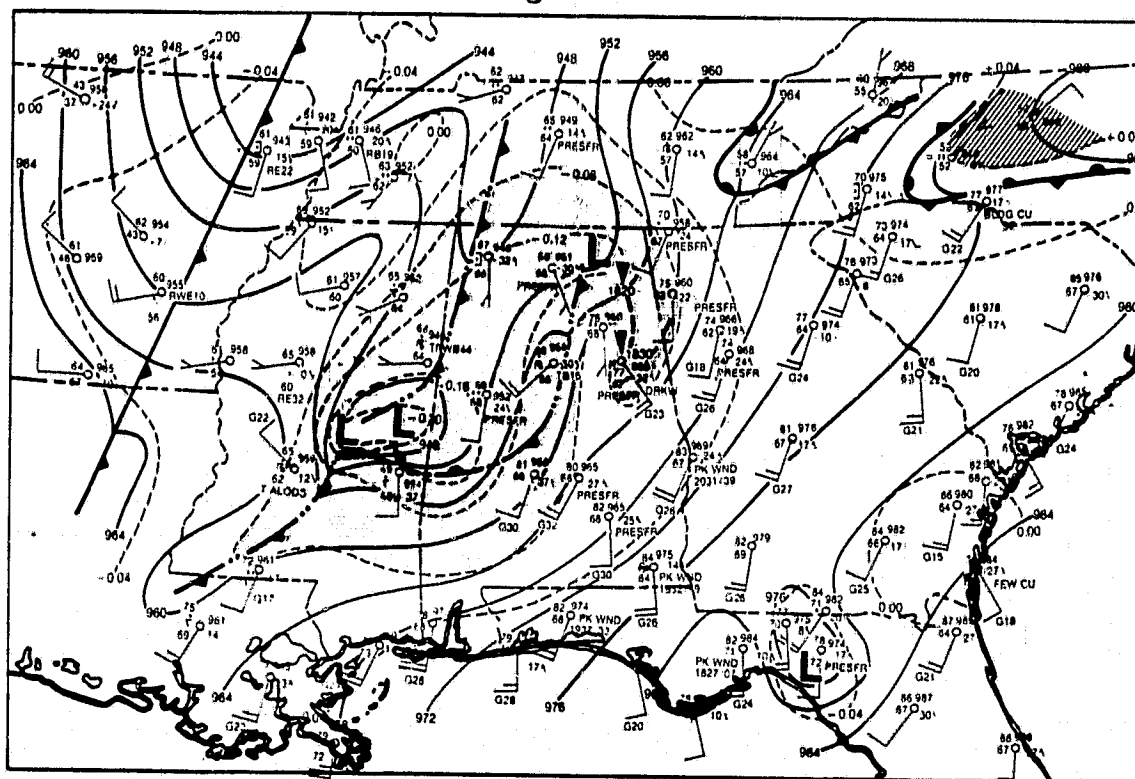


Fig. 24c. Surface mesoanalysis for 1800 GMT, 4 April 1977.
 Details as in Fig. 24a.

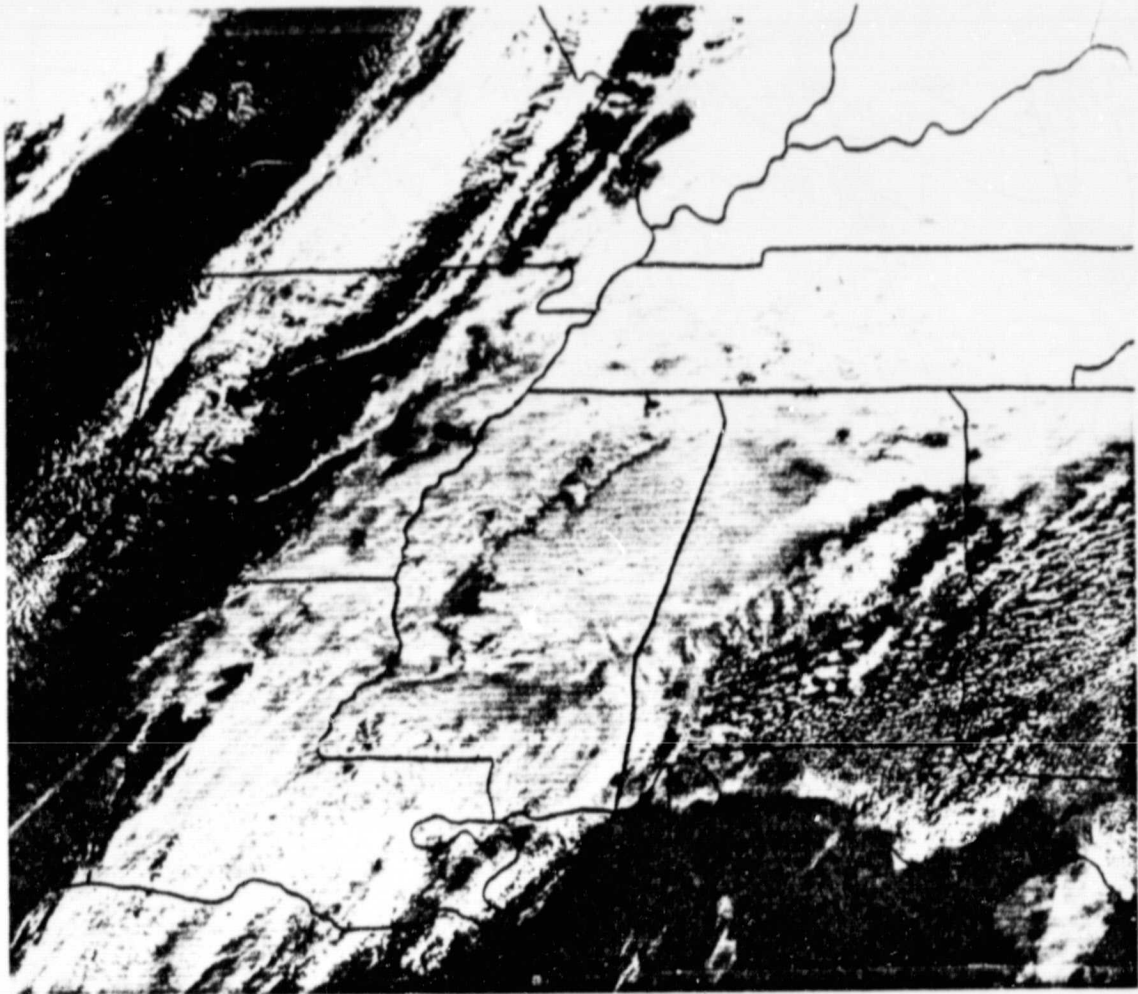


Fig. 24d. Full resolution GOES visible image for 1800 GMT,
4 April 1977.

is shown in Fig. 24d. The mesolow in eastern Mississippi was located on the southern edge of a large complex of storms; however, the low pressure perturbations over northern Alabama appeared to be located in a region of suppressed convection beneath thin cirrus anvil cloud.

Around 1800 GMT two separate mesolow pressure centers developed within the low pressure region over eastern Mississippi. Figures 24e, f, and g indicate that both of these mesoscale pressure systems moved northeastward at 60 to 65 kt! Indeed, Miller (1978) reported that radar cell motions for the severe storms on this afternoon averaged about 63 kt. The leading center became the second mesolow pressure system to cross north-central Alabama. This center was located near Tuscaloosa, Alabama, at 1900 GMT; just northeast of Birmingham by 2000 GMT; and slightly southwest of Rome, Georgia, by 2100 GMT. (Tuscaloosa is located approximately 100 km west-southwest of Birmingham and Rome is about 100 km northwest of Atlanta.) The trailing system moved along a similar path about one hour later.

Both mesolows were tornadic at 2100 GMT (Fig. 24g) with one located near Birmingham and the other just southwest of Rome. The region of rapidly falling surface pressures was located to the east and northeast of these mesosystems. A strong temperature gradient was associated with the squall-line and very strong and gusty southerly flow was indicated in the warm air mass. A concurrent satellite photograph of the thunderstorm activity is shown in Figure 24h. The mesolows were associated with intense storms characterized by multiple overshooting tops. The high tops seem to indicate a double wave structure in Alabama and Georgia with one wave crest

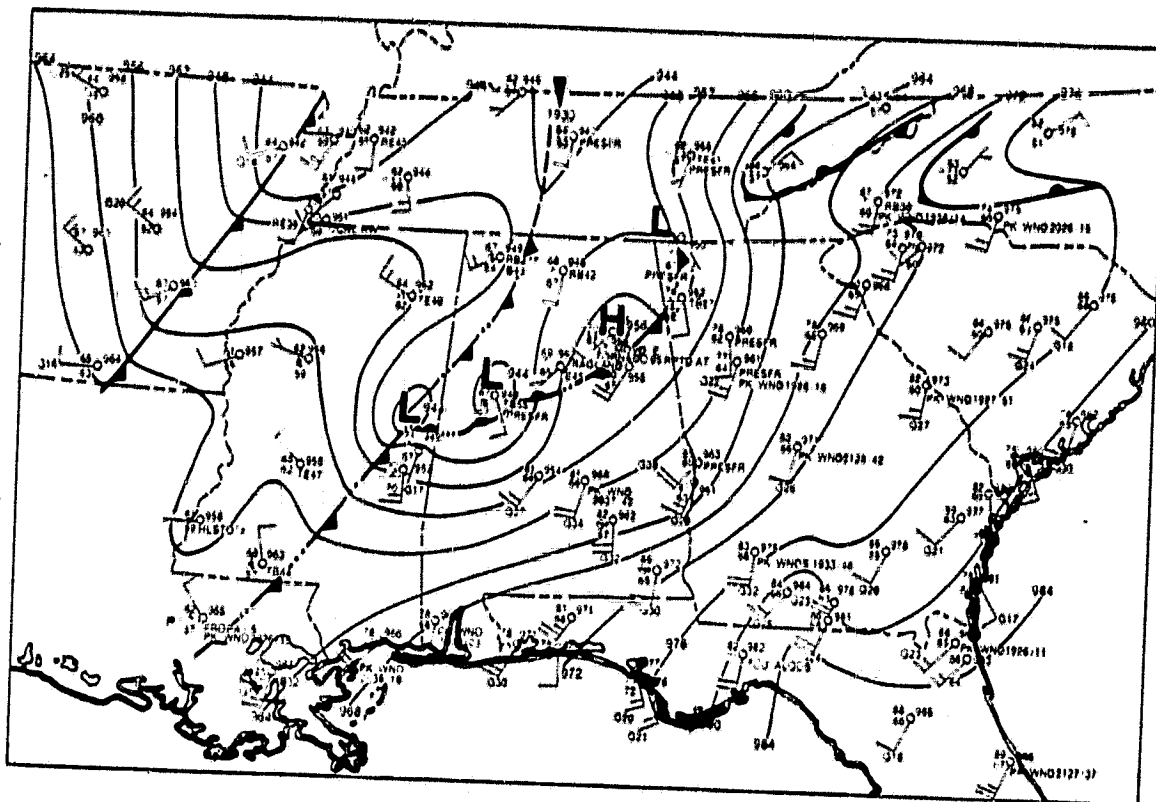


Fig. 24e. Surface mesoanalysis for 1900 GMT, 4 April 1977. Details (except for pressure perturbations) as in Fig. 24a.

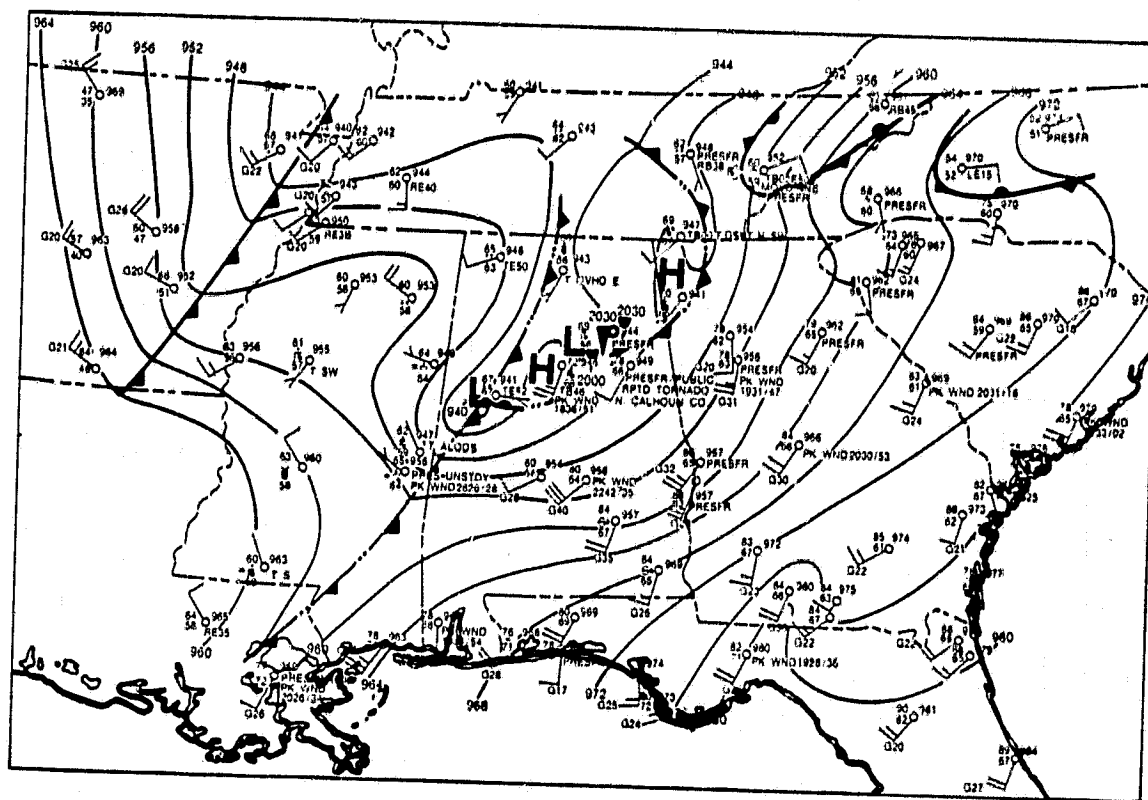


Fig. 24f. Surface mesoanalysis for 2000 GMT, 4 April 1977. Details (except for pressure perturbations) as in Fig. 24a.

located just west of Birmingham and the other just southwest of Rome, Georgia.

By 0000 GMT (Fig. 24i) the major squall-line had moved across most of northern and western Alabama and northern Georgia. The second and third mesolows that had crossed northern Alabama apparently merged as they continued to move northeastward to western North Carolina. The magnitude of the low pressure perturbation had decreased markedly. Several final tornadoes were reported as this mesosystem moved rapidly northeastward.

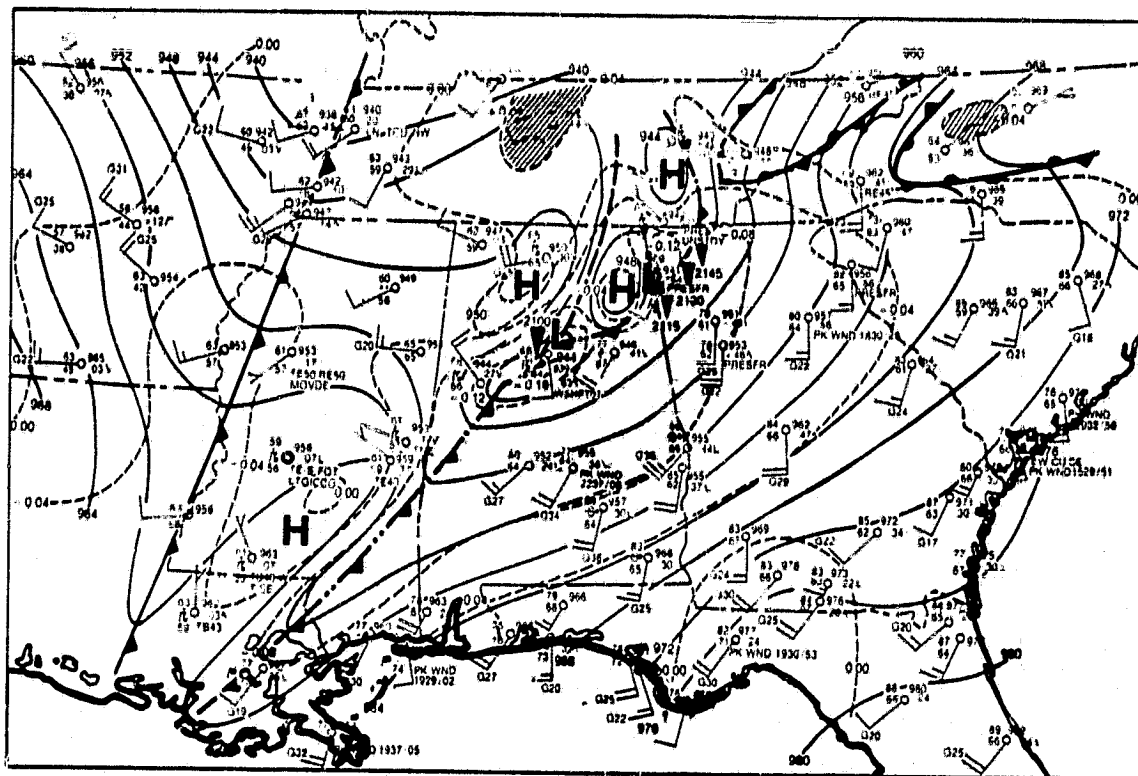


Fig. 24g. Surface mesoanalysis for 2100 GMT, 4 April 1977. Details as in Fig. 24a.



Fig. 24h. Full resolution GOES visible image for 2100 GMT,
4 April 1977.

Time series showing the surface observations at Birmingham and Rome are presented in Figs. 25 and 26. The Birmingham figure shows that the gusty southerly winds shifted to the southwest and decreased in speed as the first thunderstorm

activity moved across the station from 1700 to 1800 GMT. The pressure then fell rapidly during the next two hours as the leading (second) mesolow moved out of western Alabama and

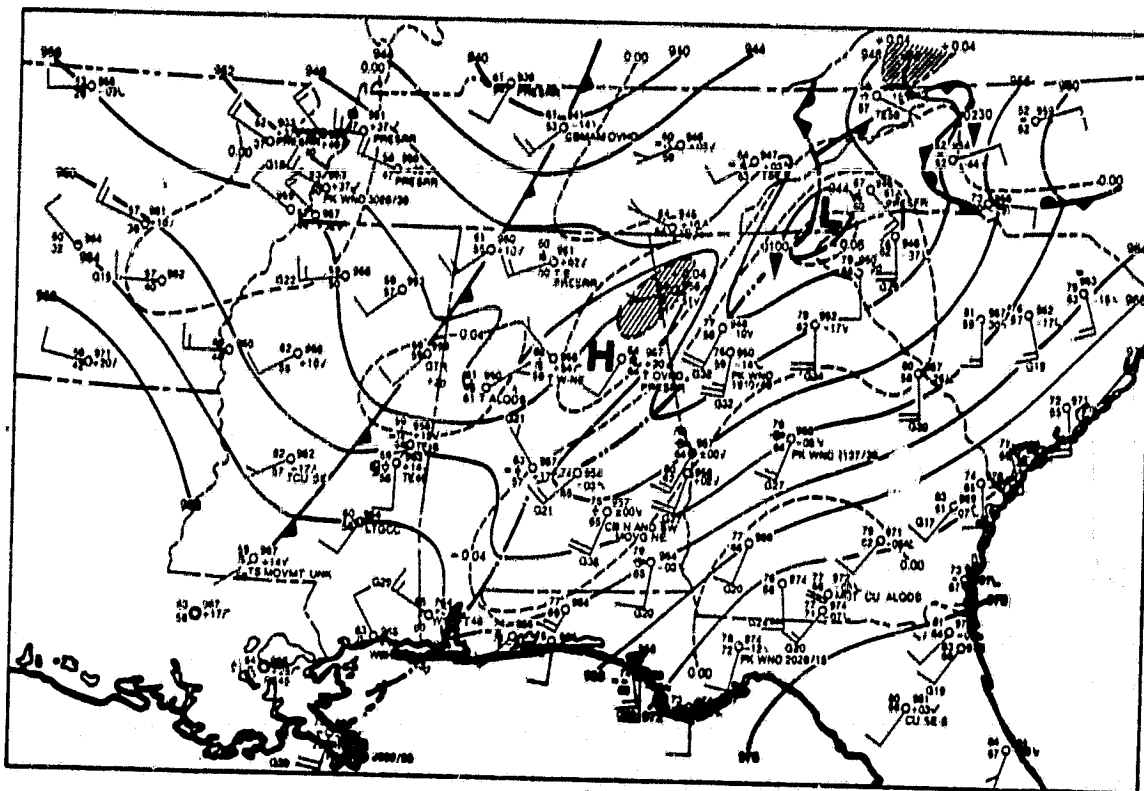


Fig. 24i. Surface mesoanalysis for 0000 GMT, 5 April 1977. Details as in Fig. 24a.

approached the station (See Figs. 24e and f). During this time the winds backed to a southerly direction and became very strong just before the mesolow passed the station. The pressure rose rapidly as thunderstorms with the mesosystem affected the station and then fell rapidly as the trailing (third) mesolow approached from the southwest. The F5 tornado was embedded in this third mesosystem. After it passed at about 2100 GMT surface winds remained west to northwest and pressures gradually rose as continuing thunderstorm activity affected the Birmingham area. Notice that during the entire period of extreme pressure fluctuations the surface temperatures and dewpoints remained relatively constant (this is similar to results already shown for the Omaha and Neosho tornadoes).

At Rome, thunderstorms moved over the station around 1900 GMT in conjunction with the first mesolow and the wind shifted to the southwest and the temperatures dropped sharply as the dewpoint increased. Surface pressures leveled off for about an hour and then fell rapidly as a second mesolow pressure system approached. The second center passed the station shortly after 2100 GMT and the low pressure remark of 28.74 inches at 2110 indicates that a tornado cyclone must have passed very near the observation site. The surface winds remained quite light during this event. The third mesolow passed between 2200 and 2300 GMT, after spawning the Birmingham tornado.

The fact that the presence of a mesolow pressure system increases the likelihood of severe convective storms has been

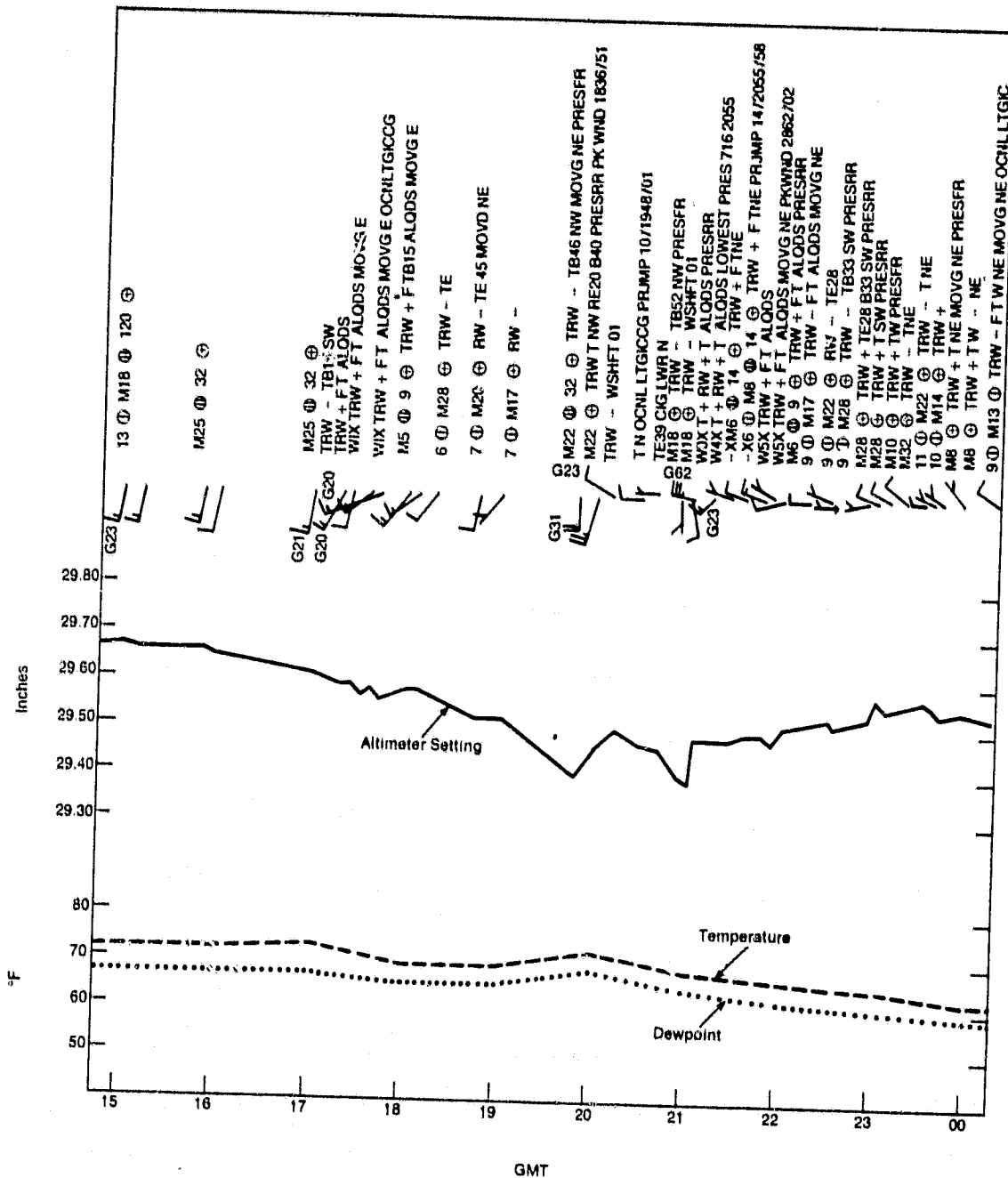


Fig. 25. Time series of surface observations for Birmingham, Alabama, on the afternoon of 4 April 1977. Winds are in knots with a full barb = 10 kt.

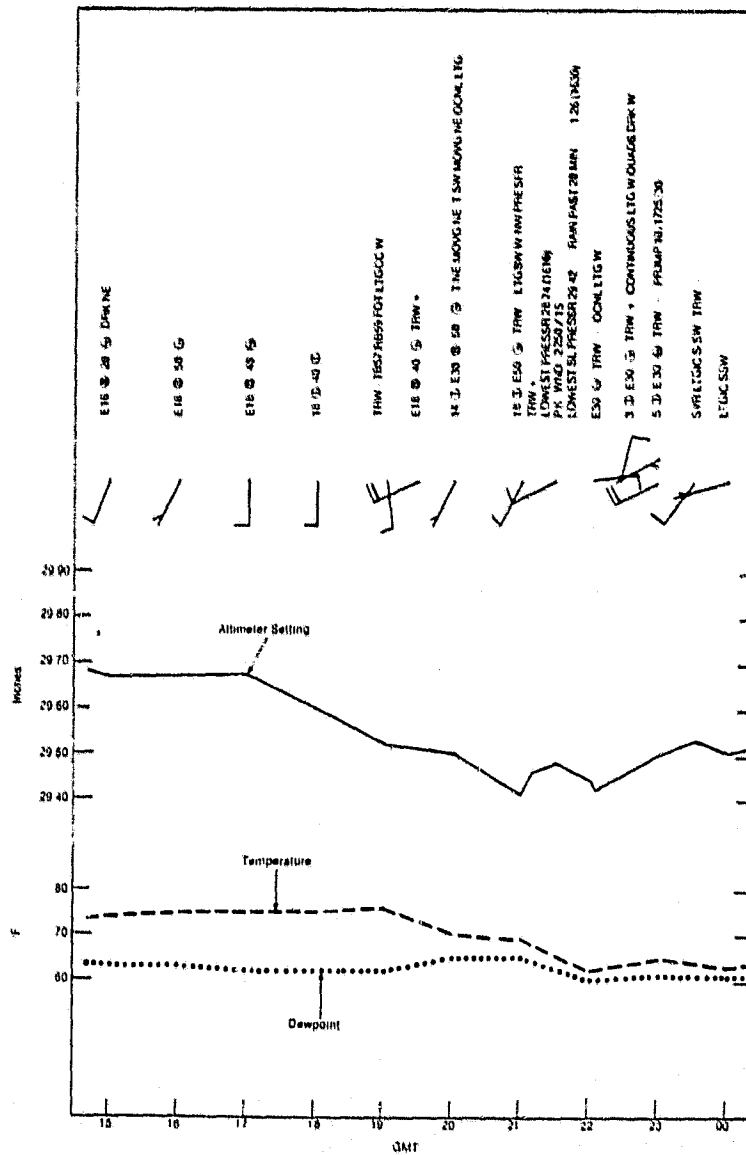


Fig. 26. Time series of surface observations for Rome, Georgia, on the afternoon of 4 April 1977. Winds are in knots with a full barb = 10 kt.

known for some time (Magor, 1958 and 1971). Hoxit et al. (1976) suggested that some mesolows may be a hydrostatic reflection of middle and upper-level subsidence warming around and downwind of thunderstorms. Earlier studies by Williams (1957) and Feteris (1961) supported the concept of compensating mesoscale circulations in the thunderstorm near environment and Fritsch (1975b) and Hoxit et al. (1976) both discussed types of feedback processes that might result.

A number of analyses of upper-air features during the 4 April 1977, event are presented in Figs. 27, 28, and 29. Isotherm analyses are for layer mean temperatures. Since the thunderstorm activity occurred well ahead of the synoptic scale front and its associated upper-level baroclinic zone, the changes in temperature that were found in the region of thunderstorms may be partially attributed to convective processes.

Figures 27a-c present analyses of lower tropospheric conditions for the period 1200 to 0000 GMT. Winds and heights are plotted for the 850 mb level and 850 mb streamlines are indicated. Mean temperatures are plotted, and isotherms drawn, for the surface to 700 mb layer. During the period, the strong baroclinic zone associated with the synoptic cold front advances slowly eastward across the Mississippi Valley. However, a cool pocket and a strong baroclinic zone develop in association with the squall-line. There is no way that advective processes could totally account for the cooling observed over central

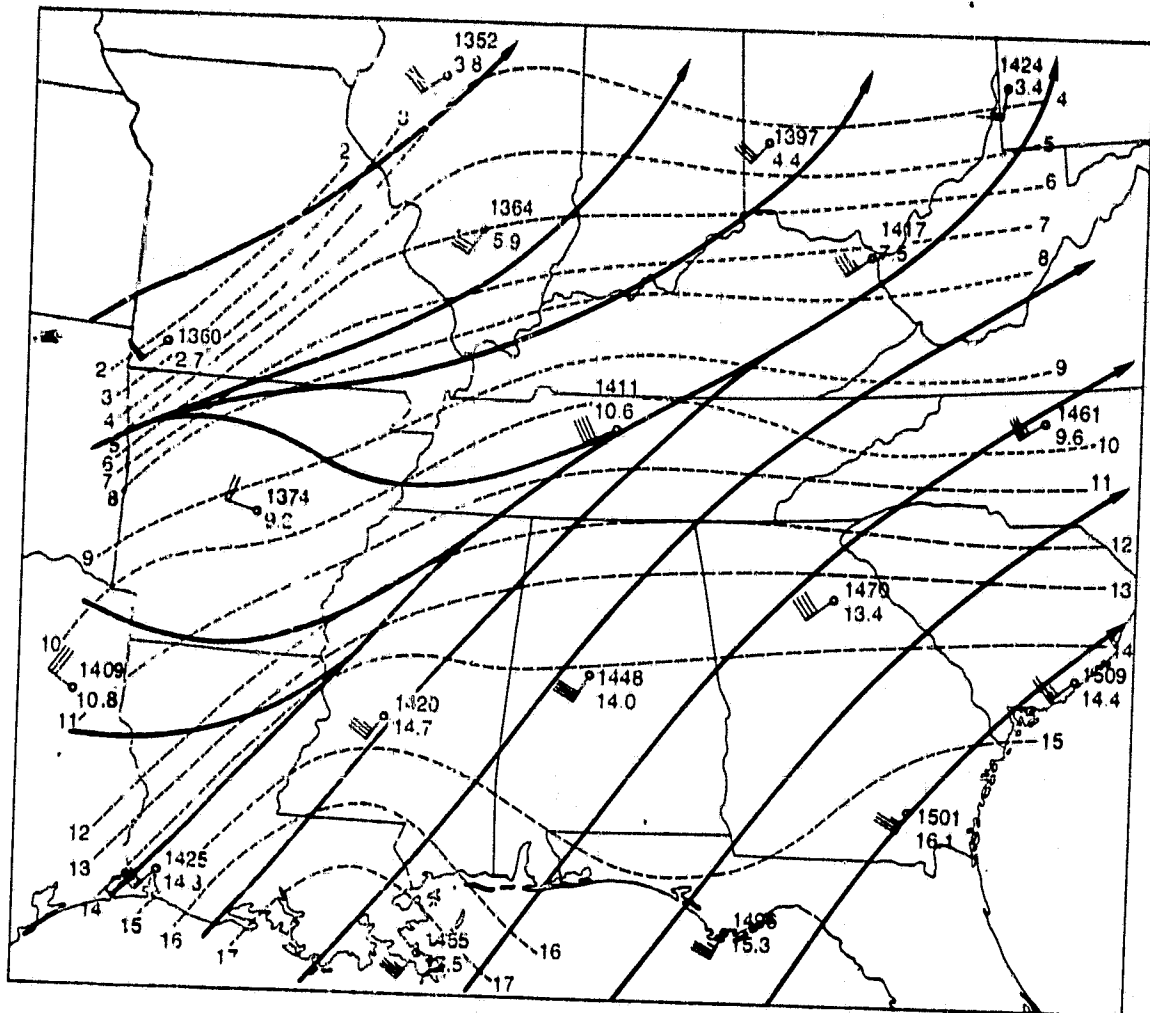


Fig. 27a. Lower tropospheric conditions for 1200 GMT, 4 April 1977. Heights, winds, and streamlines are for 850 mb. Isotherms are shown for the mean surface to 700 mb temperature (plotted below the height).

Alabama between 1800 and 0000 GMT (compare Figs. 27b and c). The eastern baroclinic zone is a mesoscale feature that has been generated by the storm activity. Low-level cooling is the primary process responsible for the development of thunderstorm mesohigh pressure systems. However, the hydrostatic surface pressure is a reflection of the temperature profile

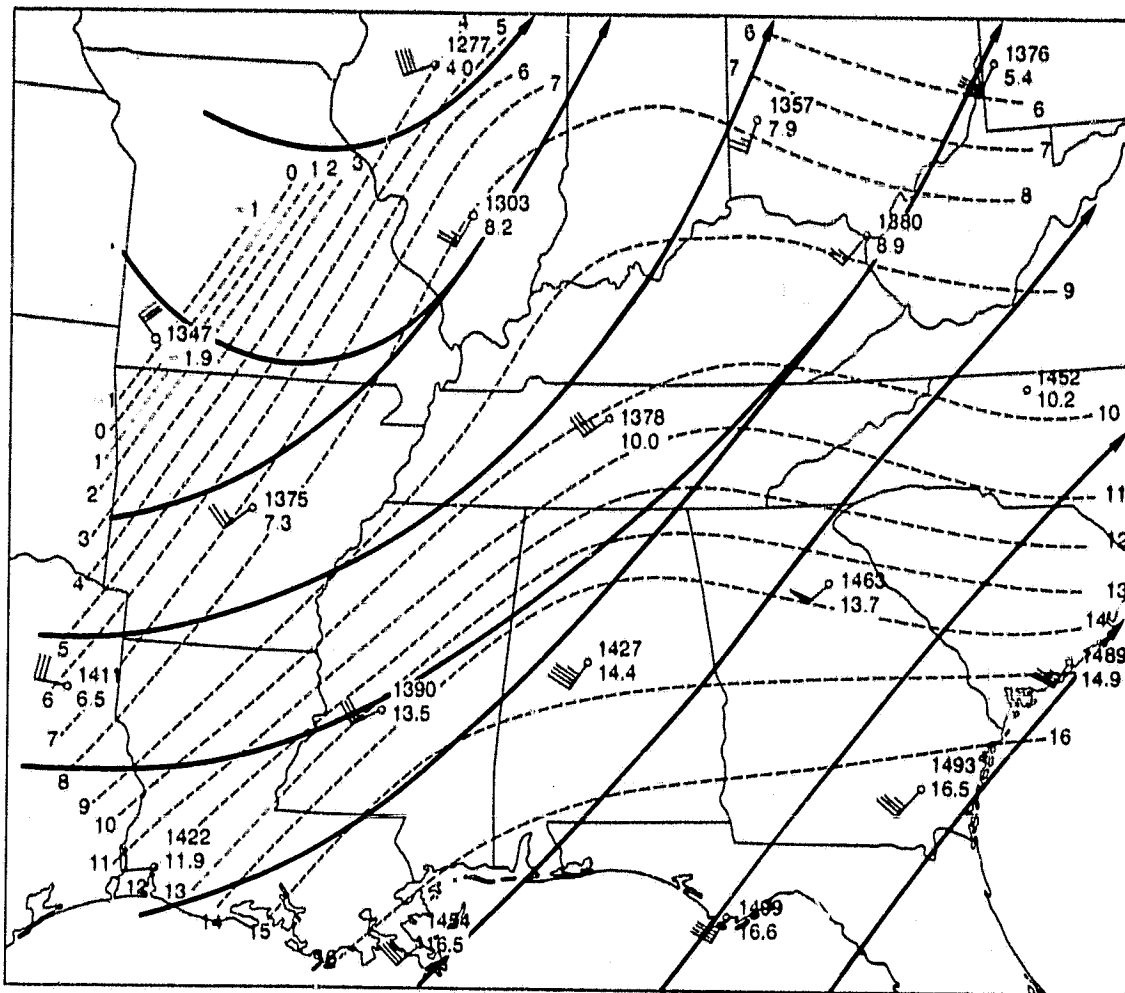


Fig. 27b. Lower tropospheric conditions for 1800 GMT, 4 April 1977. Details as in Fig. 27a.

through the depth of the atmosphere and a mesohigh can form in the cool, lower tropospheric air only if the cooling is not offset by upper-level warming.

Middle-level conditions and changes are illustrated in Figs. 28a-c. These charts show heights, winds, and streamlines for the 500 mb level and thermal analyses for mean temperature in the 700 to 250 mb layer. During the analysis period strong,

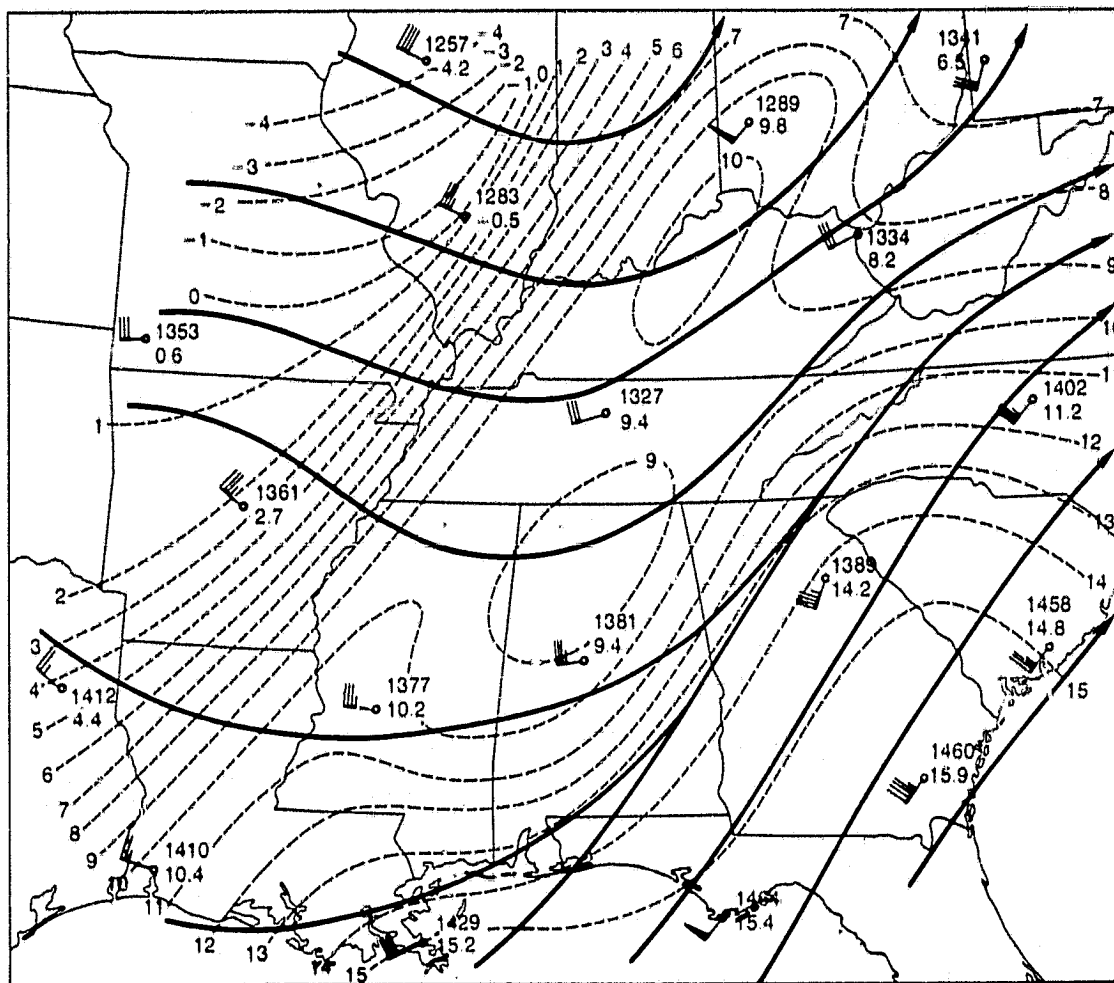


Fig. 27c. Lower tropospheric conditions for 0000 GMT, 5 April 1977. Details as in Fig. 27a.

middle-level warming occurs in the region of the severe squall-line. Mean temperatures in the layer increase from 3-5°C during the six hours from 1200 to 1800 GMT over portions of northern Mississippi, northern Alabama, and central Tennessee. Part of the increase is due to warm advection; however, the tremendous amplification of the thermal ridge during the twelve hour period suggests that the warming is partly due to the large area of convective storms. This warming could be caused by two primary processes. The first is direct warming due to persistent moist adiabatic ascent over a large area. Secondly, the warming could also be produced by compensating subsidence within the environment surrounding the thunderstorm complexes.

Upper tropospheric and lower stratospheric conditions and changes are illustrated in Figs. 29a-c. These charts show heights, winds, and streamlines for the 200 mb level and thermal analyses for mean temperature in the 225 to 175 mb layer. Although warm advection was indicated over Alabama and eastern Tennessee (see Figs. 29a and b) a large area of significant upper tropospheric cooling occurred in the region of convective activity (see Fig. 29c). Mesoscale lifting and cooling at the cloud-top level was probably the mechanism responsible for the observed changes.

Thermal changes similar to those illustrated in Figs. 27, 28 and 29 have been obtained by Fritsch (1978) in three-dimensional numerical simulations of squall-line convection.

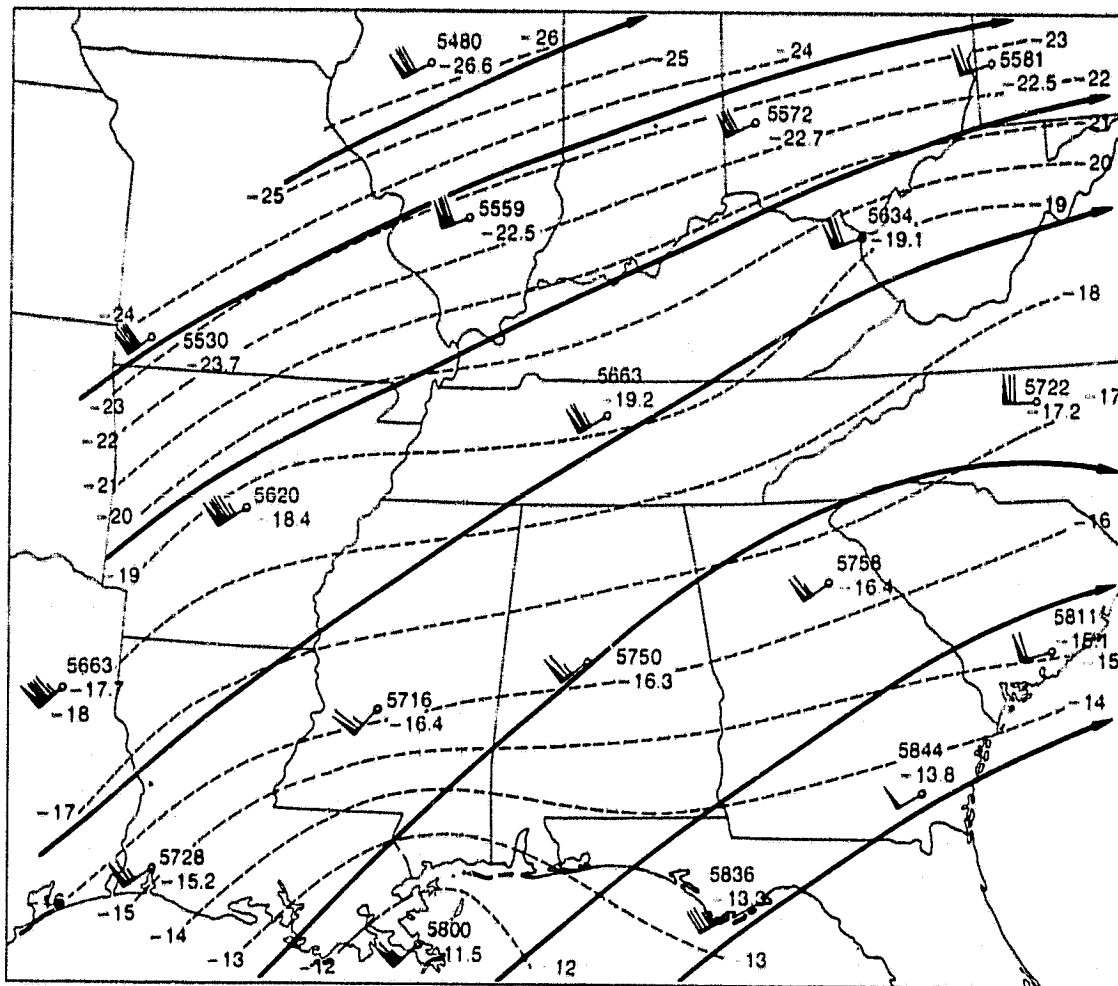


Fig. 28a. Middle tropospheric conditions for 1200 GMT, 4 April 1977. Heights, winds, and streamlines are for 500 mb. Isotherms are shown for the mean 700 to 250 mb temperature (plotted below the height).

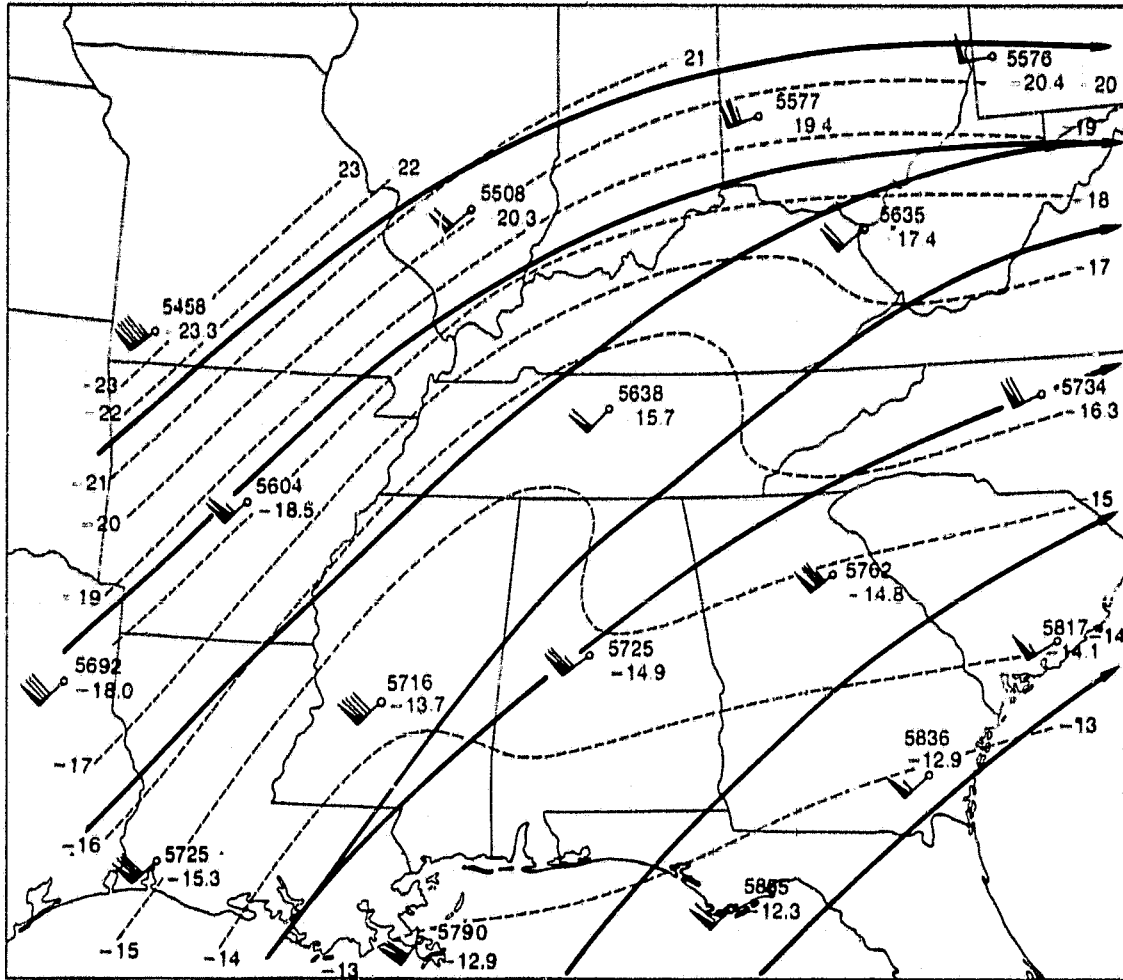


Fig. 28b. Middle tropospheric conditions for 1800 GMT, 4 April 1977. Details as in Fig. 28a.

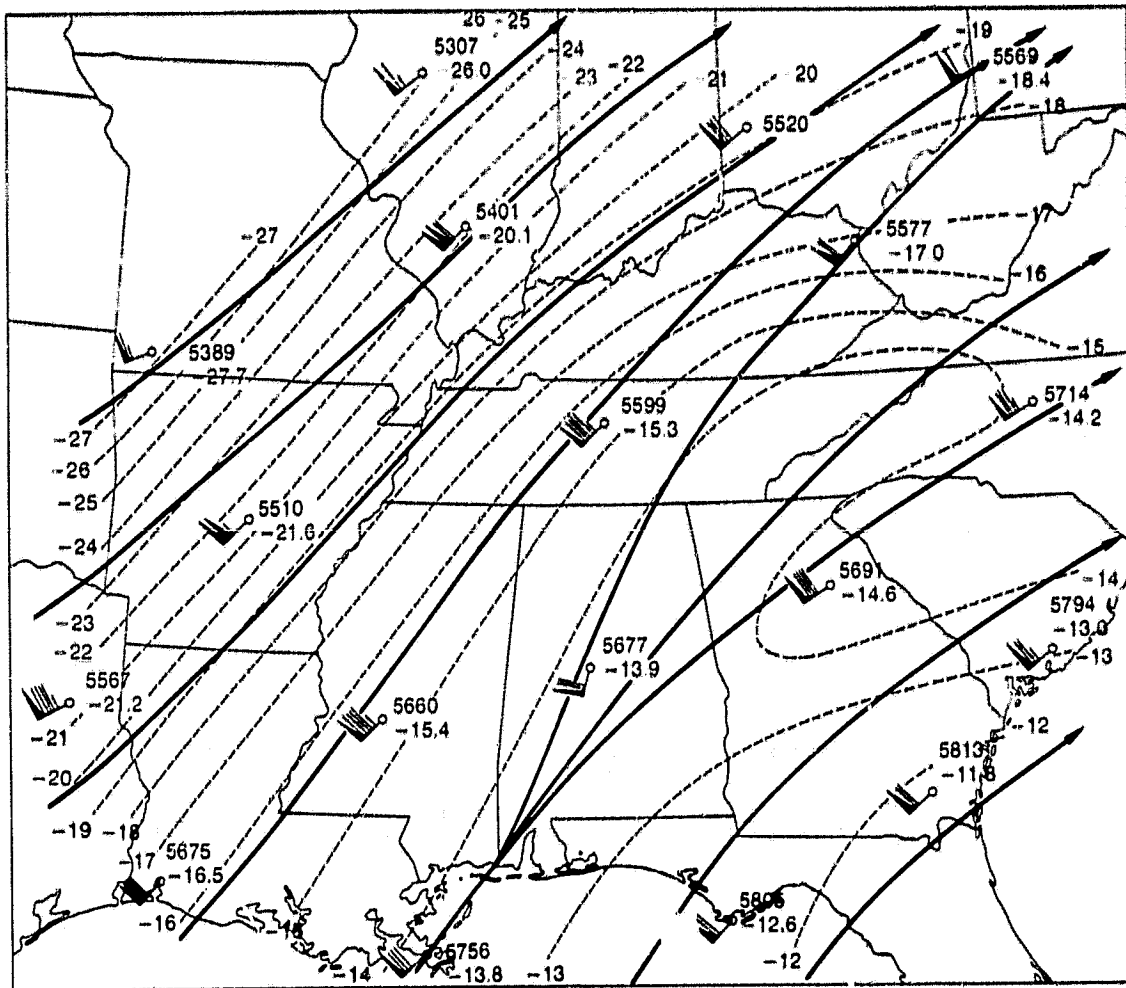


Fig. 28c. Middle tropospheric conditions for 0000 GMT, 5 April 1977. Details as in Fig. 28a.

These figures illustrate that a large region of organized convective storms can affect and modify their near environment on scales large enough to be detected in the synoptic sounding network. Convective modification can be easily detected at the surface where observations are fairly dense and the convective changes dramatic. At middle and high levels, however, convective mesoscale features are more difficult to detect because of large data separations and the superposition of mesoscale features upon strong background flow fields.

The large area of higher pressure from central Alabama into eastern Tennessee (see Figs. 24g and 24i) appears to be directly related to the area of lower tropospheric cooling evident on Fig. 27c. The exact mechanisms responsible for the series of mesolows, however, are not resolved by the coarse resolution, upper-air data. The April 4th mesolows appeared to be closely linked to active storm complexes; whereas, the April 24th mesolow (considered earlier) developed in a warm lower tropospheric region prior to storm development. The April 4th mesolows were probably a result of a combination of mesoscale effects that would include: low-level warm advection, strong moist adiabatic warming, and upper-level subsidence and warming.

b. Upper-tropospheric flow fields on 24 and 25 April 1975

Maddox (1979a) has examined the evolution of jet stream level winds using the NASA AVE IV data. His findings provide

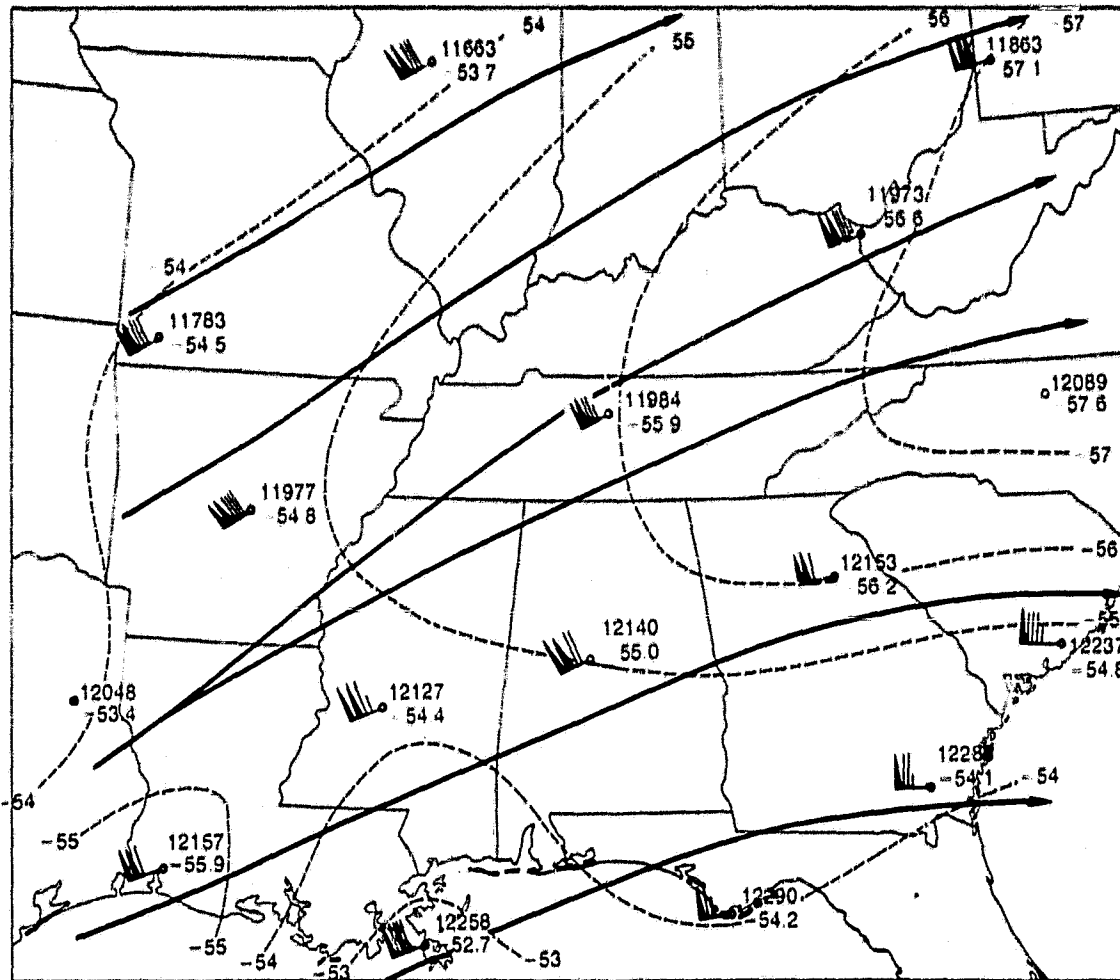


Fig. 29a. Upper tropospheric/lower stratospheric conditions for 1200 GMT, 4 April 1977. Heights, winds, and streamlines are for 200 mb. Isotherms are shown for the mean 225 to 175 mb temperature (plotted below the height).

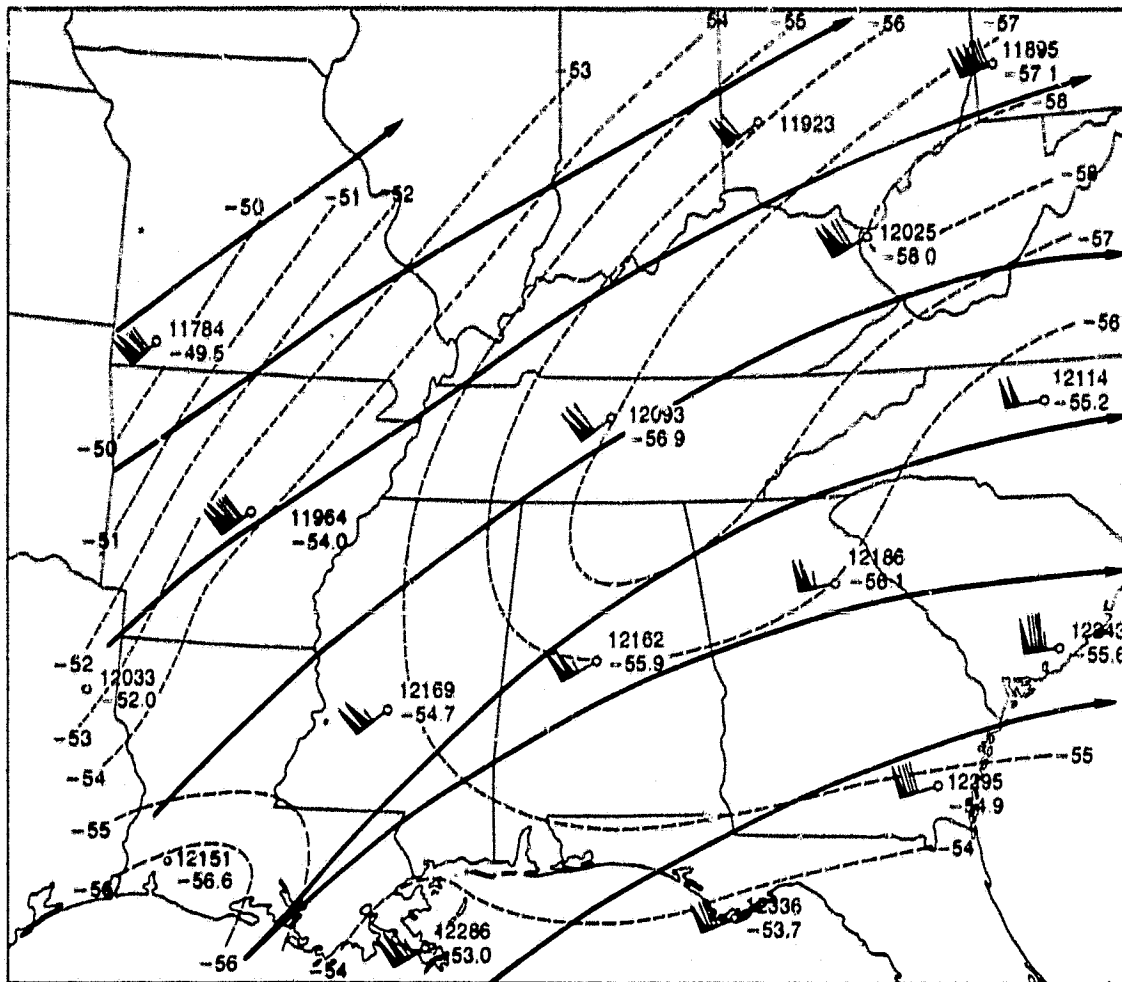


Fig. 29b. Upper tropospheric/lower stratospheric conditions for 1800 GMT, 4 April 1977. Details as in Fig. 29a.

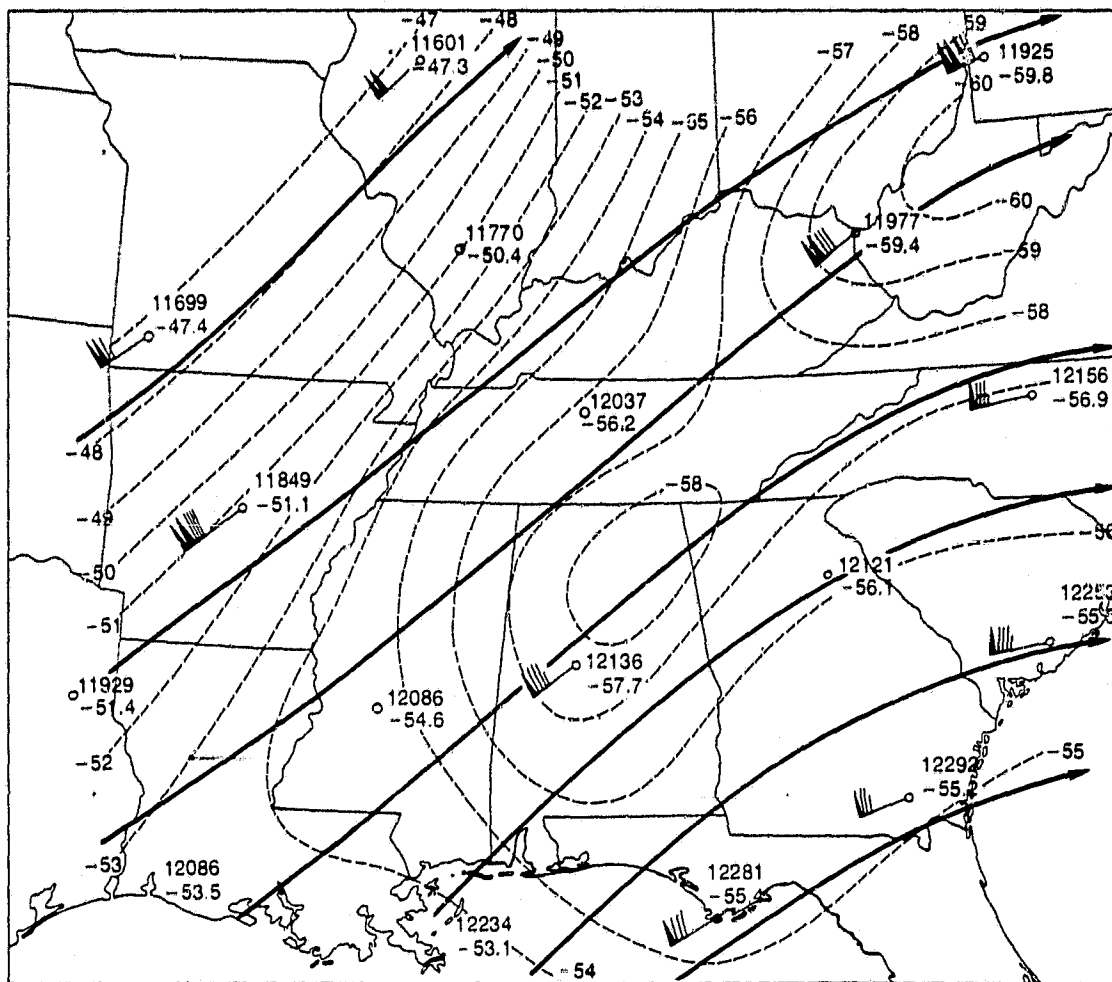


Fig. 29c. Upper tropospheric/lower stratospheric conditions for 0000 GMT, 5 April 1977. Details as in Fig. 29a.

excellent examples of convective feedbacks that affect the larger scale environment and they are briefly summarized in this section.

Figure 30a shows an analysis of jetstream winds (defined as the maximum reported wind above the 350 mb level) for 0000 GMT, 24 April 1975. Isotachs and jet axes are shown along with

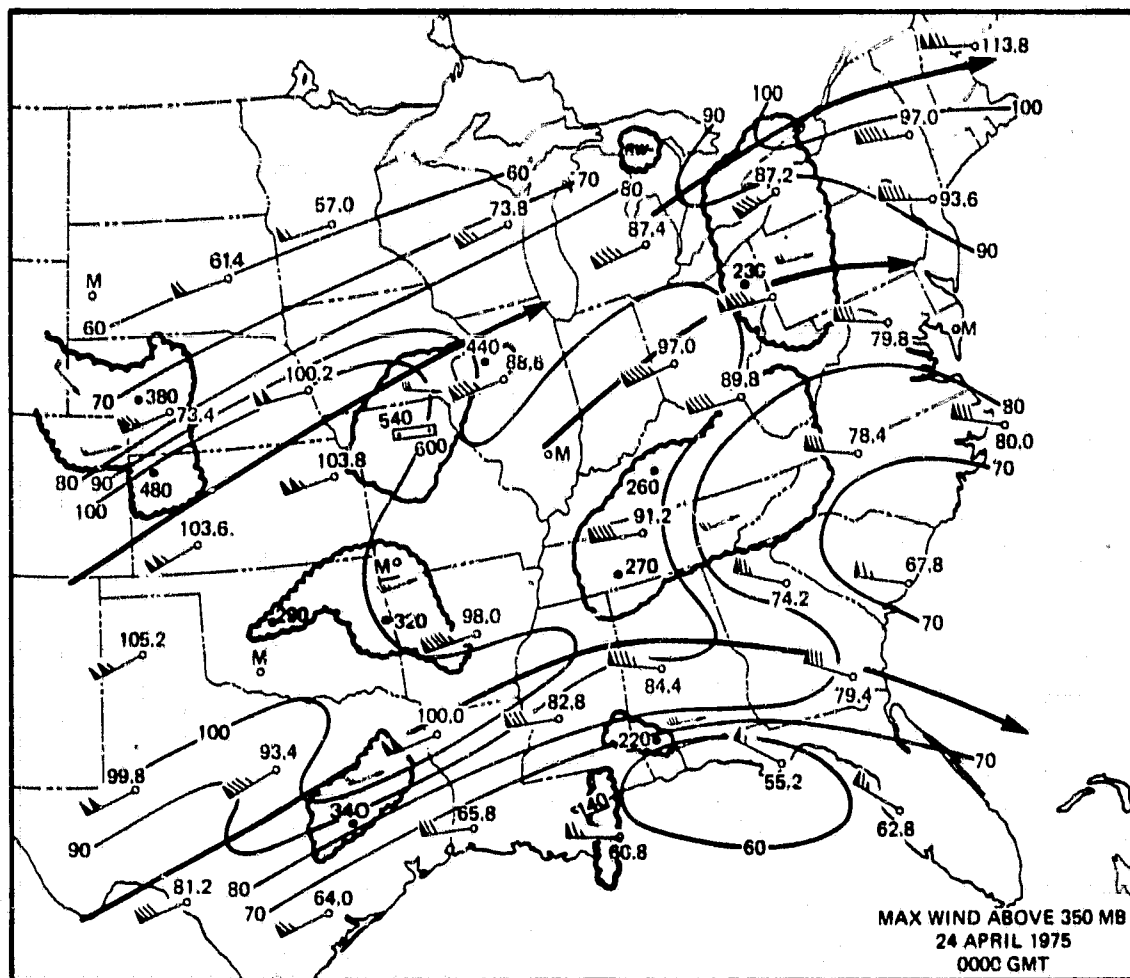


Fig. 30a. Jetstream winds (maximum wind above 350 mb) for 0000 GMT, 24 April 1975. Isotachs (kt) and jet axes are shown along with radar echoes from the 2335 GMT radar summary chart (from Maddox, 1979a).

radar echoes from the radar summary facsimile chart. The analysis shows a diffuse polar jetstream from western Kansas to New England with maximum speeds on the order of 100 kt. The subtropical jet, also with maximum speeds of about 100 kt, curves from southwest Texas across Georgia. The 0000 GMT digitized IR satellite image (Fig. 30b) shows that intense storms are occurring over northern Missouri and southern Iowa (radar tops 50-60,000 ft.). The jetstream chart for 0600 GMT 24 April 1975 (Fig. 31a) shows that tremendous changes have occurred during a period of only 6 hours. The subtropical jet is poorly defined as it crosses the Gulf Coast states. However, a significant jet, with maximum speeds exceeding 130 kt, curves from eastern Nebraska to the East Coast. Several secondary jets are also indicated. The strong flow has developed along the north edge of a region of strong thunderstorms (radar tops 40-50,000 ft. from Michigan to Kansas). The flow splits and diverges around the western end of the convective system as if a mesohigh pressure perturbation exists over the storm complex. The IR satellite image for 0600 GMT (Fig. 31b) shows that the strong jetstream is positioned along the northern edge of the cirrus shield associated with the thunderstorm complex.

Figure 32a shows the jetstream chart 18 hours later at 0000 GMT on the 25th of April. The subtropical jet was once again well defined with speeds in excess of 125 kt indicated

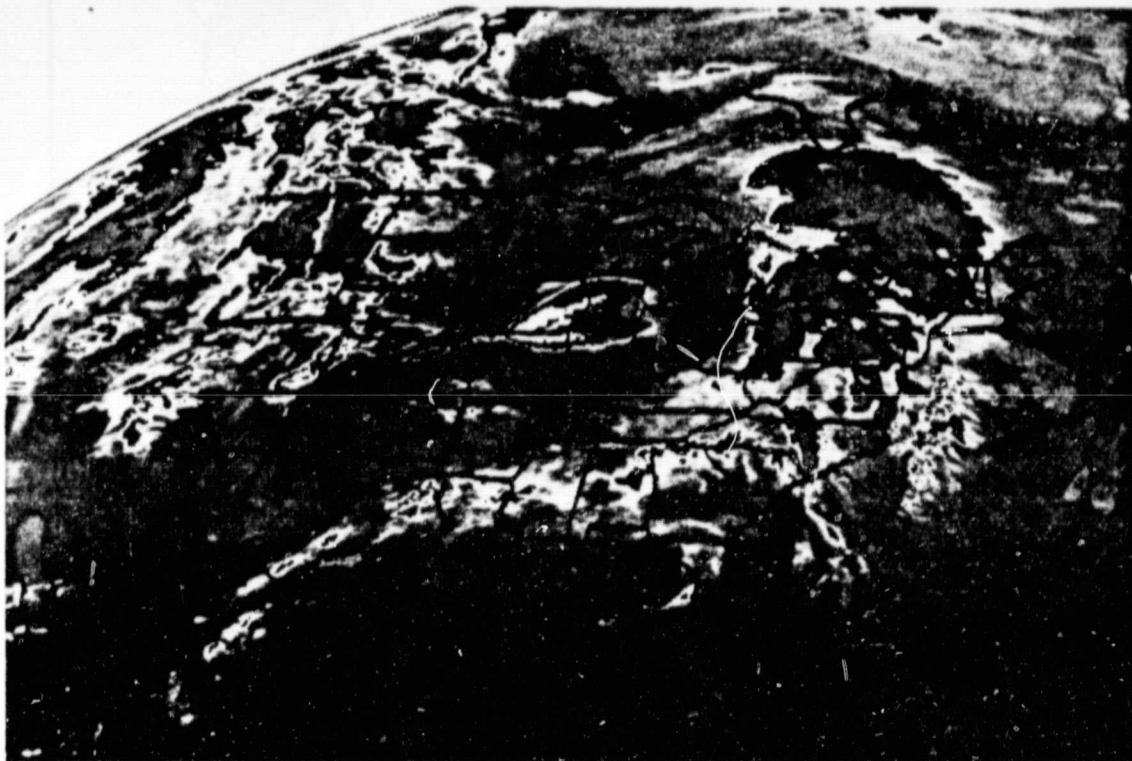


Fig. 30b. Digitized IR satellite image for 0000 GMT,
24 April 1975.

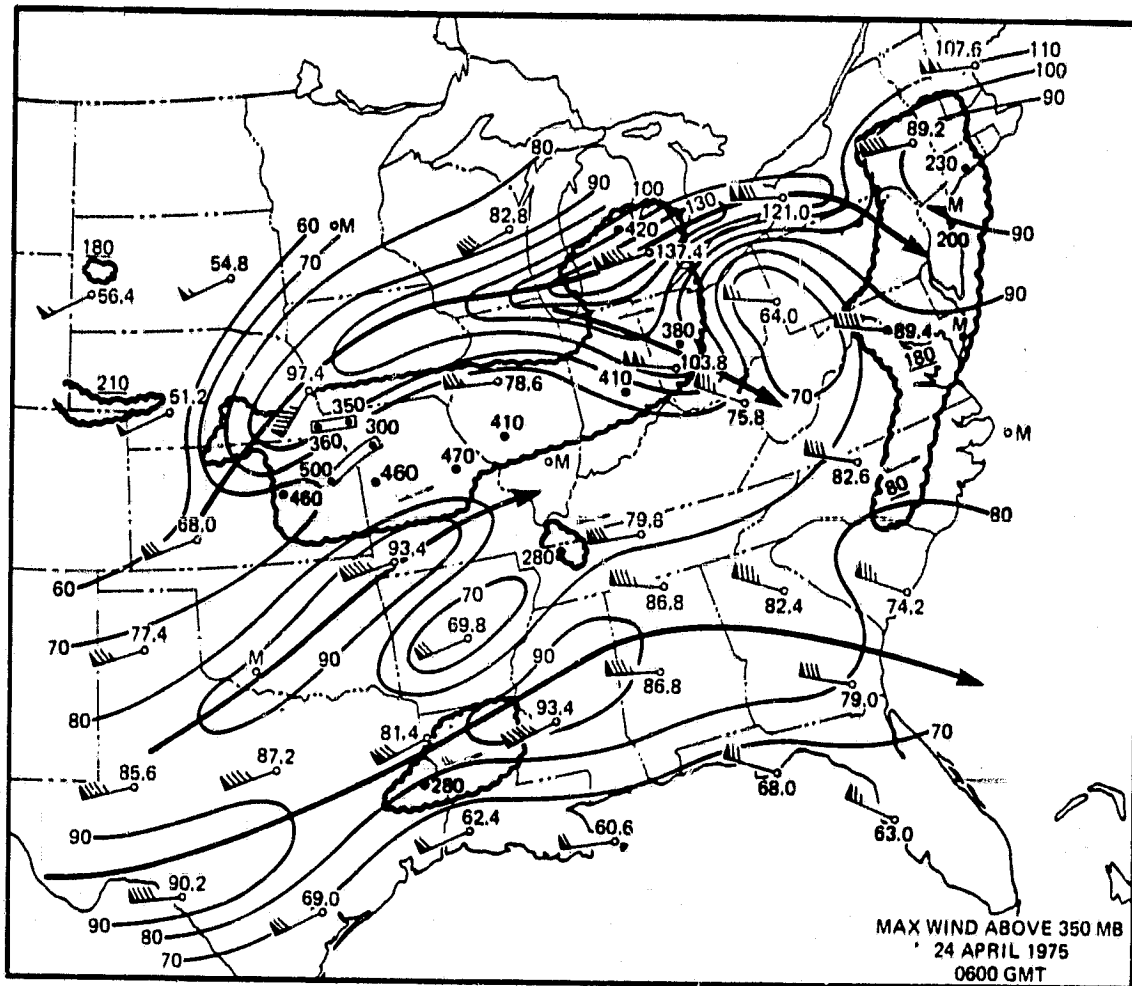


Fig. 31a. Jetstream winds for 0600 GMT and radar echoes for 0535 GMT, 24 April 1975. Details as in Fig. 30a (from Maddox, 1979a).



Fig. 31b. Digitized IR satellite image for 0600 GMT,
24 April 1975.

ORIGINAL PAGE IS
OF POOR QUALITY

over central Texas. A diffuse polar jet stretched over the northern U.S. with speeds of about 100 kt. The shower activity and slightly higher wind speeds over the East Coast were the remains of the convective system and jet shown in Fig. 31a. Intense thunderstorms were developing over western Missouri and eastern Oklahoma at the time of the figure. The satellite IR photograph shown in Fig. 32b shows these developing storms.

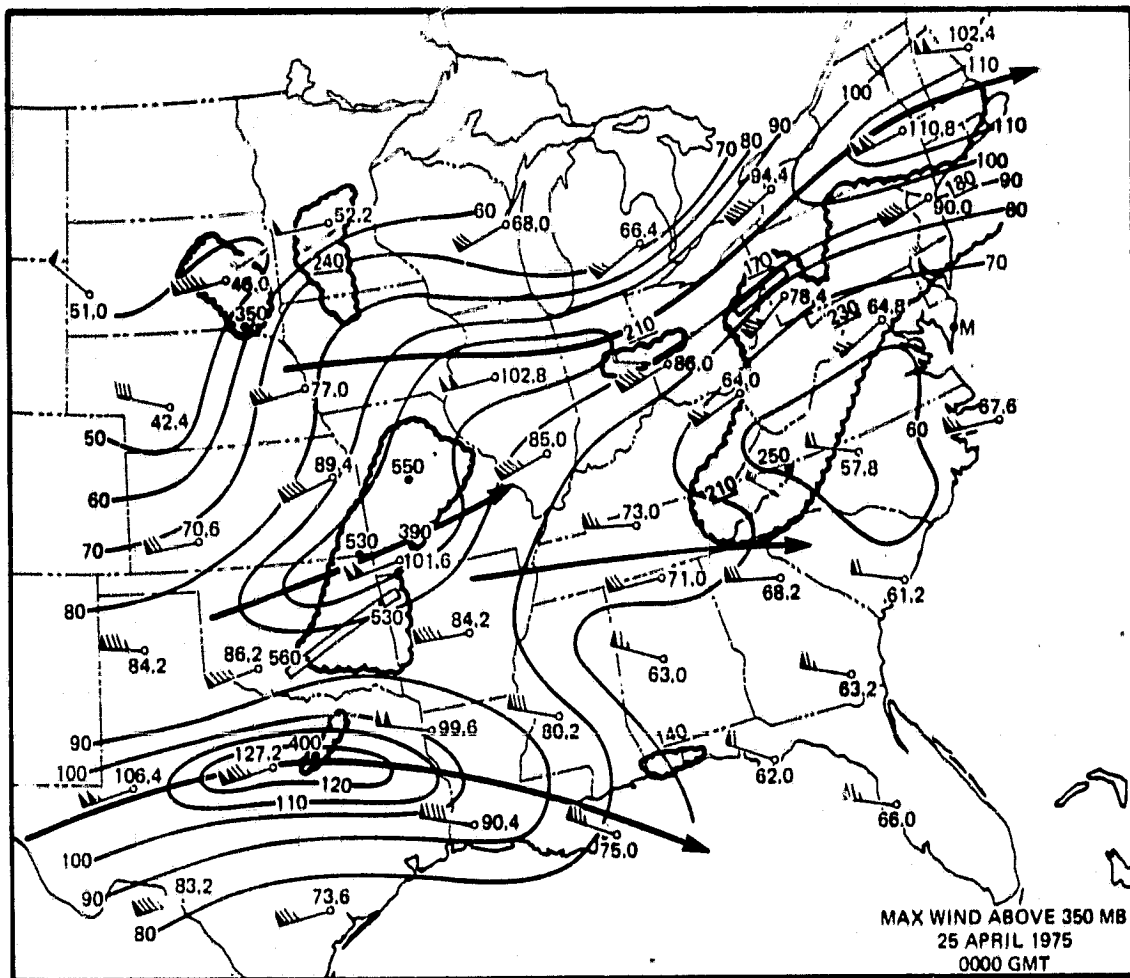


Fig. 32a. Jetstream winds for 0000 GMT and radar echoes for 2335 GMT, 25 and 24 April 1975. Details as in Fig. 30a (from Maddox, 1979a).

The wind field at the jetstream level six hours later (Fig. 33a) shows that tremendous changes have again occurred in only six hours. By 0600 GMT a large, intense thunderstorm complex (radar tops 40-55,000 ft.) extended from Kentucky westward to eastern Oklahoma. A jetstream with maximum speeds in excess of 135 kt curled anticyclonically around the northern

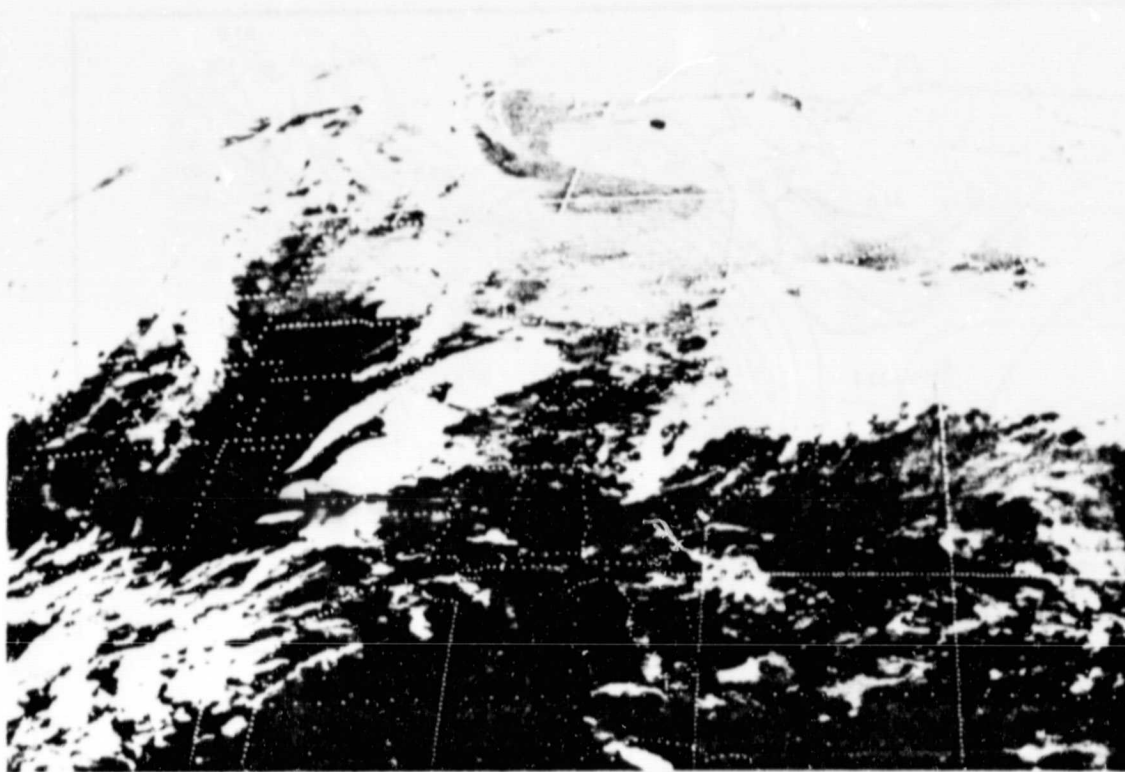


Fig. 32b. IR satellite image for 0000 GMT, 25 April 1975.

edge of the thunderstorm system and the extreme diffluence over the system again suggests the presence of a mesohigh pressure perturbation aloft. The concurrent IR satellite image (Fig. 33b) shows the intense storm system and indicates that the jetstream maximum is again located along the northern edge of the extensive cirrus shield.

ORIGINAL PAGE IS
OF POOR QUALITY

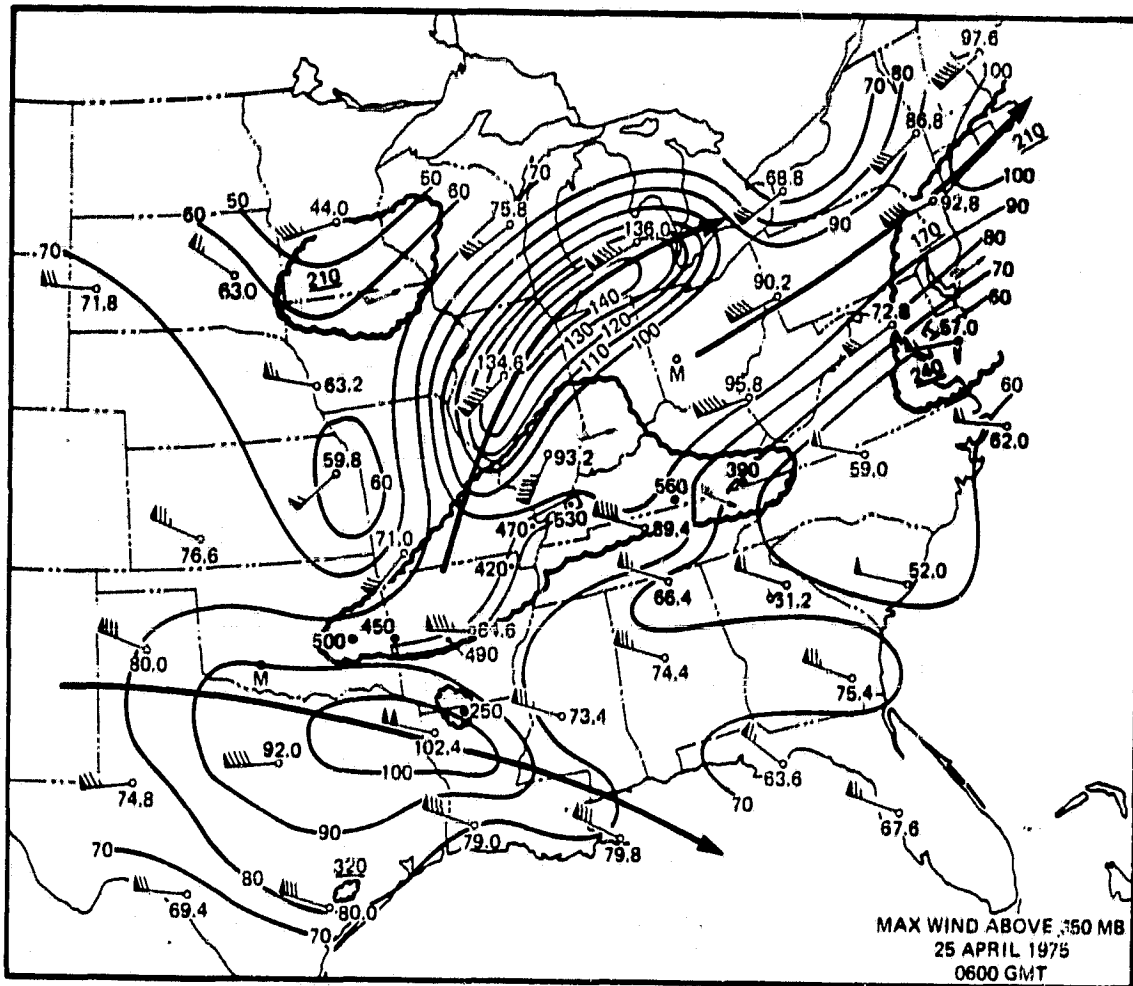


Fig. 33a. Jetstream winds for 0600 GMT and radar echoes for 0535 GMT, 25 April 1975. Details as in Fig. 30a (from Maddox, 1979a).

Maddox (1979b) has documented the existence of a large mesohigh circulation at 200 mb at the top of a similar convective system using an objective analysis scheme to isolate

mesoscale features. Fritsch et al. (1979) have shown results from numerical simulations of squall-line type convection that are similar to the features observed on 4 April 1977 and 24/25 April 1975. Ninomiya (1971a and 1971b) used satellite photographs to document similar upper-level wind perturbations. All of these examples show that when convective storms organize into large mesosystems the convectively driven circulations affect and modify the large scale flow fields on scales that may, on occasion, be detected in the synoptic upper-air data.

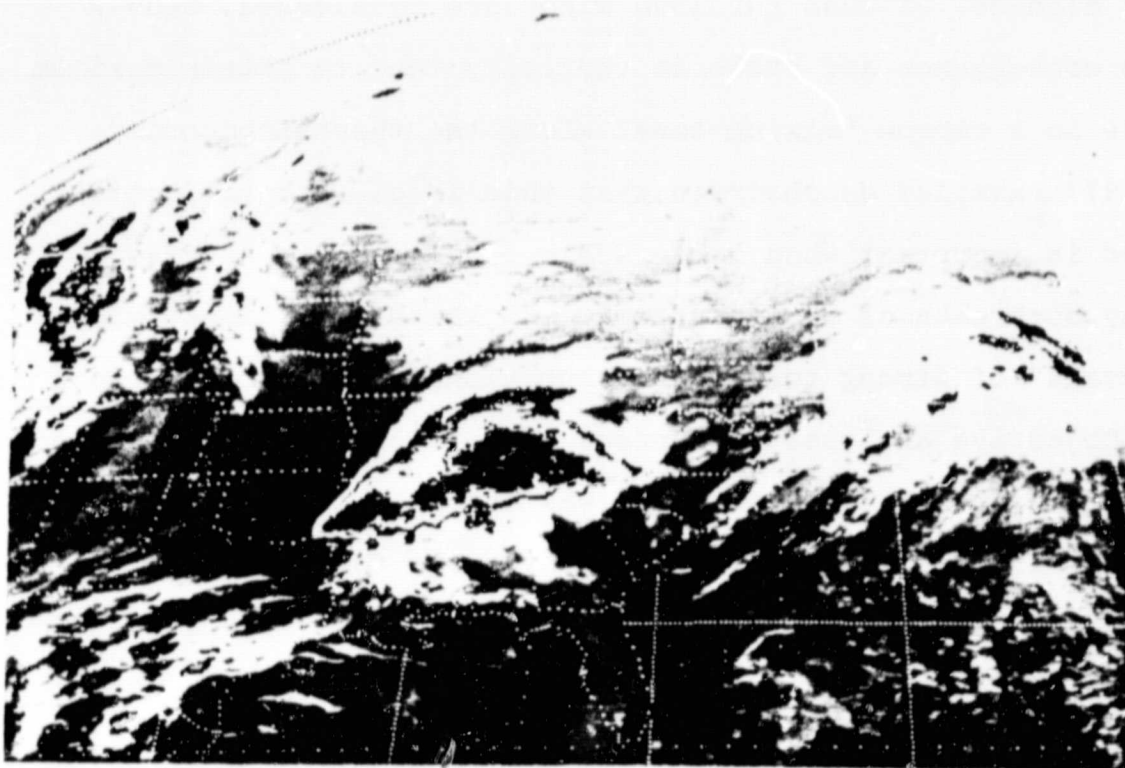


Fig. 33b. Digitized IR satellite image for 0600 GMT,
25 April 1975.

ORIGINAL PAGE IS
OF POOR QUALITY

5. SUMMARY

Results from several detailed case studies of severe storm events have been presented to document various ways in which convective storms interact with their environment. A physical model of boundary layer wind fields (both in the horizontal and vertical) was developed to explain why thunderstorms intensify as they move along or across thermal boundaries. Detailed time series data, along with three specific case studies, substantiated many aspects of the proposed model. Winds veer slowly with height on the cool side of such boundaries while winds veer rapidly through the subcloud layer in the hot, moist air mass. If mean subcloud winds are considered, meso- β scale convergence and cyclonic vorticity tend to obtain maximum values in a narrow "mixing zone" along the thermal boundary. The 1977 examples demonstrate that this local intensification effect is important when large scale conditions do not favor family outbreaks of severe storms. In these situations "mini-outbreaks" of strong tornadoes occur along thermal boundaries.

Objective analyses of surface kinematic fields were mapped onto GOES satellite imagery. It was demonstrated that meso- β scale areas where conditions were favorable for significant tornadic storms could be identified and that the satellite imagery could be used to monitor storm development in, or movement into, these dynamically favorable regions. Severe storm nowcast techniques based on these results should be tested

and studied for a number of severe storm situations. An interactive data processing and analysis facility would be desirable for use in further studies and absolutely necessary for any real-time tests or applications.

The final examples presented demonstrated that once severe thunderstorms organize into meso- α scale storm complexes the associated mesoscale circulations act to modify larger scale features. Mesoscale pressure systems, both at the surface and aloft, may develop. Once formed, these systems may act to enhance and maintain the convective storms. Many of these important features and circulations exist aloft since most of the examples showed large mesoscale pressure fluctuations occurring without corresponding fluctuations in surface temperature and dewpoint. The cases that show pronounced diffluence and jetstream maxima developing in response to large storm complexes are important. These patterns are usually thought of as precursor features that favor storm development. Convective feedbacks, such as those illustrated, cannot occur in current operational numerical models because of the simple convective parameterizations that are used.

REFERENCES

- Adler, R. F. and D. D. Fenn, 1977: Satellite-based thunderstorm intensity parameters. Preprints Tenth Conf. on Severe Local Storms (Omaha, Neb.), Amer. Meteor. Soc., Boston, Mass., 8-15.
- Arya, S. P. S., and J. C. Wyngaard, 1975: Effect of baroclinicity on wind profiles and the geostrophic drag law for the convective planetary boundary layer. J. Atmos. Sci., 32, 767-778.
- Barnes, S. L., 1964: A technique for maximizing details in numerical weather map analysis. J. Appl. Meteor., 3, 396-409.
- _____, 1973: Mesoscale objective map analysis using weighted time series observations. NOAA Tech. Memo. ERL, NSSL-62, Norman, Okla., 60 pp.
- _____, 1978a: Oklahoma thunderstorms on 29-30 April 1970. Part I: Morphology of a tornadic storm. Mon. Wea. Rev., 106, 673-684.
- _____, 1978b: Oklahoma thunderstorms on 29-30 April 1970. Part II: Radar-observed merger of twin hook echoes. Mon. Wea. Rev., 106, 685-696.
- Blackadar, A. K., 1965: A single layer theory of the vertical distribution of wind in a baroclinic neutral atmospheric boundary layer. AFCRL 65-531, Final Report Contract AF (604)-6641, Penn. State Univ., 22 pp.
- Carter, J. K., 1970: The meteorologically instrumented WKY-TV tower facility. NOAA Tech. Memo. ERL, NSSL-50, Norman, Okla., 18 pp.
- Cattle, H., 1971: The terrestrial low latitude boundary layer. Ph.D. Dissertation, Imperial College of Science and Technology, London, 201 pp.
- Doswell, C. A., III, 1977: Obtaining meteorologically significant surface divergence fields through the filtering property of objective analysis. Mon. Wea. Rev., 105, 885-892.
- Feteris, P. J., 1961: The influence of the circulation around cumulonimbus clouds on the surface humidity pattern. Swiss Aero Review, 36, 626-630.

Fritsch, J. M., 1975a: Synoptic-meso scale budget relationships for a tornado producing squall line. Preprints Ninth Conf. on Severe Storms (Norman, Okla.), Amer. Meteor. Soc., Boston, Mass., 165-172.

_____, 1975b: Cumulus dynamics: Local compensating subsidence and its implications for cumulus parameterization. Pure Appl. Geophys., 113, 851-867.

_____, 1978: Parameterization of mid-latitude organized convection. Ph.D. Dissertation, Dept. of Atmospheric Science, Colorado State University, Ft. Collins, Colo., 143 pp.

_____, R. A. Maddox, L. R. Hoxit, and C. F. Chappell, 1979: Numerical simulation of convectively driven mesoscale pressure systems aloft. Preprints Fourth Conf. on Numerical Weather Prediction (Silver Spring, Md.), Amer. Meteor. Soc., Boston, Mass.

Fucik, N. F. and R. E. Turner, 1975: Data for NASA's AVE IV experiment: 25-mb sounding data and synoptic charts. NASA TM X-64952, Marshall Space Flight Center, Al., 458 pp.

Fujita, T. T., 1971: Proposed characterization of tornadoes and hurricanes by area and intensity. SMRP Res. Paper No. 91, Univ. of Chicago, 44 pp.

Galway, J. G., 1975: Relationship of tornado deaths to severe weather watch areas. Mon. Wea. Rev., 103, 737-741.

Hill, K. and R. E. Turner, 1977: NASA's Atmospheric Variability Experiments (AVE). Bull. Amer. Meteor. Soc., 58, 170-172.

Houghton, D. D. and D. K. Lee, 1977: Mesoscale wind fields for the May 6, 1975 Omaha tornado situation derived from SMS cloud observations. Preprints Tenth Conf. on Severe Local Storms (Omaha, Neb.), Amer. Meteor. Soc., Boston, Mass., 16-21.

Hoxit, L. R., 1974: Planetary boundary layer winds in baroclinic conditions. J. Atmos. Sci., 31, 1003-1020.

_____, C. F. Chappell, and J. M. Fritsch, 1976: Formation of mesolows or pressure troughs in advance of cumulonimbus clouds. Mon. Wea. Rev., 104, 1419-1428.

- Hudson, H. R., 1971: On the relationship between horizontal moisture convergence and convective cloud formation. J. Meteor., 10, 755-762.
- Kreitzberg, C. W., 1977: SESAME '77 experiments and data availability. Bull. Amer. Meteor. Soc., 58, 1299-1301.
- Kuhn, P. M., G. L. Darkow, and V. E. Suomi, 1958: A mesoscale investigation of pre-tornado thermal environments. Bull. Amer. Meteor. Soc., 39, 224-228.
- Lettau, H., 1967: Small-to-large-scale features of boundary layer structure over mountain slopes. Proc. Symp. Mountain Meteorology, E. R. Reiter and J. L. Rasmussen, Eds., Atmos. Sci. Paper No. 122, Colo. State Univ., 1-74.
- Maddox, R. A., 1979a: The evolution of middle and upper tropospheric features during a period of intense convective storms. Preprints Eleventh Conf. on Severe Local Storms (Kansas City, Mo.), Amer. Meteor. Soc., Boston Mass.
- _____, 1979b: An objective technique for separating macroscale and mesoscale features. Submitted to Mon. Wea. Rev.
- _____, A. J. Negri, and T. H. Vonder Haar, 1977: Analysis of satellite derived winds for April 24, 1975. Preprints Tenth Conf. on Severe Local Storms (Omaha, Neb.), Amer. Meteor. Soc., Boston, Mass., 54-60
- _____, and T. H. Vonder Haar, 1979: Covariance analysis of satellite derived mesoscale wind fields. Accepted for publication in J. Appl. Meteor.
- Magor, B. W., 1958: A meso-low associated with a severe storm. Mon. Wea. Rev., 86, 81-90.
- _____, 1959: Mesoanalysis: Some operational analysis techniques utilized in tornado forecasting. Bull. Amer. Meteor. Soc., 40, 499-511
- _____, 1971: Statistics of selected surface conditions found within the hour preceding tornado occurrence, having identified a mesolow. Preprints Seventh Conf. on Severe Local Storms (Kansas City, Mo.), Amer. Meteor. Soc., Boston, Mass., 17-22
- Miller, R. C., 1967: Notes on analysis and severe storm forecasting procedures of the Military Weather Warning Center. AWS Tech. Report 200, Scott AFB, Ill., 94 pp.

- _____, 1978: Severe convective weather and the jet
airliner: A study of Southern airways Flight 242 April 4,
1977. Preprints Conf. on Weather Forecasting and Analysis
and Aviation Meteorology (Silver Spring, Md.), Amer.
Meteor. Soc., Boston, Mass., 279-283.
- Negri, A. J., D. W. Hillger, and T. H. Vonder Haar, 1977:
Moisture convergence from a combined mesoscale moisture
analysis and wind field for 24 April 1975. Preprints Tenth
Conf. on Severe Local Storms (Omaha, Neb.), Amer. Meteor.
Soc., Boston, Mass., 48-53
- Newman, W. R., 1972: The relationship between horizontal
moisture convergence and severe storm occurrences. M.S.
Thesis, The University of Oklahoma, Norman, Okla., 54 pp.
- Ninomiya, K., 1971a: Mesoscale modifications of synoptic
situations from thunderstorm development as revealed by
ATS III and aerological data. J. Appl. Meteor., 10,
1103-1121.
- _____, 1971b: Dynamic analysis of outflow from tornado-
producing thunderstorms as revealed by ATS III pictures.
J. Appl. Meteor., 10, 275-294.
- Peslen, C. A., 1977: A satellite interpretation of the dynamics
of a severe local storms area using 5 minute interval SMS
data. Preprints Tenth Conf. on Severe Local Storms (Omaha,
Neb.), Amer. Meteor. Soc., Boston, Mass., 1-7
- Purdom, J. F.W., 1975: Tornadic thunderstorms and GOES
satellite imagery. Paper presented at Ninth Conf. on
Severe Local Storms (Norman, Okla.), Amer. Meteor. Soc.
- _____, 1976: Some uses of high-resolution GOES imagery
in the mesoscale forecasting of convection and its behavior.
Mon. Wea. Rev., 104, 1474-1483.
- Sasaki, Y., 1973: Mechanisms of squall-line formation as
suggested from variational analysis of hourly surface
observations. Preprints Eight Conf. of Severe Local
Storms (Denver, Colo.), Amer. Meteor. Soc., Boston, Mass.,
300-307
- Sheppard, P. A., H. Charnock and J. R. D. Francis, 1952:
Observations of the westerlies over the sea. Quart. J.
Roy. Meteor. Soc., 78, 563-583.

Williams, D. T., 1957: A case study of the passage of a funnel bearing squall line using time cross sections of hourly rawinsonde observations. Unpublished manuscript, Severe Local Storms Project, U.S. Weather Bureau, Kansas City, Mo., 44 pp.

APPENDIX I

The Barnes Analysis Technique

The low-pass filter, exponential weight function objective analysis technique developed by Barnes (1964) was used to analyze surface data for the VTP computations presented in Sec. 3. The basic objective analysis technique follows Barnes' (1973) revision of his earlier scheme. Two dimensional meteorological data are interpolated to a cartesian grid and simultaneously smoothed. The first estimate of the gridded values of some parameter f is given by:

$$f_o(i,j) = \frac{\sum_{n=1}^N w_n f_n}{\sum_{n=1}^N w_n} \quad (A1)$$

where the weighting function, w_n , is:

$$w_n = \exp(-r_n^2/4k). \quad (A2)$$

The weight function parameter k is a constant arbitrarily chosen to fit the specific application being considered. The distance from the (i,j) grid point to the location of the data values f_n is denoted by r_n and N is the number of data observations allowed to influence the grid value.

Barnes' (1973) modification requires a correction pass through the first estimate field to achieve a desired response at specific wavelengths. The value of the weight function

parameter is reduced on the correction pass resulting in decreased computation time compared to the earlier use of successive iterations. The final grid point values are given by:

$$f(i,j) = f_0(i,j) + \sum_{n=1}^N w'_n D_n / \sum_{n=1}^N w'_n, \quad (A3)$$

where the modified weight function, w'_n , is:

$$w'_n = \exp(-r_n^2/4gk), \quad 0 < g < 1; \text{ and} \quad (A4)$$

$$D_n = f_n(x,y) - f_0(x,y). \quad (A5)$$

Thus D_n is the difference between an observed data value and the first estimate value at the same point. The first estimate value must be interpolated using $f_0(i,j)$ at the four nearest grid points. The final data field has been interpolated and filtered. Barnes has shown that the filter response is given, as a function of wavelength λ , by:

$$R = R_0(1 + R_0^{g-1} - R_0^g), \text{ where:} \quad (A6)$$

$$R_0 = \exp(-\pi^2 4k/\lambda^2). \quad (A7)$$

Advantages of this exponential weight, objective analysis technique listed by Barnes (1973) include:

1. The weight factors k and g are chosen prior to the analysis so that pattern scales supportable by the data distribution will be revealed to a known response amplitude.

2. Since $(A2)$ approaches zero asymptotically, the influence of data can be extended any distance without changing the weight function, and therefore, the response characteristics.
3. Small scale noise is adequately suppressed so that further smoothing with numerical filters is not necessary.
4. The desired pattern resolution can be achieved in only one iteration.

Barnes has also listed a number of practical guidelines to be used in specifying the values of k and g to fit particular applications. The density and distribution of the data field being analyzed is the most critical factor affecting the analysis. The response function (computed from equation A6) for the analysis runs used in this study is shown in Fig. A1.

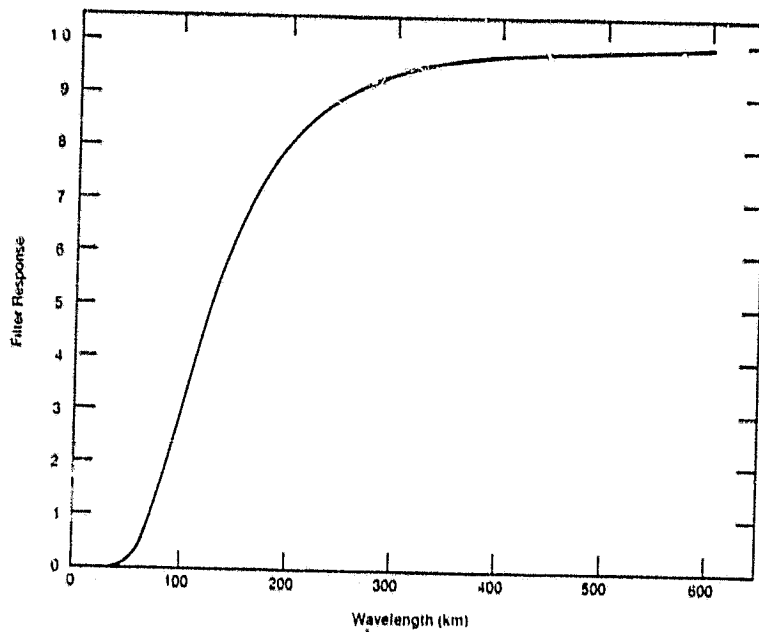


Fig. A1. Response curve as a function of wavelength.